EXPLORING DATA-DRIVEN MODELS FOR COMPOUND FLOOD FORECASTING: A COMPREHENSIVE BENCHMARK

Anonymous authors
Paper under double-blind review

ABSTRACT

Compound flood forecasting remains challenging due to complex interactions between meteorological, hydrological, and oceanographic factors, a challenge intensified by climate change. Traditional physics-based methods, such as the Hydrologic Engineering Center's River Analysis System, are often time-inefficient and non-executable due to lack of geographic data. While machine learning shows promise over traditional physics-based methods in both accuracy and efficiency, the lack of comprehensive datasets has hindered systematic evaluation of data-driven approaches. To address this gap, we introduce SF^{2}Bench, a comprehensive benchmark for compound flood forecasting using real-world data from South Florida. Our benchmark integrates four critical factors, tide, rainfall, groundwater, and human management activities, enabling systematic comparison of forecasting methods. We evaluate six modeling paradigms: Multilayer Perceptrons, Convolutional Neural Networks, Recurrent Neural Networks, Graph Neural Networks, Transformers, and Large Language Models. Through extensive experiments, we analyze the impact of key features, temporal dependencies, and spatial relationships on forecasting performance. The results across approaches highlight each method's distinct capabilities in capturing compound flood dynamics. By providing this benchmark with code and data, we aim to accelerate progress in flood forecasting through collaborative research between machine learning and environmental science communities. The code and data will be available once the paper is accepted.

1 INTRODUCTION

Floods are among the most common and hazardous natural events, causing environmental damage (Yin et al., 2023a), catastrophic loss of life (Jonkman & Vrijling, 2008), and property damage (Brody et al., 2007). Compared with single-driver flood events, such as fluvial floods and pluvial floods (Green et al., 2024), compound floods, occurring when two or more distinct flood drivers coincide in space or time (Sebastian, 2022), pose greater challenges for prediction and prevention, making it an important research topic in environmental science. Recent research indicates a rise in both the frequency and scale of compound floods due to global climate change (Wahl et al., 2015; Wing et al., 2022; Hirabayashi et al., 2013). Therefore, understanding the underlying causes of compound floods is both critical and urgent. Accurate and explainable compound flood models can support decision-making in water management, minimizing damage to human life and infrastructure.

Classical physics-based methods predict the water stage by solving complex partial differential equations (PDE) (Paniconi & Putti, 2015; Yin et al., 2023b), such as the Hydrologic Engineering Center's River Analysis System (HEC-RAS) (Brunner, 1997). Despite their accuracy and explainability, the extensive data requirements of physics-based methods, including high-resolution terrain data, reservoir characteristics, canal networks, and river geometries (Sampson et al., 2015; Zang et al., 2021), limit their widespread applications. The rapid development of machine learning (ML) has led to the application of data-centric methods, which utilize deep learning (DL) models for flood prediction and prevention. Researchers employ Convolutional Neural Networks (CNNs) (LeCun et al., 1998), Long Short-Term Memory networks (LSTMs) (Hochreiter & Schmidhuber, 1997), Graph Neural Networks (GNNs) (Kipf & Welling, 2016), and Transformers (Vaswani et al., 2017) to uncover the underlying principles of compound flood.

However, the lack of comprehensive benchmarks has significantly hindered systematic evaluation and comparison of data-driven approaches for compound flood forecasting. Existing methods (Adikari et al., 2021; Ruma et al., 2023; Miau & Hung, 2020; Shi et al., 2024; 2023; Liu et al., 2024c) largely focus on temporal causality, often underestimating the complex interplay of factors. Most prominently, compound floods have garnered increasing attention due to their capacity to analyze multiple influencing factors (Bevacqua et al., 2019; Wahl et al., 2015; Xu et al., 2023; Olbert et al., 2023; Kirschstein & Sun, 2024). Nevertheless, existing datasets (Kabir et al., 2020; Ruma et al., 2023; Shi et al., 2024) often contain limited factors and geographical scope, preventing systematic analysis and fair comparison across different modeling approaches. For example, LamaH-CE (Klingler et al., 2021) provides hydrological and topological data for the Danube River basin but lacks other important factors, such as rainfall and human management activities.

Building a comprehensive benchmark for compound flood analysis is challenging due to diverse drivers (e.g., meteorological factors, tides) and the need for long-term records. A suitable dataset must capture this complexity while supporting robust model evaluation. However, prior studies often focus on limited regions and factors, such as Haikou City in (Xu et al., 2023), limiting their representativeness and generalizability to other coastal areas.

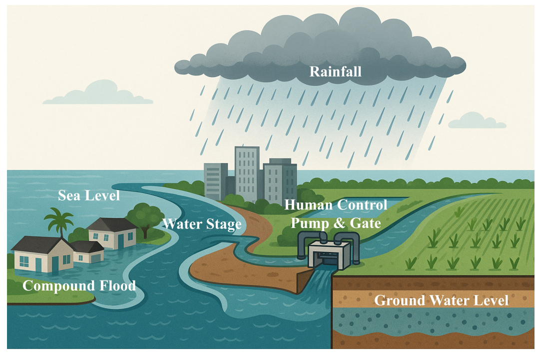

Figure 1: The schematic diagram of compound flood. The key factors include rainfall, sea, groundwater, and human control. The figure is assisted by OpenAI SORA.

In this paper, we introduce SF^{2}Bench, a benchmark for compound flood forecasting built on a curated dataset from South Florida, an ideal testbed for such analysis. South Florida exemplifies vulnerable coastal regions worldwide, facing frequent and severe compound flooding driven by interacting factors such as hurricanes and urban development. Its complex waterway system, low-lying topography, and porous geology, together with flood drivers including sea level, rainfall, river discharge, groundwater, storm surge, and waves (Jane et al., 2020), make it a comprehensive natural laboratory for studying compound flood dynamics. Our benchmark leverages this rich environment by incorporating multiple critical factors: water level, sea level, groundwater level, rainfall, and human management activities on hydraulic structures (gates and pumps), as illustrated in Figure 1. We compiled time series data from 2,452 monitoring stations across multiple counties, spanning from 1985 to 2024, providing unprecedented temporal and spatial coverage for compound flood analysis. This comprehensive dataset serves as a representative example for other coastal areas facing similar compound flooding challenges, offering insights that can inform flood management strategies in comparable regions worldwide.

To establish a rigorous evaluation framework, we benchmark a wide range of state-of-the-art forecasting methods using our dataset, including Multilayer Perceptrons (MLPs), Recurrent Neural Networks (RNNs), CNNs, GNNs, Transformers, and Large Language Models (LLM)-based approaches. Our systematic evaluation reveals that MLPs and Transformers exhibit advantages in terms of MAE and MSE metrics, while MLPs and GNNs demonstrate superior performance in extreme flood events. The benchmark results highlight the varying degrees of effectiveness of each method in capturing the complex temporal and spatial dependencies inherent in compound flooding, providing crucial insights for method selection and development. Furthermore, we conduct comprehensive experiments to demonstrate the individual and combined effectiveness of different factors across various model architectures, offering guidance for feature selection in compound flood modeling. Finally, we discuss potential strategies for improving flood forecasting performance by leveraging both spatial and temporal information, establishing a foundation for future research in this critical area.

2 Related Work

Flood Dataset. Monitoring floods presents a significant challenge due to their unpredictable nature and potentially devastating consequences. Existing flood datasets can be broadly categorized into satellite image datasets (Rahnemoonfar et al., 2021; Dottori et al., 2022; Montello et al., 2022; Papagiannaki et al., 2022; Xu et al., 2025; Bonafilia et al., 2020) and time series monitoring datasets (Xu et al., 2023; Kabir et al., 2020; Adikari et al., 2021; Ruma et al., 2023; Klingler et al., 2021; Fowler et al., 2021; Chagas et al., 2020). Satellite image datasets utilize remote sensing to capture surface water extent (Amitrano et al., 2024). While effective in delineating flood-affected areas, this type of dataset (Xu et al., 2025; Bonafilia et al., 2020) often lacks crucial temporal dynamics and information on the underlying hydrological and meteorological factors that drive flood formation, limiting its utility for in-depth modeling. Time series monitoring datasets, on the other hand, typically utilize fixed monitoring stations to record hydrological-related data such as soil moisture, water level, and temperature. A prominent example within this category is the CAMELS-x family of datasets (Addor et al., 2017; Alvarez-Garreton et al., 2018; Coxon et al., 2020; Chagas et al., 2020; Fowler et al., 2021). For instance, CAMELS-BR (Chagas et al., 2020) encompasses data from 3,679 gauges across Brazil. LamaH-CE (Klingler et al., 2021) provides daily and hourly time series data from 882 gauges, including runoff, meteorological variables, and catchment attributes. In (Kirschstein & Sun, 2024), LamaH-CE is used as a benchmark for flood forecasting, primarily focusing on temporal and spatial aspects. However, these datasets primarily focus on general hydrological modeling. Analyzing compound floods, as highlighted in (Jane et al., 2020), necessitates detailed data on rainfall, water levels, and groundwater, which are often limited in existing time series datasets.

Machine Learning for Forecasting. The task of forecasting time series data presents inherent complexities and high dimensionality. Recent advancements in time series forecasting have been significantly propelled by a data-centric approach (Zha et al., 2025), underscoring the critical role of extensive, high-quality data in training robust models. Deep learning methodologies, with their powerful representation learning capabilities, have shown considerable promise in this domain. Based on their architectural designs, deep learning methods applied to time series forecasting can be categorized as follows: **MLP-based models** (Chen et al., 2023; Zeng et al., 2023; Wang et al., 2024b; Lin et al., 2024b;a) leverage the capabilities of multilayer perceptrons for analyzing temporal sequences. **RNN-based methods** (Lai et al., 2018; Salinas et al., 2020; Wang et al., 2018; Qin et al., 2017; Jhin et al., 2024) are widely adopted in time series forecasting due to their inherent ability to model temporal dependencies within sequential data. **CNN-based methods** (Wang et al., 2024a; Cheng et al., 2024; Luo & Wang, 2024; Wu et al., 2023; Wang et al., 2023) employ convolutional operations to extract hierarchical features from time series data, enabling effective learning of underlying patterns and trends. **GNN-based methods** (Wu et al., 2020; 2019; Cao et al., 2020; Liu et al., 2022b; Yi et al., 2023; Cai et al., 2023) utilize graph structures to model intricate relationships between different time series variables, enhancing forecasting accuracy. **Transformer-based methods** (Wang et al., 2024c; Liu et al., 2024a; Nie et al., 2023; Zhou et al., 2022; Liu et al., 2022a; Wu et al., 2021; Zhou et al., 2021a) have demonstrated remarkable performance in capturing long-range dependencies and complex temporal dynamics within time series data. **LLM-based methods** (Jin et al., 2024; Pan et al., 2024; Zhou et al., 2023; Gruver et al., 2023) explore the application of prompting and reprogramming techniques to align time series data with text embeddings for forecasting tasks.

3 The SF^{2}Bench Dataset

SF^{2}Bench comprises a time series data collection from 2,452 monitoring stations across a 67,349 km^2 area in South Florida, sourced from the South Florida Water Management District (SFWMD) [1]. The dataset spans the period from 1985 to 2024 and is divided into 8 temporal splits. This dataset incorporates key factors that play critical roles in compound floods (Jane et al., 2020), including water level [2], rainfall, groundwater level, and human control data for pumps and gates. Notably, sea level data is inherently included within the water level at certain monitoring stations due to their direct connection to the sea. It is specifically collected for benchmarking data-driven forecasting approaches in the context of compound flood analysis. In Table 1, we provide a comparison with other datasets. Compared to CAMELS-x (Addor et al., 2017; Alvarez-Garreton et al., 2018; Coxon et al., 2020; Chagas et al., 2020; Fowler et al., 2021), SF^{2}Bench focuses on a region particularly susceptible to flooding, making it more relevant for compound flood analysis. In comparison to BangladeshFlood (Ruma et al., 2023), SF^{2}Bench offers a more comprehensive set of driving factors relevant to compound flooding, considering both temporal and spatial dimensions.

[1] https://www.sfwmd.gov/

[2] Water stage and water level are used interchangeably.

Table 1: **Comparison with other datasets for flood forecasting.** N/A indicates Not Available. * marks datasets with Other Attributions. Climatic indices capture climate statistics (e.g., potential evapotranspiration). Land cover attributes describe surface materials (e.g., woodland ratio). Soil attributes include properties such as porosity and depth, while geological attributes refer to subsurface features (e.g., geologic class, porosity). Anthropogenic influences cover human activities (e.g., water abstraction, discharges). Other catchment attributes include location, area, and topography.

Dataset	Time Span	Interval	Type	Gauges	Area(km^2)	Public	Other Attributions
DarlingFlood	1900-2018	Daily	Flow	12	3.5×10^4	No	Rainfall
SekongFlood	1981-2013	Daily	Flow	8	2.8×10^4	No	Rainfall
BangladeshFlood	1979-2013	Daily	Stage	24	1.5×10^5	No	N/A
Qi River	1979-2020	Hour	Flow	7	7.1×10^3	No	Rainfall
Tunxi basins	1981-2007	Hour	Flow	12	N/A	No	Rainfall
CAMELS*	1989-2009	Daily	Flow	671	1.0×10^4	Yes	Climatic Indices
CAMELS-CL*	1913-2018	Daily	Flow	516	N/A	Yes	Land Cover Attributes
CAMELS-GB*	1970-2015	Daily	Flow	671	2.1×10^5	Yes	Soil Attributes
CAMELS-BR*	1925-2024	Daily	Flow	4,025	N/A	Yes	Geological Attributes
CAMELS-AUS*	1951-2014	Daily	Flow	107	6.9×10^5	Yes	Anthropogenic Influences
LamaH-CE*	1951-2014	Daily & Hour	Flow	859	1.7×10^5	Yes	Other Catchment Attributes
SF^{2}Bench	1985-2024	Hour	Stage	2,452	6.7×10^4	Yes	Rainfall, Groundwater, Human Control

3.1 PREPROCESSING

Data Collection. The data for SF^{2}Bench was collected from DBHYDRO [3], an environmental database maintained by the SFWMD that stores a wide range of hydrologic, meteorologic, hydrogeologic, and water quality data. We initially collected data from 3731 monitoring stations and subsequently screened them based on data availability and relevance to flood analysis, resulting in a final set of 2,452 valid stations. This included 993 water stage monitoring stations, 349 rainwater monitoring stations, 582 groundwater level monitoring stations, 99 pump stations, and 429 gates.

The different types of data and their physical meanings are summarized in Table 2. To capture fine-grained temporal dynamics, all raw data is collected at their native "breakpoint" frequency, resulting in a high (up to second-level) temporal resolution for each recorded value. However, this breakpoint frequency collection method results in inconsistent data across stations, with some recording data at much higher frequencies than others. In addition, some monitoring stations have missing data for certain periods, while others provide data only for a limited duration, such as one year.

Data Processing. To provide an AI-ready dataset, we introduce data processing to unify the format. As previously mentioned, the data collection ranges vary across different monitoring stations, making it challenging to standardize all data to a uniform length. To balance the number of time series and temporal length, we divided the data into eight splits. Each time-series data is sampled with an hourly interval for all splits. During processing, for each interval, we first compute the mean of the available data points within that interval. Subsequently, we address missing values using interpolation methods. According to the characteristics of the data, we have two interpolation methods: linear interpolation and zero data filling. For water stage and groundwater level, we regard them as continuous variables and apply linear interpolation to fill missing values. For the other variables, rainfall and control data (pumps and gates), we treat them as discrete events and fill missing values with zero. The detailed information is presented in Appendix Table 7.

Table 2: The summary of the data type in SF^{2}Bench.

Type	Stations	Unit	Description
Water	993	Feet	Water Stage
Groundwater	582	Feet	Stage of Groundwater
Rainfall	349	Inches	Rainfall
Pump	99	RPM	Rotational Speed
Gate	429	Feet	Opening Level

3.2 QUALITATIVE ANALYSIS

To provide an intuitive insight of SF^{2}Bench, we provide visualization results from spatial and temporal aspects. More detailed information are provided in the Appendix A.

[3] https://apps.sfwmd.gov/dbhydroInsights/%23/homepage

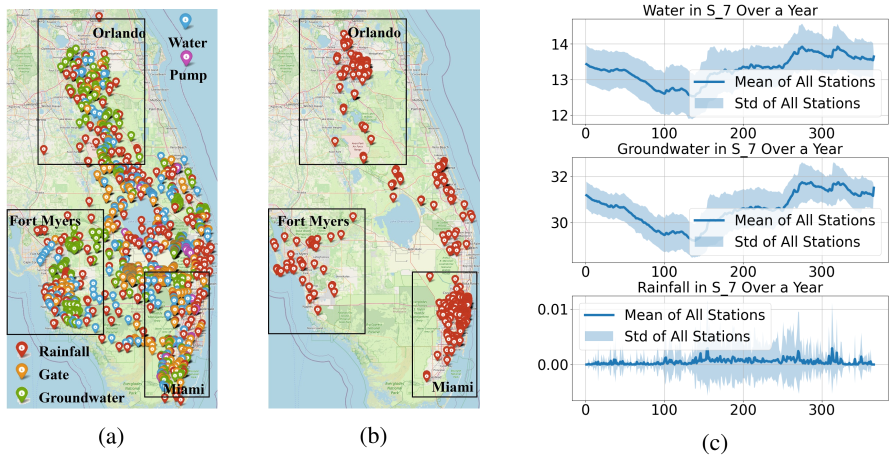

Figure 2: (a) Monitor stations location distribution. (b) Flood observation location distribution. (c) Temporal patterns of key features over a year. In (a) and (b), we highlight three interest parts: Orlando, Fort Myers, and Miami. In (c), the x-axis is the number of days in one year.

Spatial Distribution. Figure 2a illustrates the spatial distribution of all monitoring stations, which are primarily located around the intricate river system of South Florida, radiating outwards from Lake Okeechobee. The geographically staggered distribution of hydrological, groundwater, and rainwater monitoring stations enables more effective spatial analysis. For example, the water level at a specific location is likely correlated with rainfall in the surrounding area and the local groundwater level (representing the soil's water storage capacity). We also highlight the observed flood locations from 2020 to 2023 and in 2008 in Figure 2b provided by SFWMD (Office of Resilience, South Florida Water Management District, 2025), which are predominantly concentrated in urban areas.

Temporal Pattern Visualization. Figure 2c illustrates the average annual temporal patterns across all monitoring stations, using data from split S7 as a representative example. From this pattern, we observe a strong correlation between groundwater level and water level data. The water level generally rises from approximately the 150th to the 300th day of the year, followed by a gradual decrease. According to the National Weather Service (NWS) [4], Florida's climate is characterized by distinct dry and rainy seasons, with the latter typically spanning from May to October. This aligns well with the observed data patterns in our dataset. Taking rainfall as a reference, we note that increases in water level tend to correspond with rainfall events, such as the rainfall peak after the 300th day and the subsequent rise in water level. In addition, human control activities on hydraulic structures (e.g., pumps and gates) appear to influence water level changes in response to rainfall. We can infer that human intervention has played a role in mitigating potential flooding.

4 FORECASTING BENCHMARKS

4.1 PROBLEM DEFINITION

Given water stage time series data $\boldsymbol{X} \in \mathbb{R}^{N \times L}$ from N water monitoring stations, the forecasting task is to predict the water stage values for the next T time steps, denoted as $\boldsymbol{Y} \in \mathbb{R}^{N \times T}$, using a fixed look-back window of length L. We also have access to additional time series information, including groundwater levels $\boldsymbol{X}_w \in \mathbb{R}^{N_w \times L}$ (from N_w stations), rainfall $\boldsymbol{X}_r \in \mathbb{R}^{N_r \times L}$ (from N_r stations), pump control data $\boldsymbol{X}_p \in \mathbb{R}^{N_p \times L}$ (from N_p stations), gate control data $\boldsymbol{X}_g \in \mathbb{R}^{N_g \times L}$ (from N_g stations), and location information for the monitoring stations. For the primary benchmark experiments aimed at fair comparison across different models, we mainly consider the water stage data as the supervised data. However, we acknowledge that incorporating the additional information (groundwater levels, rainfall, pump and gate control data, and location) has the potential to further enhance forecasting performance.

[4] https://www.weather.gov/tbw/TBWTstmClimoQuickReference

Table 3: Benchmark of average MAE&MSE results on three interest areas across 8 splits. The best and second results are shown in bold font and underlined, respectively.

		MLP			CNN			Transformer	
Metric	T	MLP	TSMixer	NLinear	TCN	ModernTCN	TimesNet	iTransformer	PatchTST
↓MAE	1D	0.0788	0.0928	0.0817	0.1792	0.0798	0.0983	0.0756	**0.0741**
	3D	0.1351	0.1442	0.1373	0.2281	0.1441	0.1528	**0.1314**	0.1316
	5D	0.1764	0.1816	0.1769	0.2697	0.1891	0.1927	0.1722	**0.1719**
	7D	0.2063	0.2126	0.2082	0.3088	0.2248	0.2267	**0.2041**	0.2044
	Avg.	0.1492	0.1578	0.1510	0.2465	0.1594	0.1676	0.1458	**0.1455**
↓MSE	1D	0.0521	0.0648	0.0556	0.3722	0.0681	0.0704	**0.0253**	0.0531
	3D	**0.1029**	0.1132	0.1105	0.4647	0.2443	0.1358	0.1112	0.1132
	5D	**0.1432**	0.1566	0.1547	0.4173	0.2808	0.1829	0.1583	0.1566
	7D	**0.1707**	0.1903	0.1841	0.5386	0.2723	0.2241	0.1911	0.1903
	Avg.	**0.1172**	0.1283	0.1262	0.4482	0.2164	0.1533	0.1284	0.1283

		RNN			GNN			LLM	
Metric	T	LSTM	DeepAR	DilatedRNN	GCN	FourierGNN	StemGNN	GPT4TS	AutoTimes
↓MAE	1D	0.1182	0.1178	0.0919	0.1696	0.0921	0.1332	0.1256	0.0846
	3D	0.1821	0.1837	0.1573	0.2006	0.1503	0.2181	0.1521	0.1362
	5D	0.2232	0.2247	0.2022	0.2504	0.1930	0.3153	0.1911	0.1752
	7D	0.2576	0.2596	0.2374	0.2799	0.2280	0.3570	0.2247	0.2062
	Avg.	0.1953	0.1964	0.1722	0.2251	0.1658	0.2559	0.1734	0.1505
↓MSE	1D	0.1339	0.1230	0.1033	7.2299	0.0768	0.1632	0.0966	0.0584
	3D	0.1985	0.1954	0.1672	1.5645	0.1416	0.2543	0.1410	0.1125
	5D	0.2348	0.2389	0.2341	2.1341	0.2071	0.4189	0.1847	0.1522
	7D	0.2873	0.2691	0.2591	1.0374	0.2125	0.4716	0.2245	0.1823
	Avg.	0.2136	0.2066	0.1909	2.9915	0.1595	0.3270	0.1617	0.1263

Table 4: Benchmark of average SEDI results on three interest areas across 8 splits. The best and second results are shown in bold font and underlined, respectively.

	MLP			CNN			Transformer	
Metric	MLP	TSMixer	NLinear	TCN	ModernTCN	TimesNet	iTransformer	PatchTST
↑SEDI(10%)	**0.6897**	0.6144	0.6278	0.5311	0.6067	0.5829	0.6286	0.6296
↑SEDI(5%)	**0.5834**	0.4942	0.5111	0.3706	0.4846	0.4589	0.5079	0.5086
↑SEDI(1%)	**0.3666**	0.2480	0.2767	0.1387	0.2512	0.2222	0.2690	0.2685

	RNN			GNN			LLM	
Metric	LSTM	DeepAR	DilatedRNN	GCN	FourierGNN	StemGNN	GPT4TS	AutoTimes
↑SEDI(10%)	0.6097	0.5989	0.6164	0.6179	0.6623	0.5507	0.5581	0.6239
↑SEDI(5%)	0.4702	0.4643	0.5014	0.5138	0.5511	0.4270	0.4640	0.5015
↑SEDI(1%)	0.1680	0.1478	0.2499	0.2828	0.3217	0.1690	0.2268	0.2568

4.2 METRICS

We follow standard time series forecasting practices by using the Mean Absolute Error (MAE) and Mean Squared Error (MSE) as our primary evaluation metrics. To better assess the performance of our models in real-world applications, particularly for extreme flood events, we also employ the Symmetric Extremal Dependence Index (SEDI) (Han et al., 2024a; Xu et al., 2024), as suggested by (Han et al., 2024b). By selecting quantile thresholds (e.g., the 95th and 5th percentiles of the observed values), SEDI classifies each time stamp as belonging to either a normal or an extreme case and then calculates the hit rate of this classification. A higher SEDI value indicates better performance in predicting extreme events. The formulation of SEDI is as follows:

$$\mathrm{SEDI}(p) = \frac{|\hat{\boldsymbol{Y}} < V_{1-\frac{p}{2}} \& \boldsymbol{Y} < V_{1-\frac{p}{2}}| + |\hat{\boldsymbol{Y}} > V_{\frac{p}{2}} \& \boldsymbol{Y} > V_{\frac{p}{2}}|}{|\boldsymbol{Y} < V_{1-\frac{p}{2}}| + |\boldsymbol{Y} > V_{\frac{p}{2}}|}, \tag{1}$$

where $|\cdot|$ means the number of the true values satisfying the condition, $\hat{\boldsymbol{Y}}$ is the forecasting results, p is the quantile of the threshold, and $V_{1-\frac{p}{2}}, V_{\frac{p}{2}}$ are the lower and upper threshold of top and worst $\frac{p}{2}$ percent, respectively.

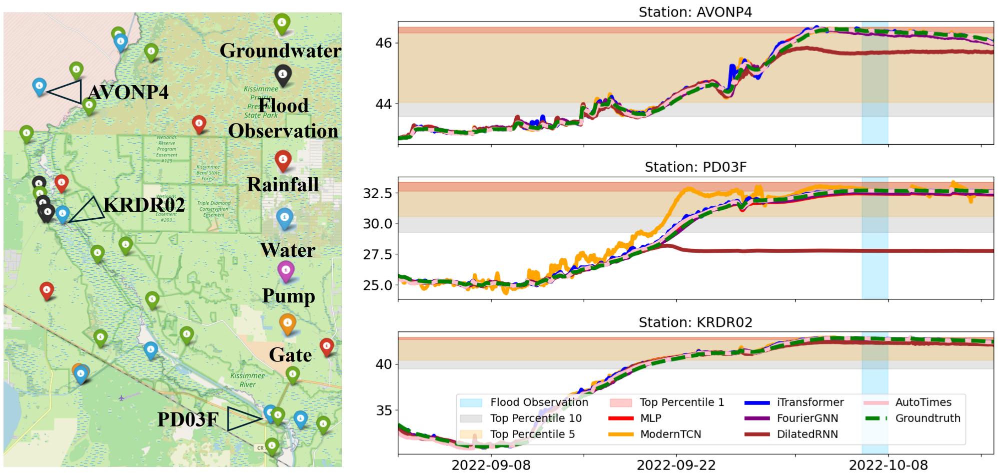

(a)

(b)

Figure 3: (a) The interest area of the case study. (b) The comparison among different methods. We mark the flood observation on the x-axis and the top percentile 10/5/1 with colors.

4.3 Methods

We benchmark six categories of time series forecasting architectures: MLP, CNN, RNN, GNN, Transformer, and LLM. We select two advanced methods as representative examples for each of these categories. Additionally, for the first four classical architectures, we also implement a basic foundational architecture. The specific advanced methods we evaluate are: MLP: NLinear (Zeng et al., 2023), TSMixer (Chen et al., 2023), CNN: ModernTCN (Luo & Wang, 2024), TimesNet (Wu et al., 2023), RNN: DeepAR (Salinas et al., 2020), DilatedRNN (Chang et al., 2017), GNN: FourierGNN (Yi et al., 2023), StemGNN (Cao et al., 2020), Transformer: PatchTST (Nie et al., 2023), iTransformer (Liu et al., 2024a), LLM: GPT4TS (Zhou et al., 2023), AutoTimes (Liu et al., 2024b). We follow the source code of NeuralForecast [5] for the implementation of these approaches. The summary of these methods can be found in Appendix B.2.

4.4 Experiment Setup

Table 5: Average results of basic methods on the whole dataset. The best and second results are shown in bold font and underlined, respectively.

Metric	MLP	LSTM	TCN	GCN
↓MAE	**0.2328**	0.3302	0.3491	<u>0.3053</u>
↓MSE	**0.3902**	2.2772	<u>0.6807</u>	1.0673
↑SEDI(10%)	**0.6853**	0.5751	0.5167	<u>0.6137</u>
↑SEDI(5%)	**0.5970**	0.4516	0.3904	<u>0.5213</u>
↑SEDI(1%)	**0.4107**	0.1828	0.1842	<u>0.3134</u>

Due to the memory and training time limitations associated with GPUs, applying some methods, particularly LLM-based approaches (Pan et al., 2024; Jin et al., 2024; Zhou et al., 2023; Liu et al., 2024b), to the entire dataset is challenging. To facilitate a fair comparison, we conduct our experiments using two setups: evaluation on three specific areas of interest and evaluation on the entire dataset. The three areas were selected based on the flood observation data presented in Figure 2. Figure 2b visualizes these flood locations alongside the selected areas. We report the performance of all evaluated methods within these areas of interest. For the entire dataset, we only report the results of the basic foundational techniques. For each data split, the last year's data is used for testing, the data of the second-to-last year is used for validation, and the remaining preceding data is used for training. In the benchmark, we maintain a consistent lookback window of two days, and we evaluate prediction windows of one, three, five, and seven days. The detailed experimental setup, including software and hardware platforms, is provided in the Appendix B.

[5] https://github.com/Nixtla/neuralforecast

Table 6: Input factors ablation study on S6. All, G, R, and C represent all factors, groundwater, rainfall, and human control(pump and gate). The best and second results are shown in bold font and underlined, respectively.

Metric	method	w/ All	w/o G	w/o R	w/o C	w/o GR	w/o RC	w/o WC	w/o WRC
↓MAE	iTransformer	0.1406	0.1407	0.1406	<u>0.1405</u>	0.1411	0.1410	**0.1402**	0.1411
	PatchTST	**0.1376**	0.1391	0.1378	<u>0.1377</u>	0.1398	0.1396	0.1385	0.1421
	TSMixer	0.1596	<u>0.1419</u>	0.2523	0.2111	**0.1418**	0.2807	0.1423	0.1422
	NLinear	0.1546	0.1577	0.1483	0.1540	0.1485	<u>0.1450</u>	0.1579	**0.1435**
	TimesNet	0.1642	0.1599	0.1662	0.1650	0.1592	0.1656	**0.1578**	<u>0.1580</u>
↓MSE	iTransformer	<u>0.0953</u>	0.0960	**0.0949**	0.0954	0.0957	0.0956	**0.0949**	0.0962
	PatchTST	<u>0.0917</u>	0.0932	0.0927	**0.0916**	0.0950	0.0938	0.0923	0.0971
	TSMixer	0.1080	0.0946	0.4061	0.2698	0.0946	0.6697	<u>0.0943</u>	**0.0941**
	NLinear	0.0992	0.1011	0.0966	0.0984	0.0973	<u>0.0954</u>	0.1006	**0.0947**
	TimesNet	0.1188	0.1154	0.1226	0.1202	0.1145	0.1237	**0.1111**	<u>0.1123</u>

4.5 Results & Observations

Overall Performance. Table 3 reports the average MSE and MAE results across three regions and eight data splits. The top-performing methods include PatchTST, iTransformer, MLP, NLinear, and AutoTimes. PatchTST and iTransformer achieve the best MAE, while MLP, NLinear, and AutoTimes perform best under MSE. A small MAE but large MSE suggests high accuracy for most points with occasional large errors, whereas the opposite indicates greater stability but lower pointwise accuracy. Table 4 shows model performance on extreme cases, where FourierGNN ranks second in SEDI despite weaker MSE and MAE. Detailed split results are provided in Appendix C. Table 5 further presents the average performance of basic methods on the full dataset (with details in Appendix C.1). Among these, MLP consistently performs best, followed by GCN and TCN, consistent with the MSE and MAE trends in Table 3. This finding aligns with prior work (Kirschstein & Sun, 2024), which also shows MLP outperforming GNNs. Overall, our results show that MLP, transformer-based models (PatchTST, iTransformer), and LLM-based models (AutoTimes, GPT4TS) achieve strong performance on MAE and MSE, while the GNN-based FourierGNN excels on SEDI. Since extreme-case predictions are crucial for assessing flood risk, SEDI provides complementary insights. Notably, MAE/MSE and SEDI results are not strongly correlated, highlighting the need for multiple evaluation metrics. We also find no clear link between performance and model size. For example, NLinear ($9K$) performs comparably to AutoTimes ($4M$) despite its far smaller parameter count.

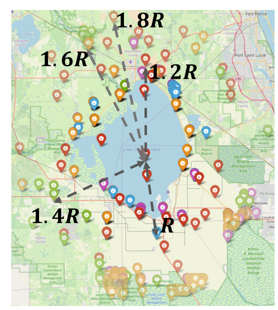

Figure 4: The different interest areas with a radius for ablation study on spatial information.

Case Study. To evaluate the performance of different models in real flood scenarios, we conduct a case study using Hurricane Ian, which struck Florida on September 28, 2022, causing widespread flooding in multiple locations, including Orlando (Hur, 2023). We select the middle stage of the Kissimmee River as our study area because the water monitoring stations are located near the observed flood zones, as shown in Figure 3a. This location provides an ideal setting for model evaluation, with available data for three key factors: water level, groundwater level, and rainfall. In the experiments, all models were trained to forecast water levels for the next 24 hours. Figure 3b presents the forecasting results from three representative water monitoring stations, revealing clear performance differences among the six methods. The results show that ModernTCN and DilatedRNN achieve lower accuracy compared to other approaches. While most methods successfully captured the overall flooding trend, iTransformer showed notably larger prediction errors in certain areas. These visualization results are consistent with the quantitative findings presented in Table 3.

Ablation of Factors. To verify and demonstrate the influence of different input factors, we conduct an ablation study using five methods. These methods contains two settings: channel-independent (including NLinear and PatchTST) and channel-dependent (including iTransformer, TimesNet, and TSMixer). For the channel-independent methods, we used all available factors as input. In contrast, for the channel-dependent methods, we primarily used the water stage data as the supervised target, while other factors were considered as potential additional inputs. As shown in Table 6, NLinear and

TSMixer achieve comparable results when the input is limited to only the water stage data, suggesting that the inclusion of other factors does not significantly improve their performance. For iTransformer, PatchTST, and TimesNet, we observe performance improvements when additional information is provided, highlighting the potential benefit of incorporating multi-faceted data for this forecasting task. Moreover, for iTransformer and PatchTST, we find excluding groundwater information (denoted as "w/o G" and "w/o GR") results in larger MSE and MAE errors compared to settings where other factors are excluded (e.g., "w/o R" for without rainfall, "w/o C" for without control data, "w/o RC", and "w/o WC"). Moreover, for iTransformer and TimesNet, providing only groundwater information as the additional input leads to the best performance among the ablation settings, suggesting that the groundwater is a particularly informative factor for these models. We also observe similar results on the SEDI(10%) metric, provided in Appendix C.2.

Impact of Temporal and Spatial Information. To provide insight into the impact of temporal input length and spatial information, we conduct ablation studies. We first select an interest area as the anchor area, where the water stages are regarded as the forecasting target. As shown in Figure 4, R is the radius of the anchor area. Then, we incorporate information from surrounding stations by incrementally increasing the radius of the interest area. In these experiments, we consider radius scale factors of 1,1.2,1.4,1.6, and 1.8. The MAE, MSE, and SEDI results, presented in Figures 5a, show that iTransformer, PatchTST, and TSMixer experience a performance improvement as the input area expands.This indicates the effectiveness of incorporating additional spatial information for the forecasting task. We provide the detailed results in Appendix C.2.

Furthermore, maintaining the anchor area as the forecasting target, we evaluate the impact of temporal input length by considering a range of durations: 6 hours, 12 hours, and 1 to 6 days. As shown in Figure 5b, we observe that PatchTST, TSMixer, and iTransformer generally show improved performance with increasing input length. However, for iTransformer, performance begins to decrease beyond an input length of 1 day. A potential reason for this phenomenon is that longer input sequences require a larger amount of training data to effectively learn the underlying patterns. The detailed results are available in Appendix C.2. Comparing these two strategies, we find that both can enhance task performance. Increasing spatial input generally leads to a relatively stable, albeit limited, improvement. In contrast, extending the temporal input length can yield more substantial gains, particularly for models like TSMixer, where a significant reduction in MSE is observed.

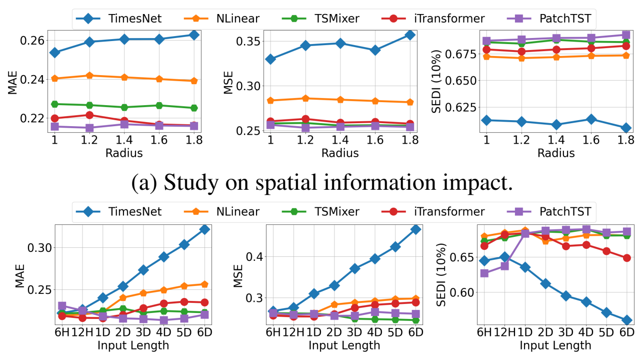

(a) Study on spatial information impact.

(b) Study on temporal information impact.

Figure 5: Combined ablation studies results.

5 CONCLUSION

In this paper, we introduce a new benchmark SF^{2}Bench, the dataset collected for comprehensive compound flood analysis. Our goal is to foster collaboration between the machine learning and environmental science communities by providing a resource that bridges domain expertise with advanced predictive modeling. SF^{2}Bench comprehensively covers the majority of South Florida and integrates five key factors: water level, sea level, groundwater table, rainfall, and human control activities. To assess its utility, we evaluate six types of time series forecasting approaches on this dataset and observe that different architectures exhibit distinct advantages. Furthermore, our ablation studies on input factors reveal that groundwater level is a particularly effective predictor compared to other information sources. Additionally, we conduct experiments to explore the effectiveness of increasing spatial and temporal information, and the results demonstrate that both strategies improve forecasting performance for this task.

Ethic Statement

All authors confirm that they have read and commit to upholding the ICLR Code of Ethics. All experiments use publicly available datasets; no human subjects or sensitive data are involved.

Reproducibility Statement

All code and datasets are included in the Supplementary Material. All experiments use publicly available datasets, and are reproducible.

References

Hurricane ian. `https://storymaps.arcgis.com/stories/4a242bae868140a394c96bc2d9415e86`, 2023. Accessed: 2025-08-20.

Nans Addor, Andrew J Newman, Naoki Mizukami, and Martyn P Clark. The camels data set: catchment attributes and meteorology for large-sample studies. *Hydrology and Earth System Sciences*, 21(10):5293–5313, 2017.

Kasuni E. Adikari, Sangam Shrestha, Dhanika T. Ratnayake, Aakanchya Budhathoki, S. Mohanasundaram, and Matthew N. Dailey. Evaluation of artificial intelligence models for flood and drought forecasting in arid and tropical regions. *Environmental Modelling & Software*, 144:105136, 2021. ISSN 1364-8152. doi: https://doi.org/10.1016/j.envsoft.2021.105136. URL `https://www.sciencedirect.com/science/article/pii/S1364815221001791`.

Camila Alvarez-Garreton, Pablo A Mendoza, Juan Pablo Boisier, Nans Addor, Mauricio Galleguillos, Mauricio Zambrano-Bigiarini, Antonio Lara, Cristóbal Puelma, Gonzalo Cortes, Rene Garreaud, et al. The camels-cl dataset: catchment attributes and meteorology for large sample studies–chile dataset. *Hydrology and Earth System Sciences*, 22(11):5817–5846, 2018.

Donato Amitrano, Gerardo Di Martino, Alessio Di Simone, and Pasquale Imperatore. Flood detection with sar: A review of techniques and datasets. *Remote Sensing*, 16(4), 2024. ISSN 2072-4292. doi: 10.3390/rs16040656. URL `https://www.mdpi.com/2072-4292/16/4/656`.

Shaojie Bai, J Zico Kolter, and Vladlen Koltun. An empirical evaluation of generic convolutional and recurrent networks for sequence modeling. *arXiv preprint arXiv:1803.01271*, 2018.

Emanuele Bevacqua, Douglas Maraun, Michalis Ioannis Vousdoukas, Evangelos Voukouvalas, Mathieu Vrac, Lorenzo Mentaschi, and Martin Widmann. Higher probability of compound flooding from precipitation and storm surge in europe under anthropogenic climate change. *Science advances*, 5(9):eaaw5531, 2019.

Derrick Bonafilia, Beth Tellman, Tyler Anderson, and Erica Issenberg. Sen1floods11: A georeferenced dataset to train and test deep learning flood algorithms for sentinel-1. In *Proceedings of the IEEE/CVF conference on computer vision and pattern recognition workshops*, pp. 210–211, 2020.

Samuel D Brody, Sammy Zahran, Praveen Maghelal, Himanshu Grover, and Wesley E Highfield. The rising costs of floods: Examining the impact of planning and development decisions on property damage in florida. *Journal of the American Planning Association*, 73(3):330–345, 2007.

Gary W Brunner. Hec-ras river analysis system. hydraulic reference manual. version 1.0. 1997.

Wanlin Cai, Yuxuan Liang, Xianggen Liu, Jianshuai Feng, and Yuankai Wu. Msgnet: Learning multi-scale inter-series correlations for multivariate time series forecasting. *arXiv preprint arXiv:2401.00423*, 2023.

Defu Cao, Yujing Wang, Juanyong Duan, Ce Zhang, Xia Zhu, Conguri Huang, Yunhai Tong, Bixiong Xu, Jing Bai, Jie Tong, and Qi Zhang. Spectral temporal graph neural network for multivariate time-series forecasting. In *Proceedings of the 34th International Conference on Neural Information Processing Systems*, NIPS '20, Red Hook, NY, USA, 2020. Curran Associates Inc. ISBN 9781713829546.

Vinícius BP Chagas, Pedro LB Chaffe, Nans Addor, Fernando M Fan, Ayan S Fleischmann, Rodrigo CD Paiva, and Vinícius A Siqueira. Camels-br: hydrometeorological time series and landscape attributes for 897 catchments in brazil. *Earth System Science Data*, 12(3):2075–2096, 2020.

Shiyu Chang, Yang Zhang, Wei Han, Mo Yu, Xiaoxiao Guo, Wei Tan, Xiaodong Cui, Michael Witbrock, Mark A Hasegawa-Johnson, and Thomas S Huang. Dilated recurrent neural networks. *Advances in neural information processing systems*, 30, 2017.

Si-An Chen, Chun-Liang Li, Sercan O Arik, Nathanael Christian Yoder, and Tomas Pfister. TSMixer: An all-MLP architecture for time series forecast-ing. *Transactions on Machine Learning Research*, 2023. ISSN 2835-8856. URL `https://openreview.net/forum?id=wbpxTuXgm0`.

Mingyue Cheng, Jiqian Yang, Tingyue Pan, Qi Liu, and Zhi Li. Convtimenet: A deep hierarchical fully convolutional model for multivariate time series analysis. *arXiv preprint arXiv:2403.01493*, 2024.

Gemma Coxon, Nans Addor, John P Bloomfield, Jim Freer, Matt Fry, Jamie Hannaford, Nicholas JK Howden, Rosanna Lane, Melinda Lewis, Emma L Robinson, et al. Camels-gb: hydrometeorological time series and landscape attributes for 671 catchments in great britain. *Earth System Science Data*, 12(4):2459–2483, 2020.

F. Dottori, L. Alfieri, A. Bianchi, J. Skoien, and P. Salamon. A new dataset of river flood hazard maps for europe and the mediterranean basin. *Earth System Science Data*, 14(4):1549–1569, 2022. doi: 10.5194/essd-14-1549-2022. URL `https://essd.copernicus.org/articles/14/1549/2022/`.

K. J. A. Fowler, S. C. Acharya, N. Addor, C. Chou, and M. C. Peel. Camels-aus: hydrometeorological time series and landscape attributes for 222 catchments in australia. *Earth System Science Data*, 13 (8):3847–3867, 2021. doi: 10.5194/essd-13-3847-2021. URL `https://essd.copernicus.org/articles/13/3847/2021/`.

Jean-Yves Franceschi, Aymeric Dieuleveut, and Martin Jaggi. Unsupervised scalable representation learning for multivariate time series. *Advances in neural information processing systems*, 32, 2019.

Joshua Green, Ivan D Haigh, Niall Quinn, Jeff Neal, Thomas Wahl, Melissa Wood, Dirk Eilander, Marleen de Ruiter, Philip Ward, and Paula Camus. A comprehensive review of coastal compound flooding literature. *arXiv preprint arXiv:2404.01321*, 2024.

Nate Gruver, Marc Finzi, Shikai Qiu, and Andrew Gordon Wilson. Large language models are zero-shot time series forecasters. In *Proceedings of the 37th International Conference on Neural Information Processing Systems*, NIPS '23, Red Hook, NY, USA, 2023. Curran Associates Inc.

Tao Han, Zhenghao Chen, Song Guo, Wanghan Xu, and Lei Bai. Cra5: Extreme compression of era5 for portable global climate and weather research via an efficient variational transformer. *arXiv preprint arXiv:2405.03376*, 2024a.

Tao Han, Song Guo, Zhenghao Chen, Wanghan Xu, and Lei Bai. How far are today's time-series models from real-world weather forecasting applications? *arXiv preprint arXiv:2406.14399*, 2024b.

Yukiko Hirabayashi, Roobavannan Mahendran, Sujan Koirala, Lisako Konoshima, Dai Yamazaki, Satoshi Watanabe, Hyungjun Kim, and Shinjiro Kanae. Global flood risk under climate change. *Nature climate change*, 3(9):816–821, 2013.

Sepp Hochreiter and Jürgen Schmidhuber. Long short-term memory. *Neural computation*, 9(8): 1735–1780, 1997.

R. Jane, L. Cadavid, J. Obeysekera, and T. Wahl. Multivariate statistical modelling of the drivers of compound flood events in south florida. *Natural Hazards and Earth System Sciences*, 20(10): 2681–2699, 2020. doi: 10.5194/nhess-20-2681-2020. URL `https://nhess.copernicus.org/articles/20/2681/2020/`.

Sheo Yon Jhin, Seojin Kim, and Noseong Park. Addressing prediction delays in time series forecasting: A continuous gru approach with derivative regularization. In *Proceedings of the 30th ACM SIGKDD Conference on Knowledge Discovery and Data Mining*, pp. 1234–1245, 2024.

Ming Jin, Shiyu Wang, Lintao Ma, Zhixuan Chu, James Y. Zhang, Xiaoming Shi, Pin-Yu Chen, Yuxuan Liang, Yuan-Fang Li, Shirui Pan, and Qingsong Wen. Time-LLM: Time series forecasting by reprogramming large language models. In *The Twelfth International Conference on Learning Representations*, 2024. URL https://openreview.net/forum?id=Unb5CVPtae.

Sebastiaan N Jonkman and Johannes K Vrijling. Loss of life due to floods. *Journal of flood risk management*, 1(1):43–56, 2008.

Syed Kabir, Sandhya Patidar, Xilin Xia, Qiuhua Liang, Jeffrey Neal, and Gareth Pender. A deep convolutional neural network model for rapid prediction of fluvial flood inundation. *Journal of Hydrology*, 590:125481, 2020.

Thomas N Kipf and Max Welling. Semi-supervised classification with graph convolutional networks. *arXiv preprint arXiv:1609.02907*, 2016.

Thomas N. Kipf and Max Welling. Semi-supervised classification with graph convolutional networks. In *International Conference on Learning Representations*, 2017. URL https://openreview.net/forum?id=SJU4ayYgl.

Nikolas Kirschstein and Yixuan Sun. The merit of river network topology for neural flood forecasting. In *International Conference on Machine Learning*, pp. 24713–24725. PMLR, 2024.

Christoph Klingler, Karsten Schulz, and Mathew Herrnegger. Lamah— large-sample data for hydrology and environmental sciences for central europe. *Earth System Science Data Discussions*, 2021:1–46, 2021.

Guokun Lai, Wei-Cheng Chang, Yiming Yang, and Hanxiao Liu. Modeling long-and short-term temporal patterns with deep neural networks. In *The 41st international ACM SIGIR conference on research & development in information retrieval*, pp. 95–104, 2018.

Yann LeCun, Léon Bottou, Yoshua Bengio, and Patrick Haffner. Gradient-based learning applied to document recognition. *Proceedings of the IEEE*, 86(11):2278–2324, 1998.

Shengsheng Lin, Weiwei Lin, Xinyi Hu, Wentai Wu, Ruichao Mo, and Haocheng Zhong. Cyclenet: Enhancing time series forecasting through modeling periodic patterns. In A. Globerson, L. Mackey, D. Belgrave, A. Fan, U. Paquet, J. Tomczak, and C. Zhang (eds.), *Advances in Neural Information Processing Systems*, volume 37, pp. 106315–106345. Curran Associates, Inc., 2024a. URL https://proceedings.neurips.cc/paper_files/paper/2024/file/bfe7998398779dde03cad7a73b1f81b6-Paper-Conference.pdf.

Shengsheng Lin, Weiwei Lin, Wentai Wu, Haojun Chen, and Junjie Yang. SparseTSF: Modeling long-term time series forecasting with *1k* parameters. In Ruslan Salakhutdinov, Zico Kolter, Katherine Heller, Adrian Weller, Nuria Oliver, Jonathan Scarlett, and Felix Berkenkamp (eds.), *Proceedings of the 41st International Conference on Machine Learning*, volume 235 of *Proceedings of Machine Learning Research*, pp. 30211–30226. PMLR, 21–27 Jul 2024b. URL https://proceedings.mlr.press/v235/lin24n.html.

Shizhan Liu, Hang Yu, Cong Liao, Jianguo Li, Weiyao Lin, Alex X. Liu, and Schahram Dustdar. Pyraformer: Low-complexity pyramidal attention for long-range time series modeling and forecasting. In *International Conference on Learning Representations*, 2022a. URL https://openreview.net/forum?id=0EXmFzUn5I.

Yijing Liu, Qinxian Liu, Jian-Wei Zhang, Haozhe Feng, Zhongwei Wang, Zihan Zhou, and Wei Chen. Multivariate time-series forecasting with temporal polynomial graph neural networks. In S. Koyejo, S. Mohamed, A. Agarwal, D. Belgrave, K. Cho, and A. Oh (eds.), *Advances in Neural Information Processing Systems*, volume 35, pp. 19414–19426. Curran Associates, Inc., 2022b. URL https://proceedings.neurips.cc/paper_files/paper/2022/file/7b102c908e9404dd040599c65db4ce3e-Paper-Conference.pdf.

Yong Liu, Tengge Hu, Haoran Zhang, Haixu Wu, Shiyu Wang, Lintao Ma, and Mingsheng Long. itransformer: Inverted transformers are effective for time series forecasting. In *The Twelfth International Conference on Learning Representations*, 2024a. URL `https://openreview.net/forum?id=JePfAI8fah`.

Yong Liu, Guo Qin, Xiangdong Huang, Jianmin Wang, and Mingsheng Long. Autotimes: Autoregressive time series forecasters via large language models. In *The Thirty-eighth Annual Conference on Neural Information Processing Systems*, 2024b. URL `https://openreview.net/forum?id=FOvZztnp1H`.

Zichuan Liu, Tianchun Wang, Jimeng Shi, Xu Zheng, Zhuomin Chen, Lei Song, Wenqian Dong, Jayantha Obeysekera, Farhad Shirani, and Dongsheng Luo. Timex++: Learning time-series explanations with information bottleneck. In *International Conference on Machine Learning*, pp. 32062–32082. PMLR, 2024c.

Ilya Loshchilov and Frank Hutter. Decoupled weight decay regularization. In *International Conference on Learning Representations*, 2019. URL `https://openreview.net/forum?id=Bkg6RiCqY7`.

Donghao Luo and Xue Wang. Moderntcn: A modern pure convolution structure for general time series analysis. In *The twelfth international conference on learning representations*, pp. 1–43, 2024.

Scott Miau and Wei-Hsi Hung. River flooding forecasting and anomaly detection based on deep learning. *Ieee Access*, 8:198384–198402, 2020.

Fabio Montello, Edoardo Arnaudo, and Claudio Rossi. Mmflood: A multimodal dataset for flood delineation from satellite imagery. *IEEE Access*, 10:96774–96787, 2022. doi: 10.1109/ACCESS.2022.3205419.

Yuqi Nie, Nam H Nguyen, Phanwadee Sinthong, and Jayant Kalagnanam. A time series is worth 64 words: Long-term forecasting with transformers. In *The Eleventh International Conference on Learning Representations*, 2023. URL `https://openreview.net/forum?id=Jbdc0vTOcol`.

Office of Resilience, South Florida Water Management District. Resiliency and flood protection, 2025. URL `https://www.sfwmd.gov/our-work/resiliency-and-flood-protection`.

Agnieszka I Olbert, Sogol Moradian, Stephen Nash, Joanne Comer, Bartosz Kazmierczak, Roger A Falconer, and Michael Hartnett. Combined statistical and hydrodynamic modelling of compound flooding in coastal areas-methodology and application. *Journal of Hydrology*, 620:129383, 2023.

Zijie Pan, Yushan Jiang, Sahil Garg, Anderson Schneider, Yuriy Nevmyvaka, and Dongjin Song. ^{2}ip-llm: Semantic space informed prompt learning with llm for time series forecasting. In *Forty-first International Conference on Machine Learning*, 2024.

Claudio Paniconi and Mario Putti. Physically based modeling in catchment hydrology at 50: Survey and outlook. *Water Resources Research*, 51(9):7090–7129, 2015.

Katerina Papagiannaki, Olga Petrucci, Michalis Diakakis, Vassiliki Kotroni, Luigi Aceto, Cinzia Bianchi, Rudolf Brázdil, Miquel Grimalt Gelabert, Moshe Inbar, Abdullah Kahraman, et al. Developing a large-scale dataset of flood fatalities for territories in the euro-mediterranean region, ffem-db. *Scientific data*, 9(1):166, 2022.

Yao Qin, Dongjin Song, Haifeng Chen, Wei Cheng, Guofei Jiang, and Garrison W Cottrell. A dual-stage attention-based recurrent neural network for time series prediction. In *Proceedings of the Twenty-Sixth International Joint Conference on Artificial Intelligence*, pp. 2627–2633. International Joint Conferences on Artificial Intelligence Organization, 2017.

Alec Radford, Jeffrey Wu, Rewon Child, David Luan, Dario Amodei, Ilya Sutskever, et al. Language models are unsupervised multitask learners. *OpenAI blog*, 1(8):9, 2019.

Maryam Rahnemoonfar, Tashnim Chowdhury, Argho Sarkar, Debvrat Varshney, Masoud Yari, and Robin Roberson Murphy. Floodnet: A high resolution aerial imagery dataset for post flood scene understanding. *IEEE Access*, 9:89644–89654, 2021. doi: 10.1109/ACCESS.2021.3090981.

Jannatul Ferdous Ruma, Mohammed Sarfaraz Gani Adnan, Ashraf Dewan, and Rashedur M. Rahman. Particle swarm optimization based lstm networks for water level forecasting: A case study on bangladesh river network. *Results in Engineering*, 17:100951, 2023. ISSN 2590-1230. doi: https://doi.org/10.1016/j.rineng.2023.100951. URL `https://www.sciencedirect.com/science/article/pii/S2590123023000786`.

David Salinas, Valentin Flunkert, Jan Gasthaus, and Tim Januschowski. Deepar: Probabilistic forecasting with autoregressive recurrent networks. *International journal of forecasting*, 36(3): 1181–1191, 2020.

Christopher C Sampson, Andrew M Smith, Paul D Bates, Jeffrey C Neal, Lorenzo Alfieri, and Jim E Freer. A high-resolution global flood hazard model. *Water resources research*, 51(9):7358–7381, 2015.

Antonia Sebastian. Chapter 7 - compound flooding. In Samuel Brody, Yoonjeong Lee, and Baukje Bee Kothuis (eds.), *Coastal Flood Risk Reduction*, pp. 77–88. Elsevier, 2022. ISBN 978-0-323-85251-7. doi: https://doi.org/10.1016/B978-0-323-85251-7.00007-X. URL `https://www.sciencedirect.com/science/article/pii/B978032385251700007X`.

Jimeng Shi, Vitalii Stebliankin, Zhaonan Wang, Shaowen Wang, and Giri Narasimhan. Graph transformer network for flood forecasting with heterogeneous covariates. *arXiv preprint arXiv:2310.07631*, 2023.

Jimeng Shi, Zeda Yin, Arturo Leon, Jayantha Obeysekera, and Giri Narasimhan. Fidlar: Forecast-informed deep learning architecture for flood mitigation. *arXiv preprint arXiv:2402.13371*, 2024.

Ashish Vaswani, Noam Shazeer, Niki Parmar, Jakob Uszkoreit, Llion Jones, Aidan N Gomez, Łukasz Kaiser, and Illia Polosukhin. Attention is all you need. *Advances in neural information processing systems*, 30, 2017.

Thomas Wahl, Shaleen Jain, Jens Bender, Steven D Meyers, and Mark E Luther. Increasing risk of compound flooding from storm surge and rainfall for major us cities. *Nature Climate Change*, 5 (12):1093–1097, 2015.

Huiqiang Wang, Jian Peng, Feihu Huang, Jince Wang, Junhui Chen, and Yifei Xiao. Micn: Multi-scale local and global context modeling for long-term series forecasting. In *The eleventh international conference on learning representations*, 2023.

Jingyuan Wang, Ze Wang, Jianfeng Li, and Junjie Wu. Multilevel wavelet decomposition network for interpretable time series analysis. In *Proceedings of the 24th ACM SIGKDD international conference on knowledge discovery & data mining*, pp. 2437–2446, 2018.

Shiyu Wang, Jiawei Li, Xiaoming Shi, Zhou Ye, Baichuan Mo, Wenze Lin, Shengtong Ju, Zhixuan Chu, and Ming Jin. Timemixer++: A general time series pattern machine for universal predictive analysis. *arXiv preprint arXiv:2410.16032*, 2024a.

Shiyu Wang, Haixu Wu, Xiaoming Shi, Tengge Hu, Huakun Luo, Lintao Ma, James Y. Zhang, and JUN ZHOU. Timemixer: Decomposable multiscale mixing for time series forecasting. In *The Twelfth International Conference on Learning Representations*, 2024b. URL `https://openreview.net/forum?id=7oLshfEIC2`.

Yuxuan Wang, Haixu Wu, Jiaxiang Dong, Guo Qin, Haoran Zhang, Yong Liu, Yunzhong Qiu, Jianmin Wang, and Mingsheng Long. Timexer: Empowering transformers for time series forecasting with exogenous variables. In *The Thirty-eighth Annual Conference on Neural Information Processing Systems*, 2024c. URL `https://openreview.net/forum?id=INAeUQ04lT`.

Oliver EJ Wing, William Lehman, Paul D Bates, Christopher C Sampson, Niall Quinn, Andrew M Smith, Jeffrey C Neal, Jeremy R Porter, and Carolyn Kousky. Inequitable patterns of us flood risk in the anthropocene. *Nature Climate Change*, 12(2):156–162, 2022.

Haixu Wu, Jiehui Xu, Jianmin Wang, and Mingsheng Long. Autoformer: decomposition transformers with auto-correlation for long-term series forecasting. In *Proceedings of the 35th International Conference on Neural Information Processing Systems*, pp. 22419–22430, 2021.

Haixu Wu, Tengge Hu, Yong Liu, Hang Zhou, Jianmin Wang, and Mingsheng Long. Timesnet: Temporal 2d-variation modeling for general time series analysis. In *The Eleventh International Conference on Learning Representations*, 2023. URL https://openreview.net/forum?id=ju_Uqw384Oq.

Zonghan Wu, Shirui Pan, Guodong Long, Jing Jiang, and Chengqi Zhang. Graph wavenet for deep spatial-temporal graph modeling, 2019. URL https://arxiv.org/abs/1906.00121.

Zonghan Wu, Shirui Pan, Guodong Long, Jing Jiang, Xiaojun Chang, and Chengqi Zhang. Connecting the dots: Multivariate time series forecasting with graph neural networks. In *Proceedings of the 26th ACM SIGKDD international conference on knowledge discovery & data mining*, pp. 753–763, 2020.

Kui Xu, Yunchao Zhuang, Lingling Bin, Chenyue Wang, and Fuchang Tian. Impact assessment of climate change on compound flooding in a coastal city. *Journal of Hydrology*, 617:129166, 2023.

Qingsong Xu, Yilei Shi, Jie Zhao, and Xiao Xiang Zhu. Floodcastbench: A large-scale dataset and foundation models for flood modeling and forecasting. *Scientific Data*, 12(1):431, 2025.

Wanghan Xu, Kang Chen, Tao Han, Hao Chen, Wanli Ouyang, and Lei Bai. Extremecast: Boosting extreme value prediction for global weather forecast. *arXiv preprint arXiv:2402.01295*, 2024.

Kun Yi, Qi Zhang, Wei Fan, Hui He, Liang Hu, Pengyang Wang, Ning An, Longbing Cao, and Zhendong Niu. Fouriergnn: rethinking multivariate time series forecasting from a pure graph perspective. In *Proceedings of the 37th International Conference on Neural Information Processing Systems*, NIPS '23, Red Hook, NY, USA, 2023. Curran Associates Inc.

Jie Yin, Yao Gao, Ruishan Chen, Dapeng Yu, Robert Wilby, Nigel Wright, Yong Ge, Jeremy Bricker, Huili Gong, and Mingfu Guan. Flash floods: why are more of them devastating the world's driest regions? *Nature*, 615(7951):212–215, 2023a.

Zeda Yin, Linglong Bian, Beichao Hu, Jimeng Shi, and Arturo S Leon. Physic-informed neural network approach coupled with boundary conditions for solving 1d steady shallow water equations for riverine system. In *World Environmental and Water Resources Congress 2023*, pp. 280–288, 2023b.

Zhihan Yue, Yujing Wang, Juanyong Duan, Tianmeng Yang, Congrui Huang, Yunhai Tong, and Bixiong Xu. Ts2vec: Towards universal representation of time series. In *Proceedings of the AAAI conference on artificial intelligence*, volume 36, pp. 8980–8987, 2022.

Shuaihong Zang, Zhijia Li, Ke Zhang, Cheng Yao, Zhiyu Liu, Jingfeng Wang, Yingchun Huang, and Sheng Wang. Improving the flood prediction capability of the xin'anjiang model by formulating a new physics-based routing framework and a key routing parameter estimation method. *Journal of Hydrology*, 603:126867, 2021.

Ailing Zeng, Muxi Chen, Lei Zhang, and Qiang Xu. Are transformers effective for time series forecasting? In *Proceedings of the AAAI conference on artificial intelligence*, volume 37, pp. 11121–11128, 2023.

Daochen Zha, Zaid Pervaiz Bhat, Kwei-Herng Lai, Fan Yang, Zhimeng Jiang, Shaochen Zhong, and Xia Hu. Data-centric artificial intelligence: A survey. *ACM Computing Surveys*, 57(5):1–42, 2025.

Haoyi Zhou, Shanghang Zhang, Jieqi Peng, Shuai Zhang, Jianxin Li, Hui Xiong, and Wancai Zhang. Informer: Beyond efficient transformer for long sequence time-series forecasting. In *The Thirty-Fifth AAAI Conference on Artificial Intelligence, AAAI 2021, Virtual Conference*, volume 35, pp. 11106–11115. AAAI Press, 2021a.

Haoyi Zhou, Shanghang Zhang, Jieqi Peng, Shuai Zhang, Jianxin Li, Hui Xiong, and Wancai Zhang. Informer: Beyond efficient transformer for long sequence time-series forecasting. In *Proceedings of the AAAI conference on artificial intelligence*, volume 35, pp. 11106–11115, 2021b.

Tian Zhou, Ziqing Ma, Qingsong Wen, Xue Wang, Liang Sun, and Rong Jin. Fedformer: Frequency enhanced decomposed transformer for long-term series forecasting. In *International conference on machine learning*, pp. 27268–27286. PMLR, 2022.

Tian Zhou, Peisong Niu, Xue Wang, Liang Sun, and Rong Jin. One fits all: power general time series analysis by pretrained lm. In *Proceedings of the 37th International Conference on Neural Information Processing Systems*, NIPS '23, Red Hook, NY, USA, 2023. Curran Associates Inc.

CONTENTS

A DETAILED INFORMATION OF SF^{2}BENCH

We provide the detailed information about the number of monitor stations in each split in Table 7. In each split, the number of water monitor stations is more than other kinds of features, which means the water level feature is the main information and others are additional parts.

Table 7: The summary of the all splits in SF^{2}Bench

Splits	Time Span	Interval	Water	Groundwater	Rainfall	Pump	Gate
S0	1985-1990	1 Hour	159	40	143	17	82
S1	1990-1995	1 Hour	227	36	139	18	104
S2	1995-2000	1 Hour	332	44	170	26	94
S3	2000-2005	1 Hour	402	178	227	31	107
S4	2005-2010	1 Hour	518	296	254	48	172
S5	2010-2015	1 Hour	585	333	216	65	256
S6	2015-2020	1 Hour	670	317	186	85	300
S7	2020-2024	1 Hour	716	352	194	89	329

We also provide the geographical distribution information of monitor stations in different splits in Figure 6. As time goes by, the number of monitoring stations gradually increases, and in terms of spatial distribution, the locations of monitoring stations remain consistent.

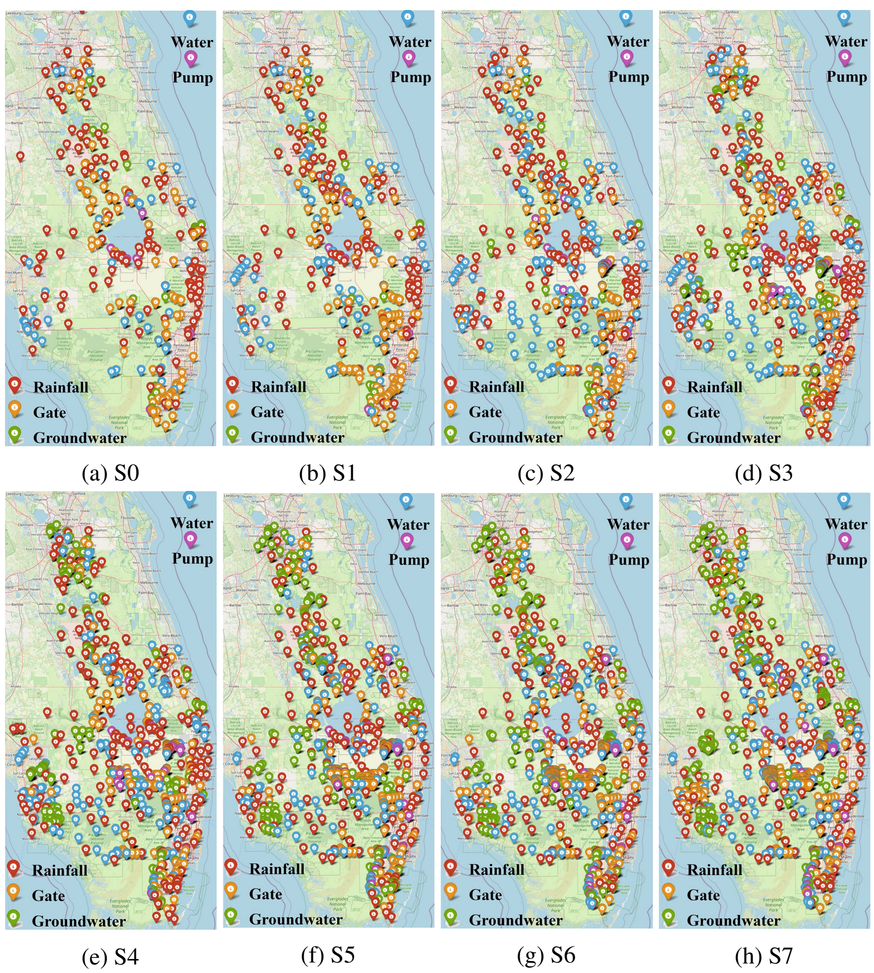

(a) S0 (b) S1 (c) S2 (d) S3

(e) S4 (f) S5 (g) S6 (h) S7

Figure 6: The location distribution in each split.

In addition, we visualize the temporal pattern of features over a year in each split. As shown in Figure 7, 8, 9, and 10, the temporal patterns in 8 splits are similar and consistent. From the view of the climate, the dry and rainy seasons are highly consistentm but the intensity of rainfall in different splits is different. These patterns that are highly aligned with the actual situation demonstrate the quality of the dataset.

B EXPERIMENTAL DETAILS

B.1 DATA PREPROCESSING

Normalization. To make the data have a zero mean and unit variance, we follow (Franceschi et al., 2019; Zhou et al., 2021b; Yue et al., 2022) using z-score to normalize the time series data. For the time series, whose variance is less than 1E-4, we regard its variance as one to avoid the variable overflow(inf or NaN). For forecasting tasks, all the report metrics are based on the normalized data.

Timestamp Features. Because of some methods, such as NLinear, we do not consider extracting the timestamp feature as part of the input. For those methods that are capable of handling the timestamp feature, we ignore this part. In our code, we also provide timestamp features extracted by following (Zhou et al., 2021b; Yue et al., 2022) for further works.

B.2 METHODS

MLP. We implement a classical three-layer MLP with ReLU as the activation function. The input layer dimension is determined by the input sequence length, and the output layer dimension corresponds to the forecast horizon. The hidden layer dimension is 64. For training, the learning rate is 1×10^{-4}, weight decay is 1×10^{-6}, and the batch size is 64. The model is trained for 15 epochs.
NLinear (Zeng et al., 2023). This is a simple linear model that treats each time series independently, modeling future values using a linear transformation of the most recent input values. Implementation is based on the NeuralForecast library[6]. The learning rate is 1×10^{-4}, weight decay is 1×10^{-6}, batch size is 64, and training is performed for 50 epochs.
TSMixer (Chen et al., 2023). Inspired by MLP-Mixer models from vision tasks, TSMixer is a neural network architecture for time series forecasting. It alternately applies MLPs along the time and feature axes, learning dependencies across both dimensions without requiring attention mechanisms or complex sequence modeling. Implementation follows the NeuralForecast default settings. The architecture includes 2 mixing layers, and the second feed-forward layer has 64 units. The learning rate is 1×10^{-4}, batch size is 32, and the model is trained for 10 epochs.
TCN (Bai et al., 2018). It incorporates causal convolutions, ensuring predictions depend only on current and past inputs, thus preserving temporal order. They also utilize dilated convolutions to efficiently capture long-range dependencies by expanding the receptive field without significantly increasing layers. Our implementation follows the official code[7] using the popular channel-wise setting. It employs a three-layer backbone with a kernel size of 3 and a fixed dilation of 1. The learning rate is 1×10^{-3}, weight decay is 1×10^{-7}, batch size is 256, and training is performed for 50 epochs.
ModernTCN (Luo & Wang, 2024). ModernTCN introduces a streamlined, fully convolutional architecture that aims to simplify design while enhancing performance. It incorporates components like depth-wise separable convolutions and Gated Linear Units (GLUs) to efficiently capture local and long-range temporal dependencies. Implementation follows the long-term forecasting settings from the source code[8], using the Weather dataset hyperparameters as defaults. The learning rate is 1×10^{-4}, batch size is 256, and the model is trained for 100 epochs.
TimesNet (Wu et al., 2023). TimesNet models temporal variations in a two-dimensional space by reshaping time series data into a pseudo-image format and applying 2D convolutional techniques. This enables it to capture both short-term dynamics and long-term dependencies. Implementation uses the Time-Series-Library[9], with default hyperparameters from the long-term forecasting setting for the Weather dataset. The learning rate is 1×10^{-4}, batch size is 32, and training is performed for

[6]`https://github.com/Nixtla/neuralforecast`
[7]`https://github.com/locuslab/TCN/tree/master`
[8]`https://github.com/luodhhh/ModernTCN`
[9]`https://github.com/thuml/Time-Series-Library`

10 epochs.

LSTM (Hochreiter & Schmidhuber, 1997). Our Long Short-Term Memory (LSTM) implementation is a two-layer model with a hidden dimension of 32. The learning rate is 1×10^{-3}, weight decay is 1×10^{-6}, batch size is 64, and the model is trained for 50 epochs.

DeepAR (Salinas et al., 2020). DeepAR is a global model trained on multiple related time series, which aids generalization, especially for series with limited history. It employs an RNN architecture to predict future values by modeling the conditional distribution of the next value given past observations. Implementation is based on the NeuralForecast library. The learning rate is 1×10^{-3}, batch size is 64, and training is performed for 20 epochs.

DilatedRNN (Chang et al., 2017). Dilated RNNs exponentially expand their receptive field by stacking layers with different dilation factors, allowing efficient capture of short- and long-range patterns without a drastic increase in parameters. This makes them suitable for forecasting tasks with wide-ranging temporal dependencies. Implementation is based on the NeuralForecast library. The learning rate is 1×10^{-3}, batch size is 64, and training is performed for 40 epochs.

GCN (Kipf & Welling, 2017). The GCN architecture consists of two layers with a hidden dimension of 32. The graph topology is derived from location information using Delaunay triangulation[10]. The learning rate is 1×10^{-4}, weight decay is 1×10^{-5}, batch size is 32, and the model is trained for 50 epochs.

FourierGNN (Yi et al., 2023). FourierGNN leverages graph neural networks and Fourier transforms to capture temporal and inter-variable dependencies. Time series variables are treated as graph nodes, with edges representing their relationships. Fourier transforms project data into the frequency domain to model periodic and long-range dependencies. Implementation follows the source code[11]. The learning rate is 1×10^{-5}, batch size is 32, and training is performed for 100 epochs.

StemGNN (Cao et al., 2020). StemGNN is designed to capture both temporal (via temporal convolutions) and spatial (via spectral graph convolutions) dependencies in time-series data, learning smooth representations over the graph structure and dynamic patterns. Implementation follows the source code[12]. The learning rate is 1×10^{-4}, batch size is 32, and the model is trained for 50 epochs.

iTransformer (Liu et al., 2024a). The iTransformer uses an encoder-decoder structure where the encoder processes the sequence in reverse order. This allows the decoder to predict future values based on this processed representation, enhancing focus on relevant temporal sequences while mitigating the computational cost of traditional transformers. Implementation is based on the NeuralForecast library. The learning rate is 1×10^{-4}, batch size is 32, and training is performed for 10 epochs.

PatchTST (Nie et al., 2023). PatchTST is a Transformer-based architecture employing patching and channel independence. Time series are divided into patches, which are transformed into tokens and processed by a transformer model to capture local and global dependencies via self-attention. This is particularly useful for long-term forecasting. Implementation is based on the NeuralForecast library. The learning rate is 1×10^{-4}, batch size is 128, and training is performed for 100 epochs.

GPT4TS (Zhou et al., 2023). GPT4TS treats time series as a language, leveraging pretrained language models (LLMs) to learn temporal patterns. Time series data is tokenized for LLM processing, enabling zero-shot or few-shot generalization. Implementation follows the source code[13], using long-term forecasting settings for the Weather dataset as default hyperparameters. The default language model is GPT-2 (Radford et al., 2019). The learning rate is 1×10^{-4}, batch size is 64, and training is performed for 10 epochs.

AutoTimes (Liu et al., 2024b). AutoTimes projects time series segments into the embedding space of language tokens, leveraging the autoregressive capabilities of LLMs for forecasting. By training the model to predict subsequent time series segments given preceding ones, AutoTimes generates multi-step forecasts. Implementation follows the source code[14], with GPT-2 (Radford et al., 2019) as the language model. The learning rate is 5×10^{-4}, batch size is 64, and training is performed for 10 epochs.

For all benchmark experiments, AdamW (Loshchilov & Hutter, 2019) is used as the optimizer, and the loss function is Mean Squared Error (MSE).

[10] `https://docs.scipy.org/doc/scipy/reference/generated/scipy.spatial.Delaunay.html`

[11] `https://github.com/aikunyi/FourierGNN`

[12] `https://github.com/microsoft/StemGNN`

[13] `https://github.com/DAMO-DI-ML/NeurIPS2023-One-Fits-All`

[14] `https://github.com/thuml/AutoTimes/tree/main`

B.3 Platform

All experiments are conducted on two Linux machines, one with 8 NVIDIA A100 GPUs, each with 40GB of memory, and another with 4 RTX 4090 GPUs. We used Python 3.12.9 and Pytorch 2.6.0 to construct our project.

C Detailed Results

C.1 Detailed Benchmark Results

In Section 4.5, we report the average of our benchmark results. In this section, we report the detailed results, including MSE, MAE, and three SEDI values on different prediction lengths, on three interest areas(Orlando, Miami, and Fort Myers) from Table 8 to 37. The best average results are presented in bold font, while the second-best are underlined. Furthermore, from Table 38 to 42, we report the detailed results of basic methods on the whole dataset. To provide qualitative analysis, from Figure 11 to 16, we demonstrate the case visualization of each method on the S7 split in the Orlando area.

C.2 Detailed Other Results

To provide more information about the ablation study, we report the detailed results of the factor ablation study in Table 43 to 45. We report the average results on three interest areas on the S6 split. For the spatial and temporal information ablation study, the results are available from Table 46 to 49.

D Limitations

While SF^{2}Bench provides five key factors, it currently lacks explicit topological linkage information between monitoring stations due to the intricate nature of South Florida's water system. Although we provide some flood observation data, the locations of these observations may not directly correspond to our monitoring stations. Therefore, this information is provided in a separate file rather than being integrated into the time series data.

E LLM Usage

In this paper, we leverage LLMs, including ChatGPT and Gemini 2.5 Pro, to refine sentence-level writing.

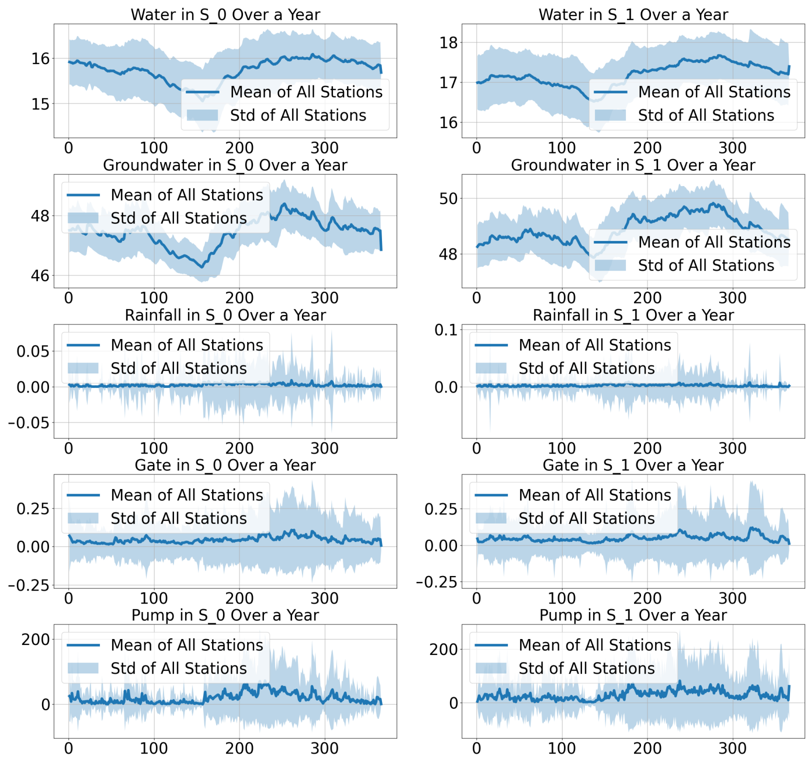

(a) S0 (b) S1

Figure 7: The temporal pattern of features of S0 and S1.

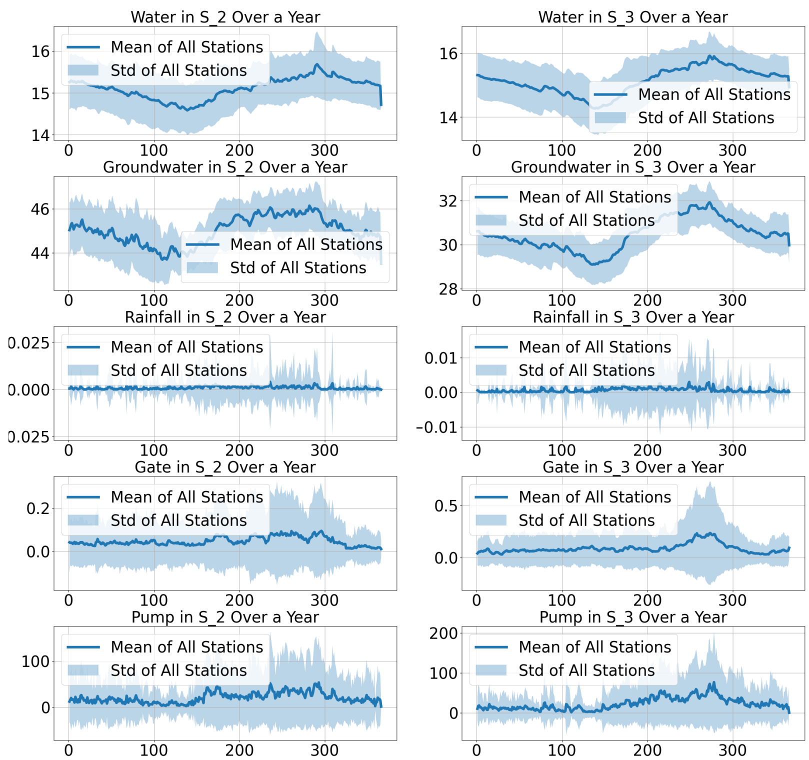

(a) S2 (b) S3

Figure 8: The temporal pattern of features of S2 and S3.

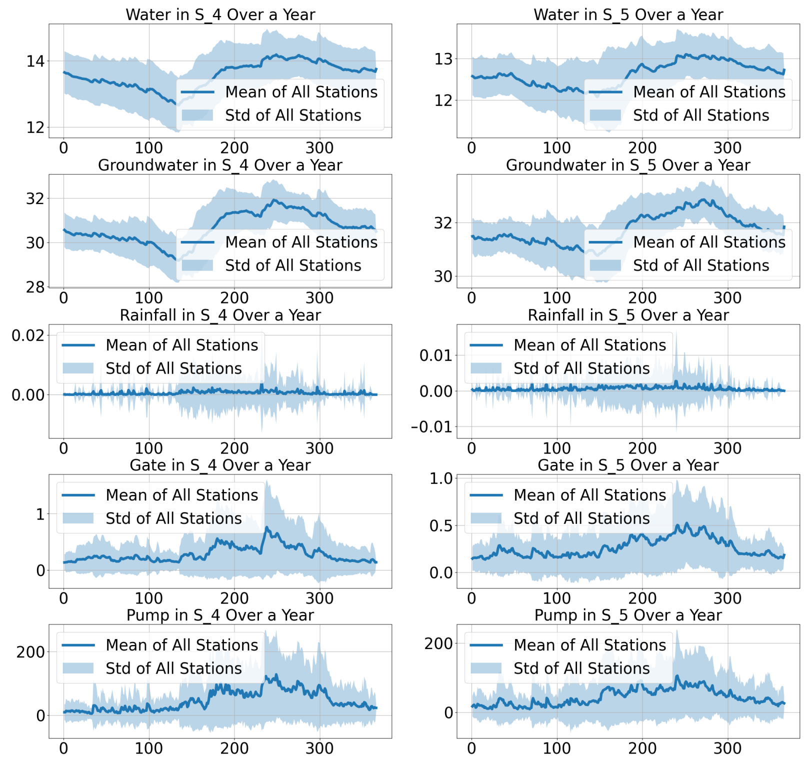

(a) S4 (b) S5

Figure 9: The temporal pattern of features of S4 and S5.

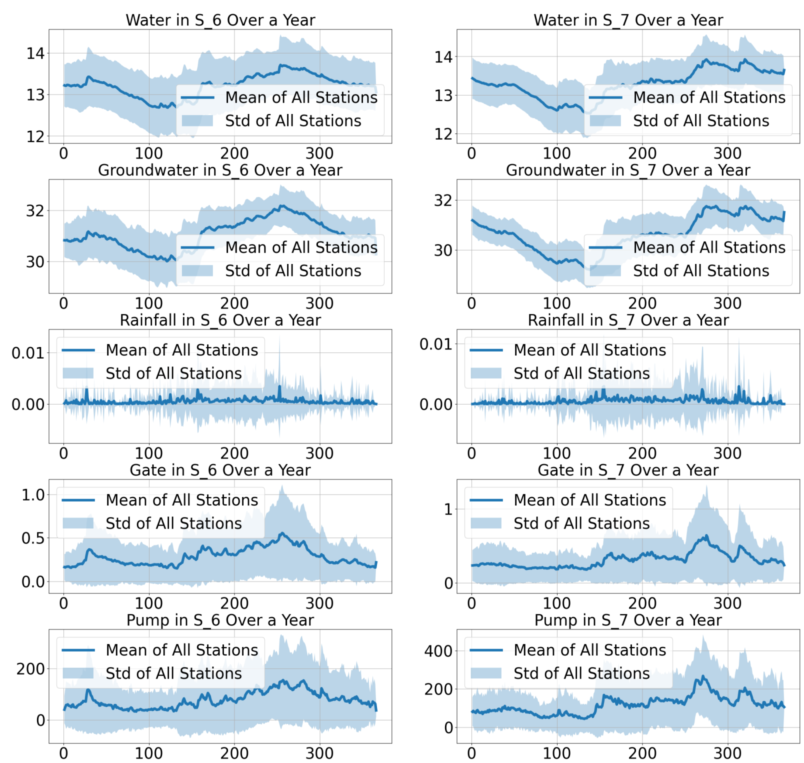

(a) S6 (b) S7

Figure 10: The temporal pattern of features of S6 and S7.

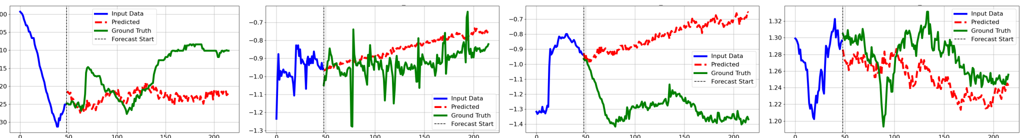

(a) MLP on ALLI (b) MLP on G103_T (c) MLP on S57_T (d) MLP on S60_H

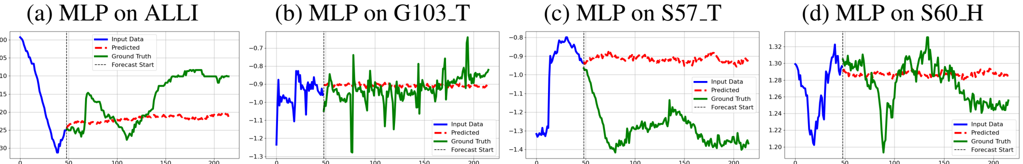

(e) TSMixer on ALLI (f) TSMixer on G103_T (g) TSMixer on S57_T (h) TSMixer on S60_H

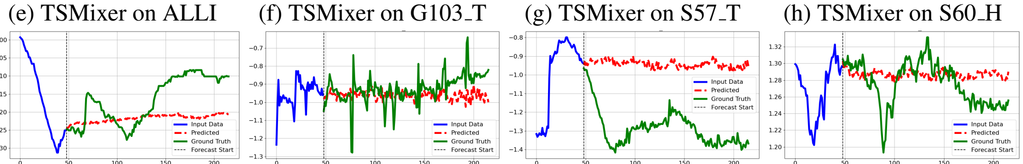

(i) NLinear on ALLI (j) NLinear on G103_T (k) NLinear on S57_T (l) NLinear on S60_H

Figure 11: Cases visualization of MLP-based architecture methods on S7(Orlando area).

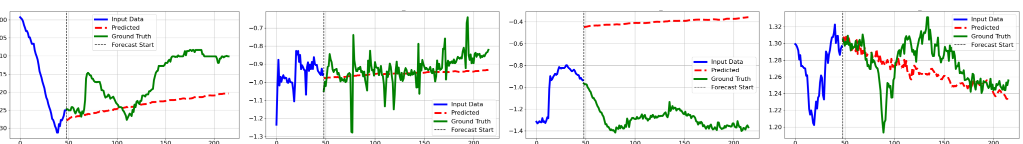

(a) TCN on ALLI (b) TCN on G103_T (c) TCN on S57_T (d) TCN on S60_H

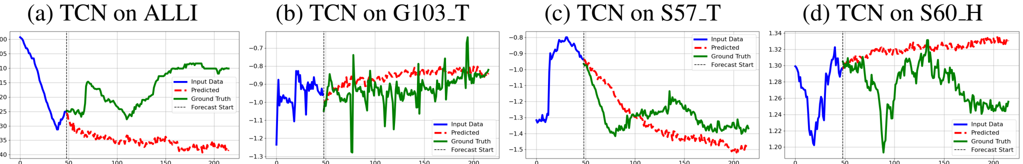

(e) Modern. on ALLI (f) Modern. on G103_T (g) Modern. on S57_T (h) Modern. on S60_H

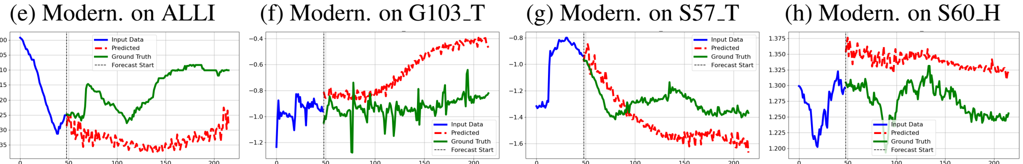

(i) TimesNet on ALLI (j) TimesNet on G103_T (k) TimesNet on S57_T (l) TimesNet on S60_H

Figure 12: Cases visualization of CNN-based architecture methods on S7(Orlando area). Modern. means ModernTCN.

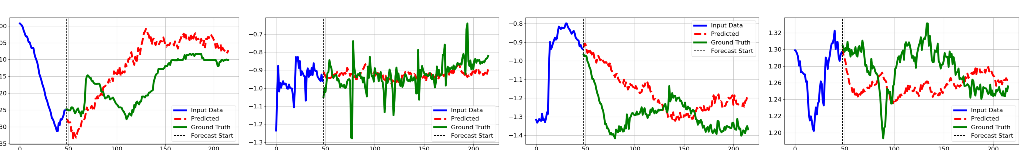

(a) iTrans. on ALLI (b) iTrans. on G103_T (c) iTrans. on S57_T (d) iTrans. on S60_H

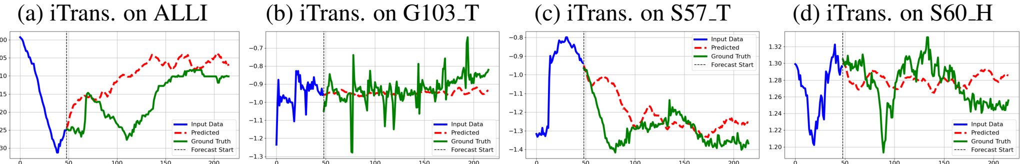

(e) PatchTST on ALLI (f) PatchTST on G103_T (g) PatchTST on S57_T (h) PatchTST on S60_H

Figure 13: Cases visualization of Transformer-based architecture methods on S7(Orlando area). iTrans. means iTransformer.

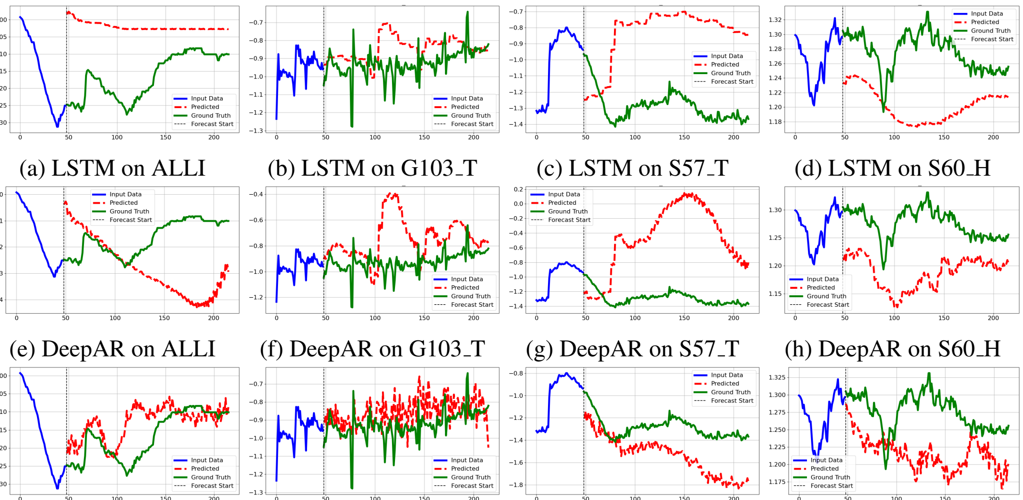

(a) LSTM on ALLI (b) LSTM on G103_T (c) LSTM on S57_T (d) LSTM on S60_H

(e) DeepAR on ALLI (f) DeepAR on G103_T (g) DeepAR on S57_T (h) DeepAR on S60_H

(i) DilatedRNN on ALLI (j) Dilated. on G103_T (k) Dilated. on S57_T (l) Dilated. on S60_H

Figure 14: Cases visualization of RNN-based architecture methods on S7(Orlando area). Dilated. means DilatedRNN.

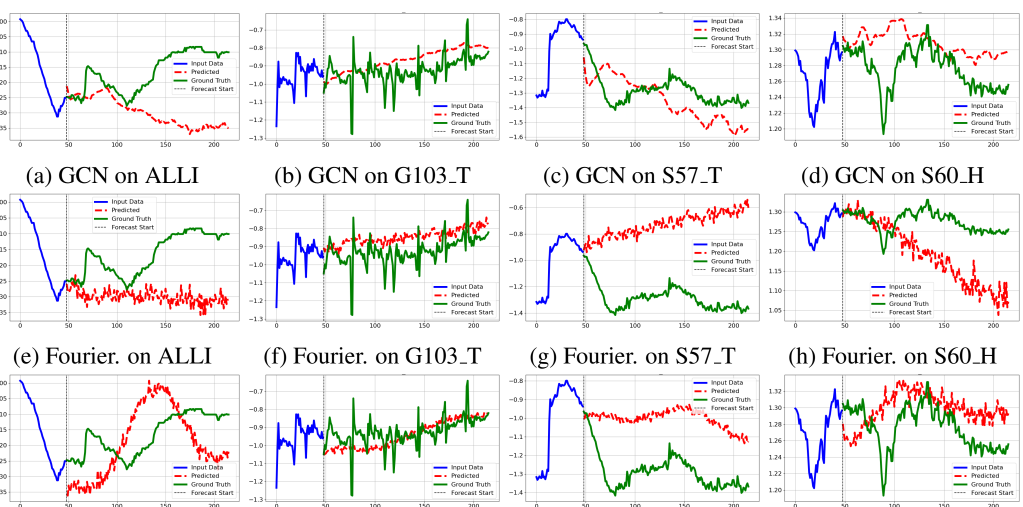

(a) GCN on ALLI (b) GCN on G103_T (c) GCN on S57_T (d) GCN on S60_H

(e) Fourier. on ALLI (f) Fourier. on G103_T (g) Fourier. on S57_T (h) Fourier. on S60_H

(i) StemGNN on ALLI (j) StemGNN on G103_T (k) StemGNN on S57_T (l) StemGNN on S60_H

Figure 15: Cases visualization of GNN-based architecture methods on S7(Orlando area). Fourier. means FourierGNN.

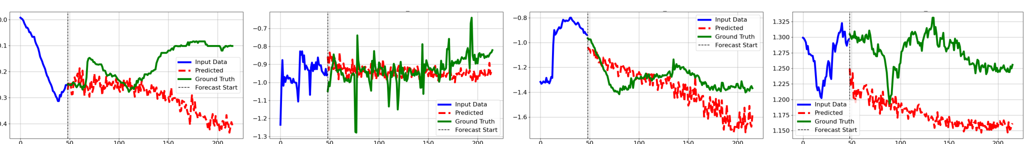

(a) GPT4TS on ALLI (b) GPT4TS on G103_T (c) GPT4TS on S57_T (d) GPT4TS on S60_H

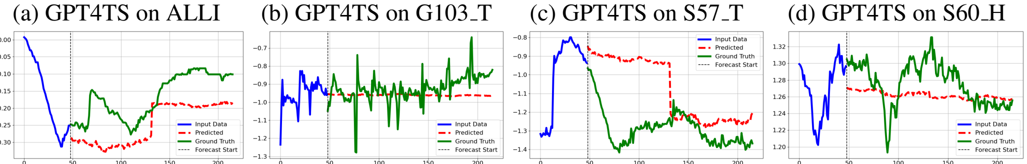

(e) AutoTimes on ALLI (f) AutoTimes on G103_T (g) AutoTimes on S57_T (h) AutoTimes on S60_H

Figure 16: Cases visualization of LLM-based architecture methods on S7(Orlando area). Dilated. means DilatedRNN.

Table 8: Benchmark(MAE) on part 1(Orlando area) stations(MLP,CNN,Transformer)

	Method	T	S0	S1	S2	S3	S4	S5	S6	S7	Avg.
MLP	MLP	1D	0.0915	0.1229	0.0679	0.0810	0.0716	0.0691	0.0598	0.0846	0.0810
		3D	0.1424	0.1928	0.1167	0.1437	0.1174	0.1154	0.1086	0.1314	0.1335
		5D	0.1746	0.2472	0.1607	0.1844	0.1503	0.1529	0.1418	0.1718	0.1730
		7D	0.1919	0.2899	0.1848	0.2244	0.1750	0.1793	0.1753	0.1970	0.2022
		Avg.	0.1501	0.2132	0.1325	0.1584	0.1286	**0.1292**	0.1214	0.1462	0.1474
	TSMixer	1D	0.1046	0.1355	0.0812	0.0846	0.0767	0.0778	0.1184	0.1015	0.0975
		3D	0.1494	0.2140	0.1252	0.1378	0.1185	0.1219	0.1500	0.1458	0.1453
		5D	0.1769	0.2673	0.1595	0.1783	0.1496	0.1547	0.1751	0.1798	0.1802
		7D	0.1938	0.3093	0.1892	0.2120	0.1765	0.1819	0.2098	0.2096	0.2103
		Avg.	0.1562	0.2315	0.1388	0.1532	0.1303	0.1341	0.1633	0.1592	0.1583
	NLinear	1D	0.0980	0.1279	0.0777	0.0820	0.0771	0.0741	0.0640	0.0929	0.0867
		3D	0.1475	0.2109	0.1234	0.1390	0.1207	0.1211	0.1079	0.1415	0.1390
		5D	0.1835	0.2663	0.1584	0.1814	0.1527	0.1541	0.1422	0.1763	0.1769
		7D	0.1964	0.3085	0.1891	0.2161	0.1803	0.1814	0.1711	0.2065	0.2062
		Avg.	0.1563	0.2284	0.1371	0.1546	0.1327	0.1327	0.1213	0.1543	0.1522
CNN	TCN	1D	0.1887	0.1417	0.2145	0.3830	0.1322	0.0889	0.1164	0.1913	0.1821
		3D	0.1588	0.2302	0.1857	0.4058	0.1968	0.1359	0.1471	0.2127	0.2091
		5D	0.2110	0.3028	0.2139	0.4483	0.2128	0.1928	0.2024	0.2579	0.2552
		7D	0.2135	0.3379	0.2605	0.5715	0.2686	0.2052	0.2102	0.2695	0.2921
		Avg.	0.1930	0.2532	0.2186	0.4522	0.2026	0.1557	0.1690	0.2329	0.2346
	ModernTCN	1D	0.0893	0.1238	0.0721	0.0760	0.0704	0.0661	0.0588	0.0802	0.0796
		3D	0.1486	0.2113	0.1366	0.1450	0.1212	0.1162	0.1073	0.1324	0.1398
		5D	0.1886	0.2685	0.1798	0.1887	0.1632	0.1537	0.1426	0.1697	0.1818
		7D	0.2140	0.3228	0.2240	0.2310	0.1936	0.1833	0.1728	0.2002	0.2177
		Avg.	0.1601	0.2316	0.1531	0.1602	0.1371	0.1298	0.1204	0.1456	0.1547
	TimesNet	1D	0.1068	0.1436	0.0805	0.0909	0.0919	0.0925	0.0787	0.1051	0.0987
		3D	0.1558	0.2190	0.1252	0.1515	0.1382	0.1402	0.1254	0.1582	0.1517
		5D	0.1813	0.2745	0.1637	0.1933	0.1735	0.1766	0.1578	0.1958	0.1896
		7D	0.2034	0.3222	0.2025	0.2309	0.2102	0.2146	0.1886	0.2263	0.2248
		Avg.	0.1618	0.2398	0.1430	0.1666	0.1534	0.1560	0.1376	0.1714	0.1662
Transformer	iTransformer	1D	0.0865	0.1227	0.0645	0.0730	0.0710	0.0700	0.0629	0.0889	0.0799
		3D	0.1395	0.1963	0.1103	0.1313	0.1193	0.1195	0.1058	0.1376	0.1325
		5D	0.1717	0.2546	0.1471	0.1723	0.1534	0.1528	0.1401	0.1775	0.1712
		7D	0.1889	0.2962	0.1801	0.2068	0.1833	0.1830	0.1708	0.2048	0.2017
		Avg.	0.1466	0.2175	0.1255	0.1459	0.1317	0.1313	0.1199	0.1522	0.1463
	PatchTST	1D	0.0843	0.1148	0.0638	0.0678	0.0711	0.0693	0.0617	0.0858	0.0773
		3D	0.1365	0.1922	0.1113	0.1269	0.1149	0.1199	0.1046	0.1362	0.1303
		5D	0.1677	0.2451	0.1471	0.1728	0.1489	0.1569	0.1409	0.1718	0.1689
		7D	0.1866	0.2927	0.1787	0.2054	0.1786	0.1859	0.1679	0.2019	0.1997
		Avg.	**0.1438**	**0.2112**	**0.1252**	**0.1432**	**0.1284**	0.1330	**0.1188**	0.1489	**0.1441**

Table 9: Benchmark(MAE) on part 1(Orlando area) stations(RNN,GNN,LLM)

	Method	T	S0	S1	S2	S3	S4	S5	S6	S7	Avg.
RNN	LSTM	1D	0.1275	0.1790	0.0935	0.1714	0.1044	0.1032	0.0865	0.1211	0.1233
		3D	0.1652	0.2751	0.1431	0.2458	0.1518	0.1528	0.1481	0.1647	0.1808
		5D	0.1972	0.3297	0.1801	0.2977	0.1871	0.1891	0.1784	0.1985	0.2197
		7D	0.2139	0.3517	0.2277	0.3351	0.2198	0.2143	0.1978	0.2266	0.2484
		Avg.	0.1759	0.2839	0.1611	0.2625	0.1658	0.1648	0.1527	0.1777	0.1931
	DeepAR	1D	0.1209	0.1855	0.0946	0.1726	0.1024	0.0971	0.0881	0.1171	0.1223
		3D	0.1667	0.2677	0.1488	0.2465	0.1534	0.1620	0.1421	0.1736	0.1826
		5D	0.1942	0.3110	0.1907	0.3237	0.1889	0.1828	0.1770	0.2045	0.2216
		7D	0.2146	0.3522	0.2210	0.3619	0.2122	0.2197	0.2123	0.2317	0.2532
		Avg.	0.1741	0.2791	0.1638	0.2762	0.1642	0.1654	0.1548	0.1817	0.1949
	DilatedRNN	1D	0.0939	0.1317	0.0700	0.1552	0.0836	0.0748	0.0672	0.1006	0.0971
		3D	0.1499	0.2318	0.1249	0.2031	0.1339	0.1318	0.1224	0.1457	0.1554
		5D	0.1794	0.2793	0.1627	0.2897	0.1678	0.1635	0.1520	0.1809	0.1969
		7D	0.2110	0.3329	0.1959	0.3061	0.1990	0.1945	0.1931	0.1478	0.2225
		Avg.	0.1586	0.2439	0.1384	0.2385	0.1461	0.1411	0.1337	**0.1437**	0.1680
GNN	GCN	1D	0.1003	0.2139	0.1034	0.3710	0.1030	0.1005	0.0775	0.0962	0.1457
		3D	0.1543	0.3137	0.1411	0.3384	0.1524	0.1517	0.1208	0.1392	0.1889
		5D	0.1862	0.3741	0.1665	0.4935	0.1893	0.1818	0.1610	0.1732	0.2407
		7D	0.2034	0.4156	0.1912	0.5967	0.2153	0.2073	0.1927	0.2024	0.2781
		Avg.	0.1610	0.3293	0.1505	0.4499	0.1650	0.1603	0.1380	0.1528	0.2134
	FourierGNN	1D	0.0985	0.1324	0.0796	0.1337	0.0863	0.0929	0.0672	0.0927	0.0979
		3D	0.1445	0.2034	0.1178	0.2733	0.1295	0.1246	0.1125	0.1392	0.1556
		5D	0.1746	0.2644	0.1524	0.3672	0.1712	0.1640	0.1513	0.1719	0.2021
		7D	0.1918	0.3028	0.1936	0.4107	0.1992	0.2019	0.1871	0.2068	0.2367
		Avg.	0.1523	0.2257	0.1358	0.2962	0.1466	0.1459	0.1295	0.1527	0.1731
	StemGNN	1D	0.1270	0.1782	0.0786	0.6896	0.1005	0.0833	0.0741	0.0969	0.1785
		3D	0.1717	0.3602	0.1536	0.6742	0.1778	0.1720	0.1498	0.1715	0.2539
		5D	0.2081	0.4895	0.2141	1.4591	0.2144	0.2729	0.2258	0.2412	0.4156
		7D	0.2477	0.5122	0.2577	1.4988	0.2552	0.3307	0.2486	0.2419	0.4491
		Avg.	0.1886	0.3850	0.1760	1.0804	0.1870	0.2147	0.1746	0.1879	0.3243
LLM	GPT4TS	1D	0.1050	0.1372	0.0833	0.0934	0.0905	0.0898	0.0778	0.1106	0.0984
		3D	0.1530	0.2169	0.1221	0.1502	0.1335	0.1380	0.1222	0.1547	0.1488
		5D	0.1817	0.2650	0.1565	0.1928	0.1666	0.1723	0.1559	0.1948	0.1857
		7D	0.1967	0.3105	0.1930	0.2294	0.1969	0.2054	0.1962	0.2224	0.2188
		Avg.	0.1591	0.2324	0.1387	0.1664	0.1469	0.1514	0.1380	0.1706	0.1629
	AutoTimes	1D	0.0967	0.1369	0.0747	0.0770	0.0768	0.0784	0.0660	0.0963	0.0878
		3D	0.1453	0.2057	0.1196	0.1296	0.1164	0.1203	0.1099	0.1409	0.1360
		5D	0.1733	0.2664	0.1499	0.1751	0.1498	0.1534	0.1411	0.1739	0.1729
		7D	0.1902	0.3029	0.1814	0.2113	0.1780	0.1823	0.1691	0.2032	0.2023
		Avg.	0.1514	0.2280	0.1314	0.1482	0.1302	0.1336	0.1215	0.1536	0.1497

Table 10: Benchmark(MSE) on part 1(Orlando area) stations(MLP,CNN,Transformer)

	Method	T	S0	S1	S2	S3	S4	S5	S6	S7	Avg.
MLP	MLP	1D	0.1472	0.1254	0.0376	0.0610	0.0379	0.0275	0.0248	0.0523	0.0642
		3D	0.2661	0.2014	0.0621	0.1232	0.0681	0.0536	0.0465	0.0913	0.1140
		5D	0.3569	0.2609	0.0875	0.1714	0.0999	0.0772	0.0670	0.1226	0.1554
		7D	0.2963	0.3124	0.1097	0.2215	0.1199	0.0975	0.0871	0.1498	0.1743
		Avg.	0.2666	**0.2250**	**0.0742**	0.1443	**0.0814**	**0.0640**	**0.0564**	0.1040	**0.1270**
	TSMixer	1D	0.1649	0.1283	0.0423	0.0696	0.0380	0.0312	0.0661	0.0633	0.0755
		3D	0.2915	0.2214	0.0679	0.1255	0.0694	0.0575	0.0862	0.1000	0.1274
		5D	0.1769	0.2903	0.0936	0.1673	0.0981	0.0812	0.1010	0.1325	0.1626
		7D	0.2817	0.3469	0.1190	0.2048	0.1248	0.1031	0.1384	0.1644	0.1854
		Avg.	0.2688	0.2467	0.0807	**0.1418**	<u>0.0826</u>	0.0682	0.0979	0.1150	0.1377
	NLinear	1D	0.1468	0.1294	0.0449	0.0678	0.0405	0.0308	0.0291	0.0580	0.0684
		3D	0.2830	0.2223	0.0699	0.1257	0.0720	0.0575	0.0510	0.0974	0.1223
		5D	0.4103	0.2915	0.0950	0.1689	0.1013	0.0812	0.0722	0.1300	0.1688
		7D	0.3001	0.3481	0.1204	0.2080	0.1291	0.1029	0.0924	0.1617	0.1828
		Avg.	0.2851	0.2478	0.0825	<u>0.1426</u>	0.0857	<u>0.0681</u>	0.0612	0.1118	0.1356
CNN	TCN	1D	0.3257	0.1416	0.1462	0.8044	0.1152	0.0344	0.0567	0.1260	0.2188
		3D	0.2475	0.2295	0.1342	0.9118	0.1694	0.0597	0.0731	0.1423	0.2459
		5D	0.2906	0.3102	0.1367	0.6579	0.1763	0.1011	0.1119	0.1884	0.2466
		7D	0.3160	0.3587	0.1805	1.3613	0.2556	0.1105	0.1087	0.2119	0.3629
		Avg.	0.2950	0.2600	0.1494	0.9338	0.1791	0.0764	0.0876	0.1671	0.2686
	ModernTCN	1D	0.1391	0.1432	0.0407	0.0778	0.0392	0.0279	0.0255	0.0520	0.0682
		3D	0.2746	0.2966	0.1185	0.1814	0.0799	0.0575	0.0505	0.0921	0.1439
		5D	0.3575	0.3305	0.1278	0.2059	0.1303	0.0850	0.0723	0.1257	0.1794
		7D	0.3067	0.4557	0.1821	0.2844	0.1657	0.1096	0.0950	0.1579	0.2196
		Avg.	0.2695	0.3065	0.1173	0.1874	0.1038	0.0700	0.0608	0.1069	0.1528
	TimesNet	1D	0.1770	0.1473	0.0429	0.0742	0.0546	0.0449	0.0394	0.0761	0.0821
		3D	0.3474	0.2545	0.0758	0.1626	0.1049	0.0829	0.0737	0.1365	0.1548
		5D	0.3436	0.3207	0.1069	0.2093	0.1475	0.1193	0.0939	0.1907	0.1915
		7D	0.3053	0.4134	0.1426	0.2522	0.2020	0.1648	0.1283	0.2267	0.2294
		Avg.	0.2933	0.2840	0.0921	0.1746	0.1273	0.1030	0.0838	0.1575	0.1644
Transformer	iTransformer	1D	0.1277	0.1337	0.0357	0.0674	0.0382	0.0314	0.0295	0.0619	0.0657
		3D	0.2760	0.2269	0.0688	0.1343	0.0755	0.0627	0.0529	0.1057	0.1254
		5D	0.3581	0.3195	0.1004	0.1846	0.1081	0.0855	0.0769	0.1483	0.1727
		7D	0.2999	0.3668	0.1288	0.2222	0.1384	0.1129	0.1003	0.1810	0.1938
		Avg.	0.2654	0.2617	0.0834	0.1521	0.0901	0.0731	0.0649	0.1242	0.1394
	PatchTST	1D	0.1315	0.1368	0.0370	0.0608	0.0385	0.0325	0.0321	0.0593	0.0661
		3D	0.3008	0.2298	0.0845	0.1276	0.0713	0.0645	0.0535	0.1041	0.1295
		5D	0.3504	0.2951	0.1222	0.1736	0.1042	0.0946	0.0777	0.1368	0.1693
		7D	0.3145	0.3605	0.1365	0.2170	0.1412	0.1198	0.0968	0.1708	0.1946
		Avg.	0.2743	0.2555	0.0951	0.1448	0.0888	0.0778	0.0650	0.1177	0.1399

Table 11: Benchmark(MSE) on part 1(Orlando area) stations(RNN,GNN,LLM)

	Method	T	S0	S1	S2	S3	S4	S5	S6	S7	Avg.
RNN	LSTM	1D	0.2408	0.2451	0.0505	0.2788	0.0655	0.0496	0.0435	0.0846	0.1323
		3D	0.2765	0.3219	0.0784	0.3653	0.1097	0.0768	0.0837	0.1162	0.1786
		5D	0.3053	0.3853	0.1085	0.4750	0.1569	0.1011	0.0953	0.1525	0.2225
		7D	0.3058	0.4057	0.1427	0.5133	0.1855	0.1226	0.1103	0.1818	0.2459
		Avg.	0.2821	0.3395	0.0950	0.4081	0.1294	0.0875	0.0832	0.1338	0.1948
	DeepAR	1D	0.2406	0.2367	0.0480	0.2190	0.0615	0.0435	0.0386	0.0782	0.1208
		3D	0.2720	0.3088	0.0793	0.4084	0.1117	0.0783	0.0652	0.1212	0.1806
		5D	0.3033	0.3441	0.1072	0.5899	0.1537	0.1003	0.0883	0.1564	0.2304
		7D	0.3046	0.4056	0.1356	0.5250	0.1639	0.1221	0.1070	0.1800	0.2430
		Avg.	0.2801	0.3238	0.0925	0.4356	0.1227	0.0860	0.0748	0.1340	0.1937
	DilatedRNN	1D	0.1818	0.1370	0.0372	0.3297	0.0496	0.0356	0.0304	0.0860	0.1109
		3D	0.2517	0.2674	0.0689	0.3124	0.0887	0.0645	0.0722	0.1150	0.1551
		5D	0.2822	0.3308	0.1004	0.6438	0.1338	0.0915	0.0916	0.1423	0.2270
		7D	0.3125	0.3989	0.1242	0.5068	0.1702	0.1159	0.1257	0.0714	0.2282
		Avg.	0.2571	0.2835	0.0827	0.4482	0.1106	0.0769	0.0800	0.1037	0.1803
GNN	GCN	1D	0.1465	0.5157	0.0443	1.1053	0.0519	0.0353	0.0275	0.0518	0.2473
		3D	0.2526	1.6031	0.0656	0.7137	0.0944	0.0654	0.0494	0.0891	0.3667
		5D	0.3055	1.9044	0.0867	1.1121	0.1266	0.0895	0.0730	0.1184	0.4770
		7D	0.2687	2.2856	0.1071	1.4113	0.1651	0.1087	0.0928	0.1471	0.5733
		Avg.	**0.2433**	1.5772	0.0759	1.0856	0.1095	0.0747	0.0607	**0.1016**	0.4161
	FourierGNN	1D	0.1619	0.1324	0.0412	0.0901	0.0442	0.0326	0.0275	0.0575	0.0734
		3D	0.2714	0.2058	0.0649	0.2944	0.0746	0.0560	0.0489	0.0941	0.1388
		5D	0.3066	0.2721	0.0891	0.4409	0.1106	0.0806	0.0705	0.1238	0.1868
		7D	0.2766	0.3139	0.1154	0.4880	0.1381	0.1065	0.0919	0.1528	0.2104
		Avg.	0.2541	0.2310	0.0777	0.3283	0.0919	0.0689	0.0597	0.1071	0.1523
	StemGNN	1D	0.2290	0.1703	0.0403	1.1688	0.0652	0.0410	0.0325	0.0723	0.2274
		3D	0.2703	0.4534	0.0903	1.2569	0.1323	0.0896	0.0743	0.1263	0.3117
		5D	0.3017	0.7711	0.1305	3.3143	0.1663	0.1663	0.1417	0.2080	0.6500
		7D	0.3225	0.7901	0.1768	3.4285	0.1979	0.2323	0.1489	0.1864	0.6854
		Avg.	0.2809	0.5462	0.1095	2.2921	0.1404	0.1323	0.0994	0.1483	0.4686
LLM	GPT4TS	1D	0.1984	0.1399	0.0456	0.0882	0.0542	0.0431	0.0387	0.0935	0.0877
		3D	0.3883	0.2385	0.0811	0.1648	0.0986	0.0788	0.0690	0.1343	0.1567
		5D	0.3668	0.3102	0.0997	0.2037	0.1304	0.1091	0.0870	0.1876	0.1868
		7D	0.2928	0.3700	0.1378	0.2503	0.1622	0.1494	0.1319	0.2233	0.2147
		Avg.	0.3116	0.2646	0.0911	0.1768	0.1114	0.0951	0.0816	0.1597	0.1615
	AutoTimes	1D	0.1531	0.1507	0.0401	0.0671	0.0390	0.0310	0.0287	0.0623	0.0715
		3D	0.3072	0.2333	0.0683	0.1278	0.0686	0.0572	0.0508	0.0978	0.1264
		5D	0.3527	0.2975	0.0916	0.1700	0.0992	0.0811	0.0715	0.1319	0.1619
		7D	0.2913	0.3428	0.1181	0.2061	0.1265	0.1031	0.0916	0.1612	0.1801
		Avg.	0.2761	0.2561	0.0795	0.1427	0.0833	0.0681	0.0606	0.1133	0.1350

Table 12: Benchmark(SEDI(10%)) on part 1(Orlando area) stations(MLP,CNN,Transformer)

	Method	T	S0	S1	S2	S3	S4	S5	S6	S7	Avg.
MLP		1D	0.8143	0.9334	0.9011	0.8780	0.6133	0.7659	0.9351	0.7772	0.8273
		3D	0.7599	0.8673	0.8592	0.9286	0.5201	0.7173	0.9040	0.7097	0.7833
	MLP	5D	0.6435	0.8095	0.8142	0.8702	0.4517	0.6956	0.8571	0.6573	0.7249
		7D	0.6022	0.8056	0.7759	0.8158	0.4198	0.6622	0.8516	0.5969	0.6912
		Avg.	**0.7050**	**0.8540**	**0.8376**	**0.8731**	**0.5012**	**0.7103**	**0.8870**	**0.6853**	**0.7567**
		1D	0.7483	0.8690	0.8917	0.9141	0.5971	0.7394	0.7901	0.7191	0.7836
		3D	0.5937	0.7493	0.8103	0.8420	0.4798	0.6766	0.7626	0.6334	0.6935
	TSMixer	5D	0.5167	0.6755	0.7538	0.7783	0.4139	0.6214	0.7289	0.5685	0.6321
		7D	0.4706	0.6241	0.7042	0.7236	0.3734	0.5854	0.6798	0.5107	0.5840
		Avg.	0.5823	0.7295	0.7900	0.8145	0.4660	0.6557	0.7403	0.6079	0.6733
		1D	0.7729	0.8803	0.8951	0.9171	0.5984	0.7844	0.9259	0.7302	0.8130
		3D	0.6007	0.7581	0.8166	0.8390	0.4784	0.6961	0.8550	0.6410	0.7106
	NLinear	5D	0.5198	0.6821	0.7576	0.7721	0.4129	0.6535	0.7956	0.5750	0.6461
		7D	0.4731	0.6290	0.7063	0.7159	0.3701	0.6155	0.7512	0.5173	0.5973
		Avg.	0.5916	0.7374	0.7939	0.8110	0.4649	0.6873	0.8319	0.6159	0.6918
CNN		1D	0.5634	0.8939	0.7243	0.7307	0.4343	0.7156	0.8132	0.5039	0.6724
		3D	0.5462	0.8010	0.6694	0.7131	0.3092	0.7072	0.7778	0.3687	0.6116
	TCN	5D	0.4606	0.7638	0.6291	0.6572	0.2804	0.6123	0.7136	0.3351	0.5565
		7D	0.4598	0.7014	0.6092	0.5674	0.2201	0.5762	0.5692	0.3620	0.5082
		Avg.	0.5075	0.7900	0.6580	0.6671	0.3110	0.6528	0.7184	0.3924	0.5872
		1D	0.7912	0.8737	0.8857	0.8915	0.6023	0.7692	0.9240	0.7395	0.8096
		3D	0.6031	0.7637	0.7893	0.8041	0.4970	0.6746	0.8469	0.6370	0.7020
	ModernTCN	5D	0.4960	0.6839	0.7201	0.7403	0.4277	0.6142	0.7898	0.5668	0.6298
		7D	0.4357	0.6233	0.6667	0.6818	0.3869	0.5726	0.7499	0.5076	0.5781
		Avg.	0.5815	0.7362	0.7654	0.7794	0.4785	0.6576	0.8277	0.6127	0.6799
		1D	0.7224	0.8584	0.8701	0.8789	0.5727	0.7000	0.9025	0.7044	0.7762
		3D	0.5820	0.7493	0.7919	0.7959	0.4368	0.6345	0.7953	0.5956	0.6727
	TimesNet	5D	0.4866	0.6771	0.7336	0.7370	0.3854	0.5657	0.7453	0.5191	0.6062
		7D	0.4083	0.6298	0.6863	0.6808	0.3325	0.5181	0.7137	0.4662	0.5545
		Avg.	0.5498	0.7286	0.7705	0.7732	0.4318	0.6045	0.7892	0.5713	0.6524
Transformer		1D	0.8049	0.8881	0.9039	0.9057	0.5997	0.7663	0.9234	0.7186	0.8138
		3D	0.6433	0.7820	0.8294	0.8350	0.4807	0.6836	0.8500	0.6270	0.7164
	iTransformer	5D	0.5540	0.7202	0.7733	0.7744	0.4121	0.6302	0.7956	0.5481	0.6510
		7D	0.5043	0.6631	0.7177	0.7288	0.3558	0.5843	0.7486	0.4997	0.6003
		Avg.	0.6266	0.7634	0.8061	0.8110	0.4621	0.6661	0.8294	0.5983	0.6954
		1D	0.8082	0.8872	0.8947	0.9082	0.5937	0.7683	0.9141	0.7252	0.8125
		3D	0.6607	0.7851	0.8203	0.8352	0.4994	0.6789	0.8537	0.6293	0.7203
	PatchTST	5D	0.5672	0.7188	0.7626	0.7659	0.4175	0.6272	0.7914	0.5625	0.6516
		7D	0.5081	0.6574	0.7167	0.7186	0.3708	0.5887	0.7506	0.5049	0.6020
		Avg.	0.6361	0.7621	0.7986	0.8070	0.4704	0.6658	0.8274	0.6055	0.6966

Table 13: Benchmark(SEDI(10%)) on part 1(Orlando area) stations(RNN, GNN,LLM)

	Method	T	S0	S1	S2	S3	S4	S5	S6	S7	Avg.
RNN	LSTM	1D	0.7709	0.8270	0.8825	0.8781	0.5134	0.7182	0.9039	0.7302	0.7780
		3D	0.6027	0.8070	0.8162	0.8833	0.4448	0.5963	0.8482	0.6473	0.7057
		5D	0.5247	0.7396	0.7646	0.7848	0.3667	0.6529	0.7852	0.5842	0.6503
		7D	0.4409	0.6678	0.7459	0.7427	0.3836	0.6063	0.7591	0.4874	0.6042
		Avg.	0.5848	0.7604	0.8023	0.8222	0.4271	0.6434	0.8241	0.6123	0.6846
	DeepAR	1D	0.7411	0.8286	0.9006	0.9469	0.5732	0.7033	0.9113	0.7681	0.7966
		3D	0.6168	0.7816	0.7859	0.7710	0.4175	0.6046	0.8704	0.6535	0.6877
		5D	0.5086	0.7014	0.7872	0.8217	0.3716	0.6180	0.7106	0.6096	0.6411
		7D	0.4686	0.7151	0.7627	0.8162	0.3346	0.6131	0.6993	0.5065	0.6145
		Avg.	0.5838	0.7567	0.8091	0.8390	0.4242	0.6348	0.7979	0.6344	0.6850
	DilatedRNN	1D	0.8033	0.9139	0.8972	0.9067	0.6086	0.7706	0.9528	0.7437	0.8246
		3D	0.6053	0.8119	0.7907	0.8376	0.4752	0.5884	0.8004	0.6515	0.6951
		5D	0.5254	0.7325	0.7443	0.8017	0.4259	0.6454	0.8208	0.6270	0.6654
		7D	0.4664	0.7255	0.7337	0.7261	0.4031	0.6275	0.7647	0.5970	0.6305
		Avg.	0.6001	0.7960	0.7915	0.8180	0.4782	0.6580	0.8347	0.6548	0.7039
GNN	GCN	1D	0.8018	0.7777	0.8496	0.7072	0.5680	0.7274	0.9103	0.7172	0.7574
		3D	0.6240	0.7415	0.8169	0.6969	0.5115	0.6977	0.8412	0.6788	0.7011
		5D	0.5324	0.7147	0.7394	0.6223	0.4217	0.6488	0.8378	0.6075	0.6406
		7D	0.4949	0.6795	0.6887	0.5567	0.3824	0.6114	0.7941	0.5809	0.5986
		Avg.	0.6133	0.7283	0.7737	0.6458	0.4709	0.6713	0.8458	0.6461	0.6744
	FourierGNN	1D	0.8505	0.8952	0.9035	0.8991	0.5899	0.7981	0.9211	0.7834	0.8301
		3D	0.6929	0.8059	0.8177	0.7987	0.5029	0.6747	0.8521	0.6853	0.7288
		5D	0.6012	0.7985	0.7753	0.7296	0.4659	0.6222	0.8349	0.6308	0.6823
		7D	0.5372	0.7731	0.7619	0.6927	0.4257	0.6830	0.8133	0.5499	0.6546
		Avg.	0.6705	0.8182	0.8146	0.7800	0.4961	0.6945	0.8554	0.6624	0.7240
	StemGNN	1D	0.6812	0.8950	0.8559	0.4137	0.5486	0.7748	0.9207	0.7578	0.7310
		3D	0.5934	0.7234	0.8229	0.3851	0.4289	0.6430	0.8470	0.6376	0.6352
		5D	0.5151	0.5492	0.6765	0.0829	0.3765	0.4472	0.7608	0.5663	0.4968
		7D	0.4576	0.5168	0.6141	0.0549	0.3011	0.4146	0.8487	0.5028	0.4638
		Avg.	0.5618	0.6711	0.7423	0.2341	0.4138	0.5699	0.8443	0.6161	0.5817
LLM	GPT4TS	1D	0.7588	0.8697	0.8790	0.8738	0.5594	0.7173	0.9066	0.6863	0.7814
		3D	0.5816	0.7515	0.8012	0.7983	0.4484	0.6322	0.8277	0.5967	0.6797
		5D	0.4917	0.6840	0.7480	0.7384	0.3970	0.5830	0.7591	0.5241	0.6157
		7D	0.4388	0.6309	0.6941	0.6878	0.3582	0.5430	0.7099	0.4672	0.5662
		Avg.	0.5677	0.7340	0.7805	0.7746	0.4408	0.6189	0.8008	0.5686	0.6607
	AutoTimes	1D	0.7957	0.8638	0.8896	0.9167	0.5985	0.7343	0.9218	0.7225	0.8054
		3D	0.6299	0.7622	0.8190	0.8520	0.4892	0.6712	0.8516	0.6389	0.7142
		5D	0.5392	0.6780	0.7622	0.7817	0.4135	0.6243	0.7982	0.5804	0.6472
		7D	0.4895	0.6363	0.7204	0.7309	0.3710	0.5879	0.7553	0.5180	0.6012
		Avg.	0.6136	0.7351	0.7978	0.8203	0.4680	0.6544	0.8317	0.6149	0.6920

Table 14: Benchmark(SEDI(5%)) on part 1(Orlando area) stations(MLP,CNN,Transformer)

	Method	T	S0	S1	S2	S3	S4	S5	S6	S7	Avg.
MLP	MLP	1D	0.5128	0.9250	0.7735	0.8437	0.4047	0.7105	0.8731	0.6329	0.7095
		3D	0.5032	0.8575	0.7227	0.9190	0.3281	0.6590	0.8035	0.5460	0.6674
		5D	0.4580	0.7990	0.6804	0.8465	0.2779	0.6314	0.7573	0.5308	0.6227
		7D	0.4174	0.8105	0.6355	0.7808	0.2684	0.5818	0.7227	0.4304	0.5809
		Avg.	**0.4729**	**0.8480**	**0.7030**	**0.8475**	0.3198	0.6457	**0.7892**	0.5350	**0.6451**
	TSMixer	1D	0.5204	0.8556	0.7619	0.8916	0.3911	0.7094	0.7193	0.6167	0.6833
		3D	0.3386	0.7182	0.6688	0.7902	0.3201	0.6698	0.6612	0.4533	0.5775
		5D	0.2734	0.6303	0.6004	0.7015	0.2664	0.5025	0.6127	0.3537	0.4926
		7D	0.2257	0.5757	0.5444	0.6277	0.2313	0.4536	0.5548	0.2847	0.4372
		Avg.	0.3395	0.6950	0.6439	0.7528	0.3022	0.5838	0.6370	0.4271	0.5477
	NLinear	1D	0.5802	0.8689	0.7743	0.9014	0.4122	0.7091	0.8529	0.6285	0.7159
		3D	0.3752	0.7312	0.6721	0.7904	0.3451	0.6185	0.7482	0.4648	0.5932
		5D	0.3456	0.6392	0.6011	0.6967	0.2872	0.5471	0.6727	0.3603	0.5187
		7D	0.2322	0.5818	0.5408	0.6184	0.2505	0.4979	0.6121	0.2912	0.4531
		Avg.	0.3833	0.7053	0.6471	0.7517	**0.3238**	0.5932	0.7215	0.4362	0.5702
CNN	TCN	1D	0.3567	0.8742	0.2636	0.6239	0.2001	0.6360	0.4088	0.4724	0.4795
		3D	0.4252	0.7796	0.3238	0.6102	0.1573	0.4839	0.4081	0.3764	0.4456
		5D	0.2808	0.7319	0.2196	0.5901	0.1484	0.3628	0.4501	0.3326	0.3895
		7D	0.3380	0.6245	0.2753	0.4466	0.1223	0.3825	0.2879	0.2875	0.3456
		Avg.	0.3502	0.7526	0.2706	0.5677	0.1570	0.4663	0.3887	0.3672	0.4150
	ModernTCN	1D	0.5274	0.8480	0.7496	0.8700	0.3762	0.7081	0.8590	0.6339	0.6965
		3D	0.3525	0.7260	0.6128	0.7416	0.3183	0.5902	0.7544	0.4769	0.5716
		5D	0.2805	0.6333	0.5298	0.6535	0.2708	0.5110	0.6824	0.3742	0.4919
		7D	0.2334	0.5539	0.4603	0.5819	0.2352	0.4597	0.6208	0.3082	0.4317
		Avg.	0.3484	0.6903	0.5881	0.7118	0.3001	0.5673	0.7292	0.4483	0.5479
	TimesNet	1D	0.4528	0.8341	0.7355	0.8507	0.3561	0.5952	0.8295	0.5725	0.6533
		3D	0.3185	0.7133	0.6279	0.7271	0.2782	0.5261	0.7186	0.4477	0.5447
		5D	0.2639	0.6133	0.5616	0.6561	0.2305	0.4305	0.6461	0.3400	0.4678
		7D	0.2184	0.5629	0.4993	0.5816	0.1851	0.3748	0.5961	0.2652	0.4104
		Avg.	0.3134	0.6809	0.6061	0.7039	0.2625	0.4816	0.6976	0.4064	0.5190
Transformer	iTransformer	1D	0.5441	0.8814	0.7818	0.8940	0.3864	0.7065	0.8510	0.5962	0.7052
		3D	0.3974	0.7637	0.6710	0.7924	0.3104	0.5943	0.7502	0.4656	0.5931
		5D	0.3080	0.6876	0.6000	0.7083	0.2453	0.5257	0.6786	0.3554	0.5136
		7D	0.2514	0.6234	0.5337	0.6420	0.2047	0.4701	0.6208	0.2896	0.4545
		Avg.	0.3752	0.7390	0.6466	0.7592	0.2867	0.5742	0.7252	0.4267	0.5666
	PatchTST	1D	0.5491	0.8715	0.7655	0.8953	0.3878	0.7004	0.8402	0.6004	0.7013
		3D	0.3800	0.7584	0.6663	0.7948	0.3210	0.5907	0.7519	0.4659	0.5911
		5D	0.3052	0.6788	0.5937	0.6959	0.2631	0.5219	0.6719	0.3734	0.5130
		7D	0.2502	0.6018	0.5339	0.6317	0.2196	0.4734	0.6156	0.3054	0.4539
		Avg.	0.3711	0.7276	0.6399	0.7544	0.2979	0.5716	0.7199	0.4363	0.5648

Table 15: Benchmark(SEDI(5%)) on part 1(Orlando area) stations(RNN,GNN,LLM)

	Method	T	S0	S1	S2	S3	S4	S5	S6	S7	Avg.
RNN	LSTM	1D	0.4017	0.8107	0.7419	0.8659	0.3198	0.6701	0.8120	0.5639	0.6483
		3D	0.3042	0.7513	0.6543	0.8644	0.2781	0.5208	0.6626	0.3957	0.5539
		5D	0.2563	0.7351	0.5817	0.7538	0.2252	0.4925	0.6287	0.3346	0.5010
		7D	0.2557	0.6068	0.5389	0.7051	0.2231	0.4831	0.5848	0.2670	0.4581
		Avg.	0.3045	0.7260	0.6292	0.7973	0.2615	0.5416	0.6720	0.3903	0.5403
	DeepAR	1D	0.5253	0.8201	0.7607	0.9462	0.3488	0.6711	0.8081	0.5904	0.6838
		3D	0.3304	0.7414	0.6407	0.7018	0.2825	0.5496	0.6188	0.4553	0.5401
		5D	0.2763	0.6725	0.5825	0.8152	0.2105	0.5123	0.5172	0.3650	0.4939
		7D	0.2556	0.6896	0.5741	0.8037	0.2025	0.4243	0.4710	0.3234	0.4680
		Avg.	0.3469	0.7309	0.6395	<u>0.8167</u>	0.2611	0.5393	0.6038	0.4335	0.5465
	DilatedRNN	1D	0.5340	0.8917	0.7632	0.8782	0.3685	0.7112	0.8792	0.6419	0.7085
		3D	0.3663	0.8079	0.6105	0.7865	0.2975	0.5017	0.6871	0.4803	0.5672
		5D	0.3059	0.6907	0.5751	0.7343	0.2560	0.5750	0.6966	0.4549	0.5361
		7D	0.3052	0.6703	0.5421	0.6376	0.2480	0.5455	0.6476	0.4271	0.5029
		Avg.	0.3779	0.7652	0.6227	0.7591	0.2925	0.5833	0.7276	0.5010	0.5787
GNN	GCN	1D	0.5137	0.7241	0.7046	0.6410	0.3511	0.7351	0.8413	0.5751	0.6357
		3D	0.3818	0.6910	0.6424	0.6378	0.3101	0.7135	0.7400	0.4640	0.5726
		5D	0.3292	0.6557	0.5711	0.5477	0.2499	0.6674	0.7444	0.4156	0.5226
		7D	0.3021	0.6169	0.5142	0.4740	0.2346	0.5327	0.6955	0.4517	0.4777
		Avg.	0.3817	0.6719	0.6081	0.5751	0.2864	**0.6622**	0.7553	0.4766	0.5522
	FourierGNN	1D	0.5676	0.8926	0.7800	0.8434	0.3851	0.7068	0.8439	0.6727	0.7115
		3D	0.4629	0.7868	0.6564	0.7028	0.3275	0.5714	0.7651	0.5707	0.6054
		5D	0.3950	0.7889	0.6028	0.6333	0.2748	0.5038	0.7352	0.5055	0.5549
		7D	0.3873	0.7530	0.6115	0.5815	0.2572	0.5880	0.7235	0.4659	0.5460
		Avg.	<u>0.4532</u>	<u>0.8053</u>	<u>0.6626</u>	0.6903	0.3112	0.5925	<u>0.7669</u>	**0.5537**	<u>0.6045</u>
	StemGNN	1D	0.3886	0.8590	0.7176	0.2562	0.3499	0.7175	0.8579	0.6320	0.5973
		3D	0.3247	0.6710	0.6642	0.1607	0.2578	0.5487	0.7490	0.5132	0.4862
		5D	0.2763	0.4268	0.4857	0.0234	0.2251	0.3075	0.6028	0.3641	0.3390
		7D	0.2189	0.3938	0.3786	0.0456	0.1851	0.2623	0.7196	0.3385	0.3178
		Avg.	0.3021	0.5877	0.5615	0.1215	0.2545	0.4590	0.7324	0.4619	0.4351
LLM	GPT4TS	1D	0.4904	0.8517	0.7383	0.8528	0.3567	0.6286	0.8333	0.5737	0.6657
		3D	0.3418	0.7131	0.6424	0.7412	0.2897	0.5298	0.7352	0.4407	0.5542
		5D	0.2811	0.6474	0.5588	0.6647	0.2451	0.4542	0.6619	0.3371	0.4813
		7D	0.2508	0.5786	0.4827	0.6002	0.2173	0.4100	0.5996	0.2547	0.4243
		Avg.	0.3410	0.6977	0.6055	0.7147	0.2772	0.5056	0.7075	0.4016	0.5314
	AutoTimes	1D	0.5235	0.8448	0.7499	0.9034	0.3786	0.6736	0.8310	0.5961	0.6876
		3D	0.3733	0.7387	0.6568	0.8177	0.3245	0.5828	0.7471	0.4660	0.5884
		5D	0.3023	0.6336	0.5923	0.7174	0.2638	0.5145	0.6738	0.3625	0.5075
		7D	0.2343	0.5856	0.5382	0.6401	0.2301	0.4620	0.6092	0.3000	0.4499
		Avg.	0.3584	0.7007	0.6343	0.7696	0.2993	0.5582	0.7153	0.4311	0.5584

Table 16: Benchmark(SEDI(1%)) on part 1(Orlando area) stations(MLP,CNN,Transformer)

	Method	T	S0	S1	S2	S3	S4	S5	S6	S7	Avg.
MLP	MLP	1D	0.2398	0.8330	0.3903	0.7439	0.2199	0.2365	0.4548	0.1809	0.4124
		3D	0.1994	0.7910	0.2967	0.7730	0.2051	0.1198	0.3723	0.1528	0.3638
		5D	0.1508	0.7647	0.2900	0.7580	0.1927	0.1346	0.3785	0.1380	0.3509
		7D	0.1877	0.7879	0.2579	0.6627	0.1935	0.1097	0.3831	0.1107	0.3367
		Avg.	**0.1944**	**0.7942**	**0.3087**	**0.7344**	**0.2028**	<u>0.1502</u>	**0.3972**	<u>0.1456</u>	**0.3660**
	TSMixer	1D	0.2154	0.7569	0.3670	0.7701	0.2092	0.1228	0.2195	0.1553	0.3520
		3D	0.1462	0.5898	0.2661	0.5455	0.1401	0.0936	0.1884	0.0939	0.2580
		5D	0.1104	0.4818	0.1939	0.4161	0.1069	0.0697	0.1647	0.0636	0.2009
		7D	0.1078	0.3947	0.1464	0.3318	0.0871	0.0548	0.1533	0.0456	0.1652
		Avg.	0.1450	0.5558	0.2433	0.5159	0.1358	0.0852	0.1815	0.0896	0.2440
	NLinear	1D	0.2205	0.7772	0.3813	0.7807	0.2302	0.2270	0.3975	0.1560	0.3963
		3D	0.1508	0.6056	0.2785	0.5478	0.1460	0.1937	0.3198	0.0888	0.2914
		5D	0.1156	0.4949	0.2062	0.4135	0.1131	0.1686	0.2773	0.0607	0.2313
		7D	0.1104	0.4048	0.1576	0.3231	0.0919	0.1536	0.2289	0.0453	0.1895
		Avg.	0.1493	0.5706	0.2559	0.5163	0.1453	**0.1857**	0.3059	0.0877	0.2771
CNN	TCN	1D	0.1520	0.7471	0.1639	0.2160	0.0801	0.0385	0.0000	0.0404	0.1797
		3D	0.1481	0.6252	0.1179	0.3218	0.0634	0.0303	0.0232	0.0397	0.1712
		5D	0.1935	0.5904	0.0941	0.2732	0.0516	0.0161	0.0496	0.0063	0.1593
		7D	0.1863	0.3808	0.1512	0.1816	0.0468	0.0121	0.0149	0.0185	0.1240
		Avg.	<u>0.1700</u>	0.5859	0.1318	0.2481	0.0605	0.0243	0.0219	0.0262	0.1586
	ModernTCN	1D	0.1937	0.7645	0.3466	0.7558	0.2153	0.2077	0.3743	0.1827	0.3801
		3D	0.1202	0.6078	0.2371	0.4858	0.1331	0.1410	0.2984	0.1105	0.2667
		5D	0.0829	0.5308	0.1742	0.3875	0.1018	0.1315	0.2742	0.0778	0.2201
		7D	0.0804	0.4283	0.1325	0.3070	0.0795	0.0623	0.2074	0.0606	0.1698
		Avg.	0.1193	0.5829	0.2226	0.4840	0.1324	0.1356	0.2886	0.1079	0.2592
	TimesNet	1D	0.1451	0.7329	0.3521	0.6753	0.1455	0.1175	0.3185	0.1265	0.3267
		3D	0.0951	0.5803	0.2451	0.4443	0.1134	0.0911	0.2359	0.0766	0.2352
		5D	0.0651	0.4805	0.1894	0.3933	0.0900	0.0482	0.2077	0.0577	0.1915
		7D	0.0372	0.3977	0.1499	0.2984	0.0631	0.0399	0.1878	0.0400	0.1518
		Avg.	0.0856	0.5479	0.2341	0.4528	0.1030	0.0742	0.2375	0.0752	0.2263
Transformer	iTransformer	1D	0.2066	0.7969	0.3789	0.7930	0.2251	0.1355	0.3441	0.1508	0.3789
		3D	0.1275	0.6825	0.2843	0.5750	0.1318	0.0913	0.2617	0.0926	0.2808
		5D	0.0961	0.5919	0.2149	0.4326	0.0930	0.0727	0.2305	0.0576	0.2237
		7D	0.0714	0.4919	0.1664	0.3504	0.0721	0.0542	0.1959	0.0448	0.1809
		Avg.	0.1254	0.6408	0.2611	0.5378	0.1305	0.0884	0.2581	0.0864	0.2661
	PatchTST	1D	0.2149	0.7937	0.3601	0.8041	0.2110	0.1291	0.3226	0.1593	0.3744
		3D	0.1327	0.6565	0.2770	0.5851	0.1429	0.0968	0.2652	0.0913	0.2809
		5D	0.0915	0.5578	0.2143	0.4411	0.1047	0.0734	0.2243	0.0673	0.2218
		7D	0.0757	0.4552	0.1661	0.3639	0.0799	0.0570	0.1975	0.0518	0.1809
		Avg.	0.1287	0.6158	0.2544	0.5485	0.1346	0.0891	0.2524	0.0924	0.2645

Table 17: Benchmark(SEDI(1%)) on part 1(Orlando area) stations(RNN,GNN,LLM)

	Method	T	S0	S1	S2	S3	S4	S5	S6	S7	Avg.
RNN	LSTM	1D	0.1231	0.5677	0.3286	0.5730	0.1160	0.1235	0.2804	0.1423	0.2818
		3D	0.0722	0.3377	0.2315	0.4083	0.1017	0.0801	0.1284	0.0580	0.1772
		5D	0.0462	0.4222	0.1899	0.1858	0.0782	0.0618	0.2246	0.0612	0.1587
		7D	0.0583	0.2870	0.0658	0.3472	0.0747	0.0526	0.1112	0.0411	0.1297
		Avg.	0.0749	0.4036	0.2040	0.3786	0.0927	0.0795	0.1862	0.0756	0.1869
	DeepAR	1D	0.1138	0.6157	0.3092	0.4319	0.1276	0.1392	0.2927	0.1144	0.2681
		3D	0.0954	0.3621	0.1573	0.2978	0.0974	0.1047	0.1110	0.0291	0.1568
		5D	0.0588	0.3228	0.1519	0.2054	0.0821	0.0691	0.0985	0.0716	0.1325
		7D	0.1016	0.2944	0.0939	0.0666	0.0793	0.0690	0.1249	0.0787	0.1135
		Avg.	0.0924	0.3987	0.1781	0.2504	0.0966	0.0955	0.1568	0.0734	0.1677
	DilatedRNN	1D	0.2111	0.7473	0.3720	0.7648	0.1895	0.1384	0.3324	0.2115	0.3709
		3D	0.1417	0.6452	0.2337	0.5917	0.1539	0.0764	0.1583	0.1111	0.2640
		5D	0.1170	0.5410	0.1941	0.4338	0.1278	0.0712	0.2353	0.1309	0.2314
		7D	0.0923	0.4478	0.1716	0.3167	0.1039	0.0766	0.1639	0.0805	0.1817
		Avg.	0.1405	0.5953	0.2428	0.5267	0.1438	0.0906	0.2225	0.1335	0.2620
GNN	GCN	1D	0.2025	0.5785	0.3234	0.4610	0.2208	0.1729	0.3612	0.1966	0.3146
		3D	0.1393	0.5720	0.2439	0.4175	0.0475	0.1439	0.3082	0.1379	0.2513
		5D	0.1185	0.5251	0.1685	0.3352	0.0296	0.1351	0.3633	0.1096	0.2231
		7D	0.1255	0.4695	0.1648	0.2308	0.0269	0.1249	0.3558	0.1684	0.2083
		Avg.	0.1465	0.5363	0.2252	0.3611	0.0812	0.1442	<u>0.3471</u>	**0.1531**	0.2493
	FourierGNN	1D	0.2074	0.7982	0.3768	0.7408	0.2155	0.1250	0.3068	0.1698	0.3675
		3D	0.1567	0.7499	0.2746	0.6374	0.1849	0.1035	0.2813	0.1395	0.3160
		5D	0.1326	0.7111	0.2177	0.5194	0.1881	0.1060	0.2724	0.1089	0.2820
		7D	0.1830	0.6629	0.2348	0.4327	0.1766	0.1203	0.3300	0.1289	0.2836
		Avg.	0.1699	<u>0.7305</u>	<u>0.2760</u>	<u>0.5826</u>	<u>0.1913</u>	0.1137	0.2976	0.1368	<u>0.3123</u>
	StemGNN	1D	0.1717	0.4968	0.3191	0.0206	0.1620	0.1239	0.2858	0.2005	0.2225
		3D	0.1410	0.3176	0.2135	0.0176	0.1152	0.0530	0.1569	0.1344	0.1437
		5D	0.1395	0.0319	0.1679	0.0013	0.0691	0.0051	0.1753	0.0661	0.0820
		7D	0.1056	0.0337	0.1386	0.0003	0.0784	0.0036	0.2534	0.0487	0.0828
		Avg.	0.1395	0.2200	0.2098	0.0100	0.1062	0.0464	0.2179	0.1124	0.1328
LLM	GPT4TS	1D	0.1732	0.7775	0.3626	0.7129	0.1662	0.1221	0.3125	0.1272	0.3443
		3D	0.1047	0.6083	0.2679	0.4717	0.1214	0.0922	0.2501	0.0771	0.2492
		5D	0.0698	0.5106	0.1923	0.3910	0.0886	0.0498	0.2192	0.0558	0.1971
		7D	0.0579	0.4151	0.1366	0.3045	0.0733	0.0356	0.2041	0.0334	0.1576
		Avg.	0.1014	0.5779	0.2399	0.4700	0.1124	0.0749	0.2465	0.0734	0.2370
	AutoTimes	1D	0.1985	0.7427	0.3622	0.8053	0.2213	0.1268	0.3335	0.1362	0.3658
		3D	0.1179	0.6341	0.2763	0.5863	0.1497	0.0970	0.2677	0.0801	0.2761
		5D	0.0788	0.5089	0.2057	0.4334	0.1039	0.0723	0.2216	0.0601	0.2106
		7D	0.0714	0.4392	0.1579	0.3310	0.0873	0.0559	0.1895	0.0444	0.1721
		Avg.	0.1167	0.5812	0.2505	0.5390	0.1406	0.0880	0.2531	0.0802	0.2562

Table 18: Benchmark(MAE) on part 2(Miami area) stations(MLP,CNN,Transformer)

	Method	T	S0	S1	S2	S3	S4	S5	S6	S7	Avg.
MLP	MLP	1D	0.0739	0.0969	0.1538	0.1234	0.1172	0.1069	0.1168	0.1548	0.1180
		3D	0.1588	0.1621	0.2502	0.2129	0.1952	0.1638	0.1855	0.2459	0.1968
		5D	0.2147	0.2079	0.3080	0.2637	0.2568	0.1984	0.2268	0.3070	0.2479
		7D	0.2650	0.2436	0.3517	0.3046	0.2989	0.2236	0.2595	0.3454	0.2865
		Avg.	0.1781	0.1776	0.2659	0.2262	0.2170	0.1732	0.1971	0.2633	0.2123
	TSMixer	1D	0.0932	0.1147	0.1777	0.1381	0.1322	0.1152	0.1279	0.2124	0.1389
		3D	0.1637	0.1770	0.2667	0.2123	0.2056	0.1680	0.1926	0.2856	0.2089
		5D	0.2179	0.2209	0.3239	0.2646	0.2615	0.2014	0.2349	0.3376	0.2578
		7D	0.2621	0.2558	0.3663	0.3055	0.3081	0.2258	0.2663	0.3779	0.2960
		Avg.	0.1842	0.1921	0.2836	0.2301	0.2269	0.1776	0.2054	0.3034	0.2254
	NLinear	1D	0.0857	0.1055	0.1672	0.1274	0.1207	0.1085	0.1191	0.1484	0.1228
		3D	0.1603	0.1709	0.2606	0.2059	0.1988	0.1642	0.1882	0.2414	0.1988
		5D	0.2153	0.2167	0.3190	0.2608	0.2560	0.1984	0.2311	0.3010	0.2498
		7D	0.2603	0.2526	0.3618	0.3022	0.3031	0.2237	0.2635	0.3457	0.2891
		Avg.	0.1804	0.1864	0.2772	0.2241	0.2196	0.1737	0.2005	0.2591	0.2151
CNN	TCN	1D	0.1747	0.1498	0.1937	0.1790	0.1882	0.1957	0.1439	0.7995	0.2531
		3D	0.2303	0.1938	0.2971	0.2766	0.2811	0.2347	0.2049	0.9442	0.3328
		5D	0.3770	0.2350	0.3711	0.3214	0.3427	0.2733	0.2633	0.8945	0.3848
		7D	0.3407	0.2960	0.3925	0.3659	0.3887	0.3089	0.2950	1.0090	0.4246
		Avg.	0.2807	0.2186	0.3136	0.2857	0.3002	0.2531	0.2268	0.9118	0.3488
	ModernTCN	1D	0.0777	0.1049	0.1764	0.1385	0.1134	0.1034	0.1154	0.1565	0.1233
		3D	0.1611	0.1813	0.2938	0.2362	0.1982	0.1669	0.1906	0.2810	0.2136
		5D	0.2289	0.2449	0.3621	0.3098	0.2576	0.2038	0.2351	0.3383	0.2726
		7D	0.2809	0.2903	0.4201	0.3565	0.3054	0.2314	0.2702	0.3758	0.3163
		Avg.	0.1871	0.2054	0.3131	0.2603	0.2186	0.1764	0.2028	0.2879	0.2315
	TimesNet	1D	0.0962	0.1269	0.1984	0.1537	0.1505	0.1309	0.1520	0.1927	0.1502
		3D	0.1684	0.1943	0.2871	0.2323	0.2249	0.1854	0.2122	0.2767	0.2227
		5D	0.2212	0.2409	0.3516	0.2849	0.2861	0.2200	0.2587	0.3347	0.2748
		7D	0.2722	0.2761	0.3937	0.3329	0.3326	0.2409	0.2915	0.3775	0.3147
		Avg.	0.1895	0.2095	0.3077	0.2509	0.2485	0.1943	0.2286	0.2954	0.2406
Transformer	iTransformer	1D	0.0731	0.0925	0.1477	0.1178	0.1129	0.1024	0.1104	0.1409	0.1122
		3D	0.1446	0.1603	0.2490	0.1975	0.1901	0.1593	0.1807	0.2334	0.1894
		5D	0.2057	0.2052	0.3095	0.2518	0.2498	0.1938	0.2248	0.3007	0.2427
		7D	0.2513	0.2460	0.3529	0.2933	0.2968	0.2193	0.2555	0.3480	0.2829
		Avg.	0.1687	**0.1760**	0.2648	**0.2151**	**0.2124**	0.1687	**0.1928**	0.2558	0.2068
	PatchTST	1D	0.0691	0.0926	0.1472	0.1158	0.1114	0.1012	0.1104	0.1394	0.1109
		3D	0.1419	0.1610	0.2449	0.1975	0.1927	0.1590	0.1828	0.2376	0.1897
		5D	0.2002	0.2094	0.3042	0.2524	0.2504	0.1943	0.2251	0.2999	0.2420
		7D	0.2463	0.2461	0.3499	0.2947	0.3005	0.2200	0.2574	0.3444	0.2824
		Avg.	**0.1644**	0.1773	**0.2615**	**0.2151**	0.2138	**0.1686**	0.1939	**0.2553**	**0.2062**

Table 19: Benchmark(MAE) on part 2(Miami area) stations(RNN,GNN,LLM)

	Method	T	S0	S1	S2	S3	S4	S5	S6	S7	Avg.
RNN	LSTM	1D	0.1150	0.1373	0.2165	0.1678	0.1691	0.1378	0.1531	0.2537	0.1688
		3D	0.2287	0.2081	0.3074	0.2574	0.2650	0.2002	0.2272	0.3706	0.2581
		5D	0.2646	0.2556	0.3832	0.3241	0.3190	0.2378	0.2694	0.4339	0.3109
		7D	0.3326	0.2989	0.4425	0.3728	0.3855	0.2579	0.2909	0.4743	0.3569
		Avg.	0.2352	0.2250	0.3374	0.2805	0.2847	0.2084	0.2352	0.3831	0.2737
	DeepAR	1D	0.1196	0.1356	0.2067	0.1678	0.1659	0.1410	0.1546	0.2557	0.1684
		3D	0.2086	0.2169	0.3113	0.2615	0.2693	0.2047	0.2301	0.3624	0.2581
		5D	0.2839	0.2586	0.3710	0.3123	0.3166	0.2299	0.2790	0.4224	0.3092
		7D	0.3404	0.2992	0.4478	0.3695	0.3657	0.2598	0.3007	0.4670	0.3562
		Avg.	0.2381	0.2276	0.3342	0.2778	0.2794	0.2088	0.2411	0.3769	0.2730
	DilatedRNN	1D	0.0781	0.1134	0.1706	0.1359	0.1309	0.1155	0.1217	0.2111	0.1347
		3D	0.1724	0.1856	0.2843	0.2268	0.2393	0.1769	0.2149	0.3164	0.2271
		5D	0.2463	0.2351	0.3483	0.2967	0.3012	0.2133	0.2548	0.3866	0.2853
		7D	0.3312	0.2732	0.4052	0.3472	0.3469	0.2460	0.2917	0.4338	0.3344
		Avg.	0.2070	0.2018	0.3021	0.2516	0.2546	0.1879	0.2208	0.3370	0.2454
GNN	GCN	1D	0.0910	0.1254	0.1880	0.1761	0.1626	0.1374	0.1528	0.9648	0.2498
		3D	0.1718	0.1904	0.2843	0.2485	0.2410	0.1928	0.2173	0.5350	0.2601
		5D	0.2460	0.2340	0.3390	0.3061	0.3085	0.2319	0.2571	0.7279	0.3313
		7D	0.2998	0.2700	0.3911	0.3452	0.3508	0.2609	0.2914	0.6410	0.3563
		Avg.	0.2022	0.2050	0.3006	0.2690	0.2657	0.2057	0.2297	0.7172	0.2994
	FourierGNN	1D	0.0825	0.1072	0.1604	0.1365	0.1226	0.1165	0.1234	0.2444	0.1367
		3D	0.1593	0.1722	0.2527	0.2059	0.2024	0.1734	0.1925	0.3399	0.2123
		5D	0.2109	0.2189	0.3114	0.2658	0.2568	0.2123	0.2320	0.4031	0.2639
		7D	0.2896	0.2506	0.3590	0.3121	0.3067	0.2357	0.2624	0.4222	0.3048
		Avg.	0.1856	0.1872	0.2709	0.2301	0.2221	0.1845	0.2026	0.3524	0.2294
	StemGNN	1D	0.0859	0.1404	0.1762	0.1382	0.1444	0.1204	0.1252	0.3656	0.1620
		3D	0.2047	0.2609	0.2958	0.2616	0.2763	0.2432	0.2227	0.4821	0.2809
		5D	0.2874	0.3173	0.3743	0.3535	0.4289	0.2839	0.2765	0.5247	0.3558
		7D	0.3603	0.3402	0.4218	0.4172	0.4253	0.3211	0.3283	0.6507	0.4081
		Avg.	0.2346	0.2647	0.3170	0.2926	0.3187	0.2422	0.2382	0.5058	0.3017
LLM	GPT4TS	1D	0.0931	0.1264	0.1860	0.1431	0.1392	0.1304	0.1510	0.1974	0.1458
		3D	0.1639	0.1959	0.2833	0.2283	0.2281	0.1895	0.2159	0.2917	0.2246
		5D	0.2256	0.2429	0.3469	0.2834	0.2897	0.2195	0.2535	0.3389	0.2751
		7D	0.2728	0.2842	0.3941	0.3275	0.3342	0.2466	0.2878	0.3960	0.3179
		Avg.	0.1888	0.2124	0.3026	0.2456	0.2478	0.1965	0.2271	0.3060	0.2408
	AutoTimes	1D	0.0863	0.1029	0.1665	0.1318	0.1270	0.1140	0.1312	0.1587	0.1273
		3D	0.1530	0.1663	0.2545	0.2069	0.2008	0.1668	0.1926	0.2450	0.1982
		5D	0.2065	0.2109	0.3079	0.2619	0.2556	0.2017	0.2342	0.3065	0.2481
		7D	0.2552	0.2469	0.3515	0.3009	0.3029	0.2267	0.2654	0.3482	0.2872
		Avg.	0.1752	0.1817	0.2701	0.2254	0.2216	0.1773	0.2058	0.2646	0.2152

Table 20: Benchmark(MSE) on part 2(Miami area) stations(MLP,CNN,Transformer)

	Method	T	S0	S1	S2	S3	S4	S5	S6	S7	Avg.
MLP	MLP	1D	0.0315	0.0629	0.1405	0.0774	0.0602	0.0525	0.0787	0.1295	0.0792
		3D	0.0808	0.1311	0.2777	0.1506	0.1289	0.0935	0.1471	0.2762	0.1607
		5D	0.1300	0.1819	0.3613	0.2040	0.1912	0.1197	0.1905	0.3950	0.2217
		7D	0.1783	0.2232	0.4256	0.2480	0.2456	0.1399	0.2230	0.4617	0.2682
		Avg.	**0.1052**	**0.1498**	**0.3012**	**0.1700**	**0.1565**	**0.1014**	**0.1599**	**0.3156**	**0.1824**
	TSMixer	1D	0.0397	0.0747	0.1695	0.0877	0.0697	0.0578	0.0868	0.2450	0.1039
		3D	0.0932	0.1486	0.3241	0.1611	0.1419	0.0985	0.1605	0.3833	0.1889
		5D	0.1460	0.2061	0.4276	0.2192	0.2111	0.1263	0.2114	0.4777	0.2532
		7D	0.1968	0.2537	0.5054	0.2679	0.2786	0.1475	0.2509	0.5544	0.3069
		Avg.	0.1189	0.1708	0.3566	0.1840	0.1753	0.1075	0.1774	0.4151	0.2132
	NLinear	1D	0.0374	0.0687	0.1605	0.0830	0.0639	0.0554	0.0816	0.1269	0.0847
		3D	0.0924	0.1442	0.3186	0.1581	0.1376	0.0974	0.1568	0.2825	0.1734
		5D	0.1450	0.2026	0.4224	0.2174	0.2065	0.1253	0.2083	0.3881	0.2395
		7D	0.1962	0.2511	0.5021	0.2666	0.2743	0.1471	0.2484	0.4696	0.2944
		Avg.	0.1177	0.1666	0.3509	0.1813	0.1706	0.1063	0.1738	<u>0.3168</u>	0.1980
CNN	TCN	1D	0.0976	0.0963	0.1756	0.1090	0.1377	0.1694	0.0984	5.8002	0.8355
		3D	0.1318	0.1480	0.3271	0.2042	0.2212	0.2113	0.1527	7.0577	1.0567
		5D	0.3490	0.2009	0.4521	0.2532	0.3033	0.2986	0.2079	5.1319	0.8996
		7D	0.2479	0.2662	0.4783	0.2929	0.3587	0.2911	0.2391	6.7494	1.1155
		Avg.	0.2066	0.1779	0.3583	0.2148	0.2552	0.2426	0.1745	6.1848	0.9768
	ModernTCN	1D	0.0395	0.0838	0.2180	0.1137	0.0630	0.0539	0.0818	0.3165	0.1213
		3D	0.1168	0.1894	0.4307	0.2323	0.1464	0.1036	0.1678	2.9814	0.5460
		5D	0.1869	0.3223	0.5611	0.3355	0.2198	0.1352	0.2221	2.7558	0.5923
		7D	0.2499	0.4475	0.7525	0.3950	0.2877	0.1613	0.2656	1.4768	0.5045
		Avg.	0.1483	0.2608	0.4906	0.2691	0.1792	0.1135	0.1843	1.8826	0.4411
	TimesNet	1D	0.0453	0.0899	0.1964	0.1033	0.0884	0.0700	0.1090	0.1729	0.1094
		3D	0.1100	0.1839	0.3598	0.1995	0.1694	0.1154	0.1857	0.3311	0.2069
		5D	0.1666	0.2634	0.4952	0.2586	0.2486	0.1484	0.2477	0.4500	0.2848
		7D	0.2283	0.3207	0.5949	0.3303	0.3296	0.1674	0.2892	0.5382	0.3498
		Avg.	0.1376	0.2145	0.4116	0.2230	0.2090	0.1253	0.2079	0.3731	0.2377
Transformer	iTransformer	1D	0.0337	0.0645	0.1413	0.0798	0.0614	0.0536	0.0766	0.1210	0.0790
		3D	0.0880	0.1424	0.3086	0.1614	0.1361	0.0964	0.1512	0.2755	0.1700
		5D	0.1486	0.2002	0.4253	0.2206	0.2052	0.1266	0.2082	0.3973	0.2415
		7D	0.2032	0.2658	0.4903	0.2697	0.2727	0.1490	0.2408	0.5022	0.2992
		Avg.	0.1184	0.1682	0.3414	0.1828	0.1688	0.1064	0.1692	0.3240	0.1974
	PatchTST	1D	0.0326	0.0667	0.1392	0.0789	0.0615	0.0525	0.0781	0.1213	0.0789
		3D	0.0872	0.1459	0.2950	0.1614	0.1389	0.0963	0.1586	0.2825	0.1707
		5D	0.1402	0.2096	0.3952	0.2208	0.2068	0.1249	0.2112	0.3960	0.2381
		7D	0.1899	0.2624	0.4758	0.2686	0.2763	0.1473	0.2494	0.4766	0.2933
		Avg.	<u>0.1125</u>	0.1711	0.3263	0.1824	0.1709	<u>0.1053</u>	0.1743	0.3191	<u>0.1952</u>

Table 21: Benchmark(MSE) on part 2(Miami area) stations(RNN,GNN,LLM)

	Method	Metric	S0	S1	S2	S3	S4	S5	S6	S7	Avg.
RNN	LSTM	1D	0.0575	0.1123	0.2405	0.1158	0.1092	0.0775	0.1224	1.1111	0.2433
		3D	0.1531	0.1869	0.3854	0.2070	0.2091	0.1206	0.1944	1.4368	0.3617
		5D	0.1983	0.2390	0.4905	0.2732	0.2894	0.1479	0.2368	1.3811	0.4070
		7D	0.2734	0.2901	0.5826	0.3426	0.3981	0.1677	0.2615	1.8380	0.5192
		Avg.	0.1706	0.2071	0.4248	0.2346	0.2515	0.1284	0.2038	1.4417	0.3828
	DeepAR	1D	0.0611	0.1108	0.2390	0.1248	0.1152	0.0790	0.1230	0.9006	0.2192
		3D	0.1276	0.1894	0.3864	0.2041	0.2173	0.1226	0.1953	1.3494	0.3490
		5D	0.1973	0.2385	0.4877	0.2623	0.2918	0.1463	0.2344	1.4248	0.4104
		7D	0.2820	0.3010	0.5995	0.3402	0.3564	0.1667	0.2657	1.4515	0.4704
		Avg.	0.1670	0.2099	0.4282	0.2328	0.2452	0.1286	0.2046	1.2816	0.3622
	DilatedRNN	1D	0.0366	0.0808	0.1810	0.0931	0.0823	0.0635	0.0944	0.8270	0.1823
		3D	0.1137	0.1710	0.3481	0.1894	0.2205	0.1151	0.1746	1.0864	0.3023
		5D	0.1970	0.2275	0.4660	0.2738	0.3055	0.1469	0.2277	1.3925	0.4046
		7D	0.2899	0.2742	0.5486	0.3313	0.3679	0.1781	0.2746	1.3743	0.4549
		Avg.	0.1593	0.1884	0.3859	0.2219	0.2441	0.1259	0.1928	1.1701	0.3360
GNN	GCN	1D	0.0333	0.0964	0.1750	0.1817	0.1209	0.0909	0.0948	170.0996	21.3616
		3D	0.0829	0.1800	0.3166	0.2245	0.1894	0.1255	0.1616	32.4988	4.2224
		5D	0.1407	0.2346	0.4015	0.2996	0.2709	0.1500	0.2053	44.7123	5.8019
		7D	0.2021	0.2599	0.4775	0.3266	0.3373	0.1828	0.2379	17.1457	2.3962
		Avg.	0.1147	0.1927	0.3426	0.2581	0.2296	0.1373	0.1749	66.1141	8.4455
	FourierGNN	1D	0.0339	0.0703	0.1442	0.0825	0.0631	0.0563	0.0809	0.6083	0.1425
		3D	0.0851	0.1359	0.2816	0.1522	0.1320	0.0988	0.1493	0.9670	0.2502
		5D	0.1331	0.1885	0.3656	0.2117	0.1916	0.1290	0.1920	1.6289	0.3800
		7D	0.2053	0.2240	0.4330	0.2525	0.2511	0.1483	0.2250	1.0897	0.3536
		Avg.	0.1144	0.1547	0.3061	0.1747	0.1594	0.1081	0.1618	1.0735	0.2816
	StemGNN	1D	0.0391	0.1055	0.1724	0.0912	0.0873	0.0665	0.0898	1.2556	0.2384
		3D	0.1283	0.2207	0.3498	0.2164	0.2680	0.1644	0.1796	1.5368	0.3830
		5D	0.2199	0.2945	0.4663	0.3239	0.5381	0.2094	0.2414	1.6949	0.4985
		7D	0.3149	0.3582	0.5362	0.3986	0.4688	0.2426	0.3031	2.0180	0.5801
		Avg.	0.1755	0.2447	0.3812	0.2575	0.3406	0.1707	0.2035	1.6263	0.4250
LLM	GPT4TS	1D	0.0473	0.0949	0.1828	0.0977	0.0819	0.0735	0.1124	0.1921	0.1103
		3D	0.1163	0.1995	0.3605	0.2009	0.1762	0.1251	0.1953	0.3751	0.2186
		5D	0.1908	0.2827	0.4853	0.2619	0.2654	0.1534	0.2487	0.4691	0.2947
		7D	0.2394	0.3739	0.5955	0.3207	0.3350	0.1826	0.2946	0.5944	0.3670
		Avg.	0.1484	0.2377	0.4060	0.2203	0.2146	0.1337	0.2127	0.4077	0.2477
	AutoTimes	1D	0.0375	0.0718	0.1582	0.0879	0.0687	0.0581	0.0900	0.1373	0.0887
		3D	0.0889	0.1438	0.3015	0.1598	0.1410	0.0984	0.1615	0.2986	0.1742
		5D	0.1406	0.2011	0.3952	0.2175	0.2057	0.1265	0.2115	0.4012	0.2374
		7D	0.1944	0.2496	0.4659	0.2653	0.2754	0.1485	0.2510	0.4759	0.2908
		Avg.	0.1154	0.1666	0.3302	0.1826	0.1727	0.1079	0.1785	0.3283	0.1978

Table 22: Benchmark(SEDI10) on part 2(Miami area) stations(MLP,CNN,Transformer)

	Method	T	S0	S1	S2	S3	S4	S5	S6	S7	Avg.
MLP	MLP	1D	0.8741	0.8301	0.8503	0.8179	0.8890	0.5135	0.4864	0.7414	0.7503
		3D	0.8258	0.7763	0.8076	0.7682	0.8627	0.4220	0.4150	0.6270	0.6881
		5D	0.7627	0.7409	0.7604	0.7023	0.8228	0.3802	0.3853	0.6126	0.6459
		7D	0.7108	0.7069	0.7572	0.6765	0.8028	0.3550	0.3867	0.5522	0.6185
		Avg.	**0.7933**	**0.7636**	**0.7939**	**0.7412**	**0.8443**	**0.4177**	**0.4183**	**0.6333**	**0.6757**
	TSMixer	1D	0.8506	0.7672	0.8000	0.7572	0.8709	0.4446	0.4225	0.5891	0.6878
		3D	0.7622	0.6598	0.7016	0.6497	0.7979	0.3370	0.3233	0.4826	0.5893
		5D	0.6958	0.5955	0.6414	0.5820	0.7421	0.2694	0.2707	0.4073	0.5255
		7D	0.6433	0.5499	0.5962	0.5360	0.6957	0.2335	0.2379	0.3550	0.4810
		Avg.	0.7380	0.6431	0.6848	0.6312	0.7767	0.3211	0.3136	0.4585	0.5709
	NLinear	1D	0.8486	0.7786	0.8039	0.7660	0.8697	0.4931	0.4452	0.7005	0.7132
		3D	0.7606	0.6705	0.7059	0.6597	0.7969	0.3753	0.3424	0.5532	0.6081
		5D	0.6961	0.6019	0.6452	0.5928	0.7418	0.3265	0.2868	0.4605	0.5439
		7D	0.6445	0.5544	0.6000	0.5465	0.6962	0.2868	0.2522	0.3980	0.4973
		Avg.	0.7374	0.6514	0.6887	0.6412	0.7761	0.3704	0.3316	0.5280	0.5906
CNN	TCN	1D	0.7593	0.7900	0.8204	0.6993	0.7827	0.2702	0.4436	0.2651	0.6038
		3D	0.7316	0.6984	0.7447	0.5739	0.7257	0.1869	0.3902	0.1932	0.5306
		5D	0.5618	0.6040	0.6806	0.5003	0.6732	0.1566	0.3651	0.1776	0.4649
		7D	0.6365	0.5666	0.6778	0.4988	0.5719	0.1185	0.2944	0.1443	0.4386
		Avg.	0.6723	0.6647	0.7309	0.5681	0.6884	0.1831	0.3733	0.1951	0.5095
	ModernTCN	1D	0.8450	0.7649	0.7755	0.7226	0.8710	0.4506	0.4383	0.6989	0.6959
		3D	0.7464	0.6562	0.6524	0.5939	0.7859	0.3206	0.3270	0.5369	0.5774
		5D	0.6737	0.5673	0.5828	0.5158	0.7293	0.2661	0.2691	0.4358	0.5050
		7D	0.6180	0.5240	0.5309	0.4738	0.6825	0.2327	0.2278	0.3797	0.4587
		Avg.	0.7208	0.6281	0.6354	0.5766	0.7672	0.3175	0.3156	0.5128	0.5592
	TimesNet	1D	0.8231	0.7314	0.7478	0.7043	0.8409	0.3910	0.3584	0.6258	0.6528
		3D	0.7335	0.6302	0.6612	0.6004	0.7609	0.2651	0.2711	0.4914	0.5517
		5D	0.6745	0.5599	0.5876	0.5382	0.7072	0.2241	0.2204	0.4053	0.4896
		7D	0.6158	0.5245	0.5430	0.4907	0.6482	0.1888	0.1921	0.3477	0.4438
		Avg.	0.7117	0.6115	0.6349	0.5834	0.7393	0.2672	0.2605	0.4675	0.5345
Transformer	iTransformer	1D	0.8637	0.8038	0.8207	0.7756	0.8762	0.4669	0.4545	0.7247	0.7233
		3D	0.7686	0.7074	0.7133	0.6568	0.8054	0.3441	0.3459	0.5810	0.6153
		5D	0.6971	0.6270	0.6584	0.5889	0.7435	0.2774	0.2809	0.4665	0.5424
		7D	0.6451	0.5751	0.6083	0.5437	0.6964	0.2396	0.2535	0.3979	0.4949
		Avg.	0.7436	0.6783	0.7002	0.6412	0.7803	0.3320	0.3337	<u>0.5425</u>	0.5940
	PatchTST	1D	0.8595	0.7994	0.8269	0.7725	0.8746	0.4772	0.4750	0.7220	0.7259
		3D	0.7678	0.6914	0.7225	0.6534	0.7956	0.3561	0.3503	0.5633	0.6125
		5D	0.7022	0.6194	0.6605	0.5880	0.7365	0.3018	0.2951	0.4659	0.5462
		7D	0.6513	0.5667	0.6103	0.5407	0.6906	0.2540	0.2564	0.4046	0.4968
		Avg.	0.7452	0.6692	0.7051	0.6386	0.7743	<u>0.3473</u>	0.3442	0.5389	0.5954

Table 23: Benchmark(SEDI10) on part 2(Miami area) stations(RNN,GNN,LLM)

	Method	T	S0	S1	S2	S3	S4	S5	S6	S7	Avg.
RNN	LSTM	1D	0.8360	0.7782	0.8055	0.7590	0.8905	0.4015	0.3896	0.6608	0.6901
		3D	0.7519	0.6710	0.6999	0.6089	0.8233	0.2542	0.2837	0.5149	0.5760
		5D	0.6692	0.6430	0.6611	0.5801	0.7650	0.2298	0.2401	0.3879	0.5220
		7D	0.6402	0.5991	0.6269	0.4682	0.7060	0.1930	0.2364	0.3669	0.4796
		Avg.	0.7243	0.6728	0.6984	0.6041	0.7962	0.2696	0.2874	0.4826	0.5669
	DeepAR	1D	0.8152	0.7886	0.7825	0.7384	0.8582	0.3910	0.4268	0.6741	0.6843
		3D	0.7450	0.6511	0.7208	0.6443	0.8068	0.2397	0.2744	0.5008	0.5729
		5D	0.6943	0.6334	0.6518	0.5570	0.7574	0.2019	0.2405	0.4519	0.5235
		7D	0.6155	0.5923	0.6195	0.5072	0.7319	0.2241	0.2245	0.3572	0.4840
		Avg.	0.7175	0.6664	0.6936	0.6117	0.7886	0.2642	0.2916	0.4960	0.5662
	DilatedRNN	1D	0.8692	0.7880	0.8197	0.7892	0.8793	0.4684	0.4362	0.6942	0.7180
		3D	0.7796	0.7056	0.7306	0.6319	0.7575	0.2916	0.3150	0.5490	0.5951
		5D	0.6999	0.6585	0.6645	0.5788	0.7220	0.2488	0.2843	0.4543	0.5389
		7D	0.6469	0.5807	0.5970	0.5429	0.6725	0.2202	0.2308	0.3934	0.4856
		Avg.	0.7489	0.6832	0.7029	0.6357	0.7578	0.3072	0.3166	0.5227	0.5844
GNN	GCN	1D	0.8394	0.7752	0.8086	0.7437	0.8631	0.4585	0.4685	0.6737	0.7038
		3D	0.7913	0.7114	0.7760	0.6987	0.8134	0.4180	0.3846	0.5844	0.6472
		5D	0.7726	0.6603	0.7433	0.6416	0.8037	0.3545	0.3369	0.5404	0.6067
		7D	0.7195	0.6370	0.7368	0.6266	0.7624	0.2961	0.3282	0.5247	0.5789
		Avg.	0.7807	0.6960	0.7662	0.6777	0.8107	0.3818	0.3795	0.5808	0.6342
	FourierGNN	1D	0.8842	0.8339	0.8446	0.8034	0.8794	0.4924	0.4661	0.5660	0.7213
		3D	0.8071	0.7862	0.7878	0.6988	0.8383	0.3740	0.3840	0.5319	0.6510
		5D	0.7275	0.6700	0.7674	0.6396	0.8200	0.3434	0.3735	0.5033	0.6056
		7D	0.7208	0.6275	0.7505	0.6695	0.7939	0.3157	0.3493	0.4627	0.5863
		Avg.	<u>0.7849</u>	<u>0.7294</u>	<u>0.7876</u>	<u>0.7028</u>	<u>0.8329</u>	0.3814	<u>0.3932</u>	0.5160	<u>0.6410</u>
	StemGNN	1D	0.8646	0.7785	0.7954	0.7146	0.8769	0.4439	0.4379	0.4597	0.6714
		3D	0.7744	0.6132	0.7012	0.6006	0.7568	0.2438	0.2951	0.3788	0.5455
		5D	0.6814	0.6045	0.6612	0.5584	0.5665	0.2083	0.2529	0.3115	0.4806
		7D	0.6648	0.5171	0.6013	0.4415	0.5642	0.1738	0.2100	0.2598	0.4291
		Avg.	0.7463	0.6283	0.6898	0.5788	0.6911	0.2674	0.2990	0.3525	0.5316
LLM	GPT4TS	1D	0.8216	0.7340	0.7701	0.7331	0.8414	0.3715	0.3565	0.6124	0.6551
		3D	0.7389	0.6277	0.6603	0.6071	0.7518	0.2678	0.2655	0.4756	0.5493
		5D	0.6746	0.5605	0.5939	0.5327	0.6894	0.2279	0.2255	0.3964	0.4876
		7D	0.6139	0.5161	0.5541	0.4812	0.6419	0.1929	0.1982	0.3275	0.4407
		Avg.	0.7123	0.6096	0.6446	0.5885	0.7311	0.2650	0.2614	0.4530	0.5332
	AutoTimes	1D	0.8574	0.7975	0.8157	0.7598	0.8726	0.4113	0.4080	0.7040	0.7033
		3D	0.7652	0.6858	0.7175	0.6466	0.8032	0.3067	0.3215	0.5668	0.6017
		5D	0.7002	0.6266	0.6601	0.5837	0.7408	0.2576	0.2676	0.4668	0.5379
		7D	0.6453	0.5683	0.6149	0.5348	0.6967	0.2213	0.2319	0.4040	0.4896
		Avg.	0.7420	0.6695	0.7021	0.6312	0.7783	0.2992	0.3073	0.5354	0.5831

Table 24: Benchmark(SEDI5) on part 2(Miami area) stations(MLP,CNN,Transformer)

	Method	T	S0	S1	S2	S3	S4	S5	S6	S7	Avg.
MLP	MLP	1D	0.8203	0.8018	0.8453	0.6927	0.8843	0.3386	0.3853	0.6361	0.6755
		3D	0.7427	0.7459	0.8080	0.6251	0.8496	0.2768	0.3320	0.5376	0.6147
		5D	0.6747	0.7152	0.7456	0.5607	0.8084	0.2658	0.3134	0.5075	0.5739
		7D	0.6180	0.6833	0.7520	0.5447	0.7774	0.2555	0.3284	0.4584	0.5522
		Avg.	**0.7139**	**0.7366**	**0.7878**	**0.6058**	**0.8299**	**0.2842**	**0.3398**	**0.5349**	**0.6041**
	TSMixer	1D	0.7829	0.7231	0.7853	0.6187	0.8603	0.2823	0.3224	0.4521	0.6034
		3D	0.6518	0.5942	0.6704	0.5094	0.7743	0.2085	0.2223	0.3548	0.4982
		5D	0.5559	0.5210	0.5950	0.4429	0.7069	0.1762	0.1753	0.2891	0.4328
		7D	0.4809	0.4667	0.5379	0.3967	0.6516	0.1424	0.1484	0.2437	0.3835
		Avg.	0.6179	0.5763	0.6471	0.4919	0.7483	0.2023	0.2171	0.3349	0.4795
	NLinear	1D	0.7842	0.7341	0.7857	0.6272	0.8583	0.3155	0.3398	0.5837	0.6286
		3D	0.6549	0.6065	0.6750	0.5297	0.7740	0.2379	0.2452	0.4378	0.5201
		5D	0.5606	0.5291	0.6000	0.4519	0.7081	0.2114	0.1966	0.3530	0.4513
		7D	0.4881	0.4734	0.5439	0.4077	0.6537	0.1884	0.1690	0.2964	0.4026
		Avg.	0.6220	0.5858	0.6512	0.5041	0.7485	0.2383	0.2377	0.4177	0.5007
CNN	TCN	1D	0.6732	0.7264	0.8085	0.4636	0.6769	0.1780	0.3211	0.1701	0.5022
		3D	0.6003	0.6072	0.7341	0.3332	0.6076	0.1251	0.2746	0.1106	0.4241
		5D	0.3759	0.4967	0.6449	0.3185	0.5094	0.0967	0.2207	0.1031	0.3457
		7D	0.3713	0.4688	0.6172	0.2808	0.4117	0.0658	0.1851	0.0710	0.3089
		Avg.	0.5052	0.5748	0.7012	0.3490	0.5514	0.1164	0.2504	0.1137	0.3952
	ModernTCN	1D	0.7753	0.7152	0.7470	0.5845	0.8521	0.2784	0.3290	0.5653	0.6058
		3D	0.6425	0.5891	0.6141	0.4597	0.7544	0.1988	0.2123	0.4098	0.4851
		5D	0.5456	0.4885	0.5393	0.3821	0.6921	0.1645	0.1691	0.3149	0.4120
		7D	0.4749	0.4345	0.4788	0.3437	0.6387	0.1410	0.1413	0.2653	0.3648
		Avg.	0.6096	0.5568	0.5948	0.4425	0.7343	0.1957	0.2129	0.3888	0.4669
	TimesNet	1D	0.7487	0.6768	0.7300	0.5653	0.8128	0.2235	0.2528	0.4910	0.5626
		3D	0.6236	0.5582	0.6225	0.4521	0.7272	0.1473	0.1642	0.3592	0.4568
		5D	0.5369	0.4827	0.5380	0.3935	0.6590	0.1184	0.1226	0.2851	0.3920
		7D	0.4596	0.4353	0.4911	0.3486	0.5869	0.1043	0.0991	0.2359	0.3451
		Avg.	0.5922	0.5383	0.5954	0.4399	0.6965	0.1484	0.1597	0.3428	0.4391
Transformer	iTransformer	1D	0.7985	0.7670	0.8047	0.6444	0.8568	0.2787	0.3549	0.6033	0.6385
		3D	0.6767	0.6518	0.6871	0.5192	0.7699	0.1998	0.2785	0.4604	0.5304
		5D	0.5748	0.5559	0.6193	0.4492	0.6981	0.1652	0.1791	0.3529	0.4493
		7D	0.5036	0.4938	0.5666	0.4040	0.6433	0.1402	0.1705	0.2874	0.4012
		Avg.	0.6384	0.6171	0.6694	0.5042	0.7420	0.1960	0.2457	0.4260	0.5049
	PatchTST	1D	0.7948	0.7663	0.8131	0.6364	0.8546	0.2859	0.3648	0.6001	0.6395
		3D	0.6706	0.6408	0.6990	0.5158	0.7641	0.2161	0.2558	0.4454	0.5260
		5D	0.5757	0.5538	0.6241	0.4486	0.6977	0.1833	0.2059	0.3516	0.4551
		7D	0.5016	0.4906	0.5665	0.4029	0.6450	0.1581	0.1751	0.2979	0.4047
		Avg.	0.6357	0.6129	0.6757	0.5009	0.7404	0.2108	0.2504	0.4238	0.5063

Table 25: Benchmark(SEDI5) on part 2(Miami area) stations(RNN,GNN,LLM)

	Method	T	S0	S1	S2	S3	S4	S5	S6	S7	Avg.
RNN	LSTM	1D	0.7782	0.7372	0.7975	0.6088	0.8707	0.2226	0.2661	0.5371	0.6023
		3D	0.6193	0.6102	0.6635	0.4559	0.7919	0.1437	0.1772	0.4233	0.4856
		5D	0.5323	0.5690	0.6237	0.3969	0.7194	0.1253	0.1418	0.3040	0.4266
		7D	0.4947	0.4718	0.5666	0.3301	0.6305	0.1009	0.1329	0.2593	0.3734
		Avg.	0.6061	0.5971	0.6628	0.4479	0.7531	0.1481	0.1795	0.3809	0.4720
	DeepAR	1D	0.7506	0.7444	0.7702	0.5797	0.8298	0.2470	0.2639	0.5466	0.5915
		3D	0.6252	0.6021	0.6902	0.4647	0.7750	0.1426	0.1678	0.4273	0.4869
		5D	0.5361	0.5584	0.5951	0.3839	0.7114	0.1120	0.1259	0.3603	0.4229
		7D	0.4436	0.5078	0.5647	0.3391	0.6956	0.0967	0.1104	0.2599	0.3772
		Avg.	0.5889	0.6032	0.6551	0.4419	0.7530	0.1496	0.1670	0.3985	0.4696
	DilatedRNN	1D	0.8054	0.7393	0.8027	0.6504	0.8471	0.3023	0.3125	0.5724	0.6290
		3D	0.6871	0.6505	0.7110	0.5126	0.7126	0.1749	0.2102	0.4345	0.5117
		5D	0.5834	0.5993	0.6388	0.4463	0.6757	0.1499	0.1713	0.3450	0.4512
		7D	0.5413	0.4900	0.5612	0.4197	0.6188	0.1372	0.1388	0.2847	0.3990
		Avg.	0.6543	0.6198	0.6784	0.5072	0.7136	0.1911	0.2082	0.4092	0.4977
GNN	GCN	1D	0.7502	0.7320	0.8148	0.6321	0.8439	0.3394	0.3757	0.5786	0.6333
		3D	0.6899	0.6528	0.7953	0.5605	0.7889	0.2891	0.3176	0.5118	0.5757
		5D	0.6957	0.5923	0.7658	0.5245	0.7818	0.2388	0.2643	0.4678	0.5414
		7D	0.6440	0.5577	0.7625	0.4949	0.7402	0.2244	0.2587	0.4532	0.5169
		Avg.	0.6949	0.6337	0.7846	0.5530	0.7887	0.2729	0.3041	0.5029	0.5668
	FourierGNN	1D	0.8279	0.7998	0.8378	0.6750	0.8669	0.3249	0.3500	0.4899	0.6465
		3D	0.7233	0.7394	0.7814	0.5680	0.8201	0.2450	0.2873	0.4436	0.5760
		5D	0.6198	0.6098	0.7593	0.5051	0.7966	0.2324	0.2902	0.4006	0.5267
		7D	0.6588	0.5544	0.7447	0.5131	0.7637	0.2154	0.2739	0.4022	0.5158
		Avg.	0.7074	0.6758	0.7808	0.5653	0.8118	0.2544	0.3003	0.4340	0.5662
	StemGNN	1D	0.8015	0.7321	0.7884	0.5807	0.8594	0.2851	0.3385	0.3684	0.5943
		3D	0.6608	0.5265	0.7032	0.4503	0.7169	0.1409	0.1868	0.2969	0.4603
		5D	0.5775	0.5009	0.6416	0.4189	0.3915	0.1244	0.1569	0.2450	0.3821
		7D	0.4858	0.4275	0.5752	0.2864	0.4690	0.0999	0.1371	0.1949	0.3345
		Avg.	0.6314	0.5468	0.6771	0.4341	0.6092	0.1626	0.2048	0.2763	0.4428
LLM	GPT4TS	1D	0.7424	0.6726	0.7407	0.5721	0.8175	0.2057	0.2580	0.4738	0.5604
		3D	0.6382	0.5471	0.6227	0.4534	0.7177	0.1509	0.1622	0.3482	0.4550
		5D	0.5484	0.4662	0.5447	0.3914	0.6360	0.1230	0.1265	0.2813	0.3897
		7D	0.4653	0.4102	0.4972	0.3462	0.5821	0.1040	0.1057	0.2184	0.3411
		Avg.	0.5986	0.5240	0.6013	0.4408	0.6883	0.1459	0.1631	0.3304	0.4366
	AutoTimes	1D	0.7923	0.7578	0.8113	0.6238	0.8590	0.2414	0.3024	0.5828	0.6213
		3D	0.6587	0.6310	0.6989	0.5032	0.7737	0.1776	0.2137	0.4392	0.5120
		5D	0.5670	0.5597	0.6312	0.4430	0.7028	0.1544	0.1690	0.3459	0.4466
		7D	0.4857	0.4895	0.5722	0.3936	0.6512	0.1312	0.1424	0.2904	0.3945
		Avg.	0.6259	0.6095	0.6784	0.4909	0.7467	0.1761	0.2069	0.4146	0.4936

Table 26: Benchmark(SEDI1) on part 2(Miami area) stations(MLP,CNN,Transformer)

	Method	T	S0	S1	S2	S3	S4	S5	S6	S7	Avg.
MLP	MLP	1D	0.6392	0.7486	0.7968	0.4636	0.7523	0.1510	0.1849	0.4622	0.5248
		3D	0.5460	0.6948	0.7434	0.4294	0.6635	0.1429	0.1752	0.3631	0.4698
		5D	0.5736	0.6829	0.6508	0.3551	0.6734	0.1527	0.1643	0.3667	0.4524
		7D	0.5641	0.6625	0.7139	0.4331	0.6920	0.1401	0.1617	0.3547	0.4653
		Avg.	**0.5807**	**0.6972**	**0.7263**	**0.4203**	**0.6953**	0.1467	**0.1715**	**0.3867**	**0.4781**
	TSMixer	1D	0.5899	0.6011	0.6559	0.3407	0.6954	0.1186	0.1495	0.2268	0.4222
		3D	0.4351	0.4299	0.4696	0.2279	0.5486	0.0778	0.0867	0.1369	0.3016
		5D	0.3255	0.3379	0.3531	0.1776	0.4431	0.0599	0.0690	0.1006	0.2333
		7D	0.2522	0.2693	0.2787	0.1494	0.3661	0.0524	0.0697	0.0791	0.1896
		Avg.	0.4007	0.4096	0.4393	0.2239	0.5133	0.0772	0.0937	0.1359	0.2867
	NLinear	1D	0.6032	0.6324	0.6721	0.3915	0.7185	0.1412	0.1508	0.3811	0.4613
		3D	0.4433	0.4556	0.4838	0.2745	0.5680	0.1052	0.1023	0.2296	0.3328
		5D	0.3408	0.3553	0.3639	0.2278	0.4626	0.0956	0.0801	0.1734	0.2624
		7D	0.2637	0.2851	0.2905	0.1992	0.3820	0.0851	0.0702	0.1435	0.2149
		Avg.	0.4128	0.4321	0.4526	0.2732	0.5328	0.1068	0.1008	0.2319	0.3179
CNN	TCN	1D	0.1324	0.4480	0.7226	0.2066	0.2128	0.0640	0.1211	0.0506	0.2448
		3D	0.0330	0.3732	0.5677	0.1723	0.1441	0.0387	0.1129	0.0265	0.1835
		5D	0.0258	0.2706	0.4580	0.1274	0.1506	0.0312	0.1130	0.0283	0.1506
		7D	0.0571	0.2566	0.4746	0.1193	0.1263	0.0128	0.0770	0.0104	0.1418
		Avg.	0.0621	0.3371	0.5557	0.1564	0.1584	0.0367	0.1060	0.0289	0.1802
	ModernTCN	1D	0.6055	0.5939	0.6605	0.3129	0.7173	0.1196	0.1522	0.3788	0.4426
		3D	0.4336	0.4005	0.4627	0.1837	0.5687	0.0721	0.0722	0.2224	0.3020
		5D	0.3390	0.2918	0.3464	0.1267	0.4670	0.0555	0.0590	0.1442	0.2287
		7D	0.2672	0.2162	0.2717	0.1025	0.3878	0.0519	0.0415	0.1163	0.1819
		Avg.	0.4113	0.3756	0.4353	0.1814	0.5352	0.0748	0.0812	0.2154	0.2888
	TimesNet	1D	0.5404	0.5278	0.6337	0.2851	0.6289	0.0906	0.0988	0.2989	0.3880
		3D	0.4211	0.3841	0.4394	0.1624	0.5016	0.0434	0.0522	0.1626	0.2708
		5D	0.3299	0.2943	0.3291	0.1157	0.3647	0.0295	0.0269	0.1104	0.2001
		7D	0.2249	0.2508	0.2616	0.0851	0.3262	0.0234	0.0230	0.0944	0.1612
		Avg.	0.3791	0.3643	0.4160	0.1621	0.4554	0.0467	0.0502	0.1666	0.2550
Transformer	iTransformer	1D	0.6163	0.6752	0.7437	0.3883	0.7228	0.1268	0.1668	0.4121	0.4815
		3D	0.4566	0.5015	0.5470	0.2322	0.5716	0.0745	0.0972	0.2676	0.3435
		5D	0.3503	0.3820	0.4225	0.1779	0.4512	0.0560	0.0565	0.1561	0.2566
		7D	0.2829	0.2964	0.3415	0.1450	0.3636	0.0446	0.0921	0.1163	0.2103
		Avg.	0.4265	0.4638	0.5137	0.2359	0.5273	0.0755	0.1031	0.2380	0.3230
	PatchTST	1D	0.6112	0.6690	0.7429	0.3695	0.7238	0.1261	0.1691	0.4179	0.4787
		3D	0.4618	0.4940	0.5613	0.2286	0.5741	0.0822	0.0949	0.2473	0.3430
		5D	0.3572	0.3782	0.4444	0.1734	0.4708	0.0668	0.0695	0.1708	0.2664
		7D	0.2791	0.3030	0.3527	0.1388	0.3865	0.0589	0.0600	0.1358	0.2143
		Avg.	0.4273	0.4610	0.5253	0.2276	0.5388	0.0835	0.0984	0.2429	0.3256

Table 27: Benchmark(SEDI1) on part 2(Miami area) stations(RNN,GNN,LLM)

	Method	T	S0	S1	S2	S3	S4	S5	S6	S7	Avg.
RNN	LSTM	1D	0.5173	0.5951	0.6803	0.2523	0.4421	0.0731	0.0896	0.3249	0.3718
		3D	0.3565	0.3467	0.4334	0.1171	0.2033	0.0380	0.0398	0.1530	0.2110
		5D	0.3267	0.2902	0.3336	0.0565	0.2339	0.0143	0.0343	0.1030	0.1740
		7D	0.2477	0.2608	0.4109	0.0553	0.0981	0.0078	0.0051	0.0914	0.1471
		Avg.	0.3621	0.3732	0.4646	0.1203	0.2443	0.0333	0.0422	0.1681	0.2260
	DeepAR	1D	0.4712	0.6332	0.6489	0.2446	0.4433	0.0756	0.1161	0.3283	0.3701
		3D	0.3647	0.3977	0.4097	0.0820	0.1804	0.0310	0.0387	0.1553	0.2074
		5D	0.2339	0.2331	0.2853	0.0355	0.1330	0.0220	0.0048	0.1158	0.1329
		7D	0.1074	0.2155	0.2837	0.0609	0.0813	0.0165	0.0063	0.1074	0.1099
		Avg.	0.2943	0.3699	0.4069	0.1058	0.2095	0.0363	0.0415	0.1767	0.2051
	DilatedRNN	1D	0.6372	0.5916	0.7119	0.4065	0.7022	0.1088	0.1333	0.3922	0.4605
		3D	0.5222	0.4714	0.6236	0.2306	0.4730	0.0741	0.0689	0.2576	0.3402
		5D	0.3632	0.4556	0.5025	0.1754	0.4427	0.0560	0.0513	0.1841	0.2789
		7D	0.3681	0.3293	0.4419	0.1630	0.4273	0.0491	0.0411	0.1600	0.2475
		Avg.	0.4727	0.4620	0.5700	0.2439	0.5113	0.0720	0.0737	0.2485	0.3317
GNN	GCN	1D	0.5814	0.5680	0.7359	0.3744	0.6712	0.1554	0.1852	0.4307	0.4628
		3D	0.5052	0.5117	0.7286	0.2892	0.5979	0.1691	0.1555	0.3875	0.4181
		5D	0.4462	0.4254	0.6934	0.2584	0.5692	0.1573	0.1310	0.3559	0.3796
		7D	0.4309	0.3783	0.6980	0.2593	0.5114	0.1639	0.1560	0.3369	0.3668
		Avg.	0.4909	0.4709	0.7140	0.2953	0.5874	**0.1614**	0.1569	0.3777	0.4068
	FourierGNN	1D	0.6570	0.6977	0.7677	0.4359	0.7147	0.1492	0.1707	0.3647	0.4947
		3D	0.5526	0.6366	0.6920	0.3083	0.6153	0.1285	0.1482	0.2883	0.4212
		5D	0.4619	0.4865	0.6791	0.2633	0.5934	0.1286	0.1450	0.2778	0.3794
		7D	0.6103	0.4415	0.7151	0.3320	0.6158	0.1261	0.1514	0.2791	0.4089
		Avg.	0.5705	0.5656	0.7135	0.3349	0.6348	0.1331	0.1538	0.3025	0.4261
	StemGNN	1D	0.5891	0.5290	0.7186	0.3042	0.6594	0.1308	0.1546	0.2231	0.4136
		3D	0.3107	0.2996	0.6110	0.1650	0.4861	0.0484	0.0712	0.1342	0.2658
		5D	0.3170	0.2849	0.5104	0.1400	0.1212	0.0405	0.0469	0.1600	0.2026
		7D	0.2300	0.2427	0.3921	0.0846	0.1728	0.0315	0.0513	0.0838	0.1611
		Avg.	0.3617	0.3391	0.5580	0.1735	0.3599	0.0628	0.0810	0.1503	0.2608
LLM	GPT4TS	1D	0.5577	0.5380	0.6412	0.2952	0.6627	0.0716	0.0904	0.2589	0.3895
		3D	0.4106	0.3726	0.4585	0.1692	0.4833	0.0402	0.0416	0.1690	0.2681
		5D	0.3439	0.2834	0.3346	0.1284	0.3308	0.0317	0.0291	0.1154	0.1997
		7D	0.2543	0.2254	0.2716	0.0894	0.2808	0.0250	0.0233	0.0790	0.1561
		Avg.	0.3917	0.3548	0.4265	0.1706	0.4394	0.0421	0.0461	0.1556	0.2533
	AutoTimes	1D	0.5904	0.6595	0.7269	0.3583	0.6964	0.1035	0.1381	0.3728	0.4557
		3D	0.4307	0.4794	0.5365	0.2296	0.5553	0.0609	0.0708	0.2425	0.3257
		5D	0.3386	0.3883	0.4334	0.2038	0.4503	0.0524	0.0534	0.1652	0.2607
		7D	0.2539	0.2968	0.3465	0.1403	0.3743	0.0457	0.0386	0.1488	0.2056
		Avg.	0.4034	0.4560	0.5108	0.2330	0.5191	0.0656	0.0752	0.2323	0.3119

Table 28: Benchmark(MAE) on part 3(Fort Myers area) stations(MLP,CNN,Transformer)

	Method	T	S0	S1	S2	S3	S4	S5	S6	S7	Avg.
MLP	MLP	1D	0.0251	0.0246	0.0207	0.0463	0.0302	0.0628	0.0505	0.0380	0.0373
		3D	0.0526	0.0607	0.0523	0.0777	0.0603	0.1228	0.0977	0.0757	0.0750
		5D	0.0839	0.0940	0.0814	0.1102	0.0958	0.1610	0.1305	0.1105	0.1084
		7D	0.1005	0.1202	0.1013	0.1327	0.1143	0.1891	0.1558	0.1281	0.1303
		Avg.	0.0655	**0.0749**	0.0639	0.0917	0.0752	<u>0.1339</u>	<u>0.1086</u>	0.0881	0.0877
	TSMixer	1D	0.0247	0.0327	0.0265	0.0477	0.0353	0.0684	0.0548	0.0461	0.0420
		3D	0.0503	0.0683	0.0560	0.0821	0.0665	0.1226	0.0987	0.0811	0.0782
		5D	0.0734	0.0989	0.0827	0.1093	0.0899	0.1596	0.1307	0.1108	0.1069
		7D	0.0946	0.1254	0.1081	0.1330	0.1100	0.1873	0.1561	0.1368	0.1314
		Avg.	0.0608	0.0813	0.0683	0.0930	0.0754	0.1345	0.1101	0.0937	0.0896
	NLinear	1D	0.0184	0.0243	0.0200	0.0427	0.0307	0.0615	0.0480	0.0377	0.0354
		3D	0.0463	0.0613	0.0516	0.0798	0.0636	0.1196	0.0947	0.0752	0.0740
		5D	0.0705	0.0931	0.0796	0.1089	0.0880	0.1577	0.1279	0.1055	0.1039
		7D	0.0933	0.1207	0.1053	0.1334	0.1078	0.1861	0.1545	0.1322	0.1292
		Avg.	**0.0571**	**0.0749**	0.0641	0.0912	0.0725	**0.1312**	**0.1063**	0.0877	<u>0.0856</u>
CNN	TCN	1D	0.0577	0.0505	0.0318	0.0970	0.1129	0.0920	0.2015	0.1758	0.1024
		3D	0.0968	0.1382	0.0689	0.1048	0.1373	0.1937	0.1485	0.2512	0.1424
		5D	0.1406	0.1002	0.0931	0.1558	0.1816	0.2363	0.1885	0.2557	0.1690
		7D	0.2256	0.1780	0.1241	0.1633	0.2116	0.2240	0.2846	0.2676	0.2098
		Avg.	0.1302	0.1167	0.0795	0.1302	0.1608	0.1865	0.2058	0.2376	0.1559
	ModernTCN	1D	0.0221	0.0265	0.0205	0.0443	0.0278	0.0654	0.0491	0.0357	0.0364
		3D	0.0567	0.0702	0.0510	0.0861	0.0603	0.1332	0.1010	0.0719	0.0788
		5D	0.0871	0.1048	0.0834	0.1215	0.0883	0.1774	0.1384	0.1015	0.1128
		7D	0.1202	0.1362	0.1056	0.1499	0.1094	0.2057	0.1686	0.1280	0.1405
		Avg.	0.0715	0.0845	0.0651	0.1005	0.0714	0.1454	0.1143	0.0843	0.0921
	TimesNet	1D	0.0199	0.0288	0.0242	0.0513	0.0445	0.0809	0.0651	0.0528	0.0459
		3D	0.0467	0.0651	0.0558	0.0875	0.0724	0.1426	0.1164	0.0866	0.0841
		5D	0.0703	0.0970	0.0838	0.1148	0.0988	0.1852	0.1484	0.1127	0.1139
		7D	0.0923	0.1284	0.1121	0.1438	0.1158	0.2145	0.1759	0.1417	0.1406
		Avg.	0.0573	0.0798	0.0690	0.0993	0.0829	0.1558	0.1264	0.0984	0.0961
Transformer	iTransformer	1D	0.0190	0.0253	0.0192	0.0383	0.0278	0.0641	0.0482	0.0345	0.0346
		3D	0.0469	0.0617	0.0487	0.0726	0.0576	0.1244	0.0959	0.0706	0.0723
		5D	0.0709	0.0948	0.0766	0.1023	0.0834	0.1633	0.1331	0.0977	0.1028
		7D	0.0914	0.1226	0.1041	0.1275	0.1048	0.1889	0.1596	0.1214	0.1275
		Avg.	**0.0571**	0.0761	<u>0.0621</u>	**0.0852**	**0.0684**	0.1352	0.1092	**0.0811**	**0.0843**
	PatchTST	1D	0.0183	0.0241	0.0177	0.0381	0.0288	0.0637	0.0481	0.0349	0.0342
		3D	0.0464	0.0654	0.0545	0.0765	0.0588	0.1242	0.1007	0.0714	0.0747
		5D	0.0762	0.0951	0.0761	0.1057	0.0835	0.1651	0.1354	0.1014	0.1048
		7D	0.0984	0.1266	0.1032	0.1319	0.1053	0.1955	0.1608	0.1257	0.1309
		Avg.	0.0598	0.0778	0.0629	<u>0.0881</u>	<u>0.0691</u>	0.1371	0.1112	<u>0.0833</u>	0.0862

Table 29: Benchmark(MAE) on part 3(Fort Myers area) stations(RNN,GNN,LLM)

	Method	T	S0	S1	S2	S3	S4	S5	S6	S7	Avg.
RNN	LSTM	1D	0.0486	0.0447	0.0393	0.0640	0.0465	0.1120	0.0839	0.0606	0.0625
		3D	0.0895	0.0878	0.0788	0.1048	0.0828	0.1775	0.1299	0.1091	0.1075
		5D	0.1246	0.1247	0.1167	0.1344	0.1172	0.2057	0.1590	0.1281	0.1388
		7D	0.1621	0.1584	0.1496	0.1725	0.1389	0.2203	0.1823	0.1567	0.1676
		Avg.	0.1062	0.1039	0.0961	0.1189	0.0964	0.1789	0.1388	0.1136	0.1191
	DeepAR	1D	0.0569	0.0461	0.0381	0.0632	0.0486	0.1023	0.0763	0.0694	0.0626
		3D	0.0859	0.0950	0.0851	0.1180	0.0949	0.1640	0.1403	0.0993	0.1103
		5D	0.1086	0.1219	0.1137	0.1424	0.1388	0.2005	0.1742	0.1466	0.1433
		7D	0.1496	0.1542	0.1549	0.1745	0.1467	0.2247	0.2012	0.1485	0.1693
		Avg.	0.1003	0.1043	0.0980	0.1245	0.1073	0.1729	0.1480	0.1159	0.1214
	DilatedRNN	1D	0.0394	0.0268	0.0277	0.0441	0.0472	0.0691	0.0596	0.0372	0.0439
		3D	0.0726	0.0714	0.0679	0.0978	0.0648	0.1390	0.1186	0.0837	0.0895
		5D	0.1100	0.1028	0.0887	0.1257	0.0966	0.2000	0.1578	0.1128	0.1243
		7D	0.1312	0.1500	0.1175	0.1499	0.1234	0.2363	0.1870	0.1478	0.1554
		Avg.	0.0883	0.0877	0.0754	0.1043	0.0830	0.1611	0.1308	0.0954	0.1033
GNN	GCN	1D	0.0543	0.0596	0.0264	0.3354	0.1422	0.0789	0.0946	0.1151	0.1133
		3D	0.0858	0.0942	0.0598	0.3643	0.1756	0.1443	0.1374	0.1593	0.1526
		5D	0.1006	0.1192	0.0851	0.3859	0.2002	0.1767	0.1713	0.1952	0.1793
		7D	0.1196	0.1408	0.1141	0.4079	0.2197	0.2033	0.2068	0.2315	0.2055
		Avg.	0.0901	0.1034	0.0713	0.3734	0.1845	0.1508	0.1525	0.1753	0.1627
	FourierGNN	1D	10.0224	0.0295	0.0262	0.0462	0.0370	0.0732	0.0543	0.0436	0.0415
		3D	0.0548	0.0673	0.0538	0.0829	0.0784	0.1336	0.1087	0.0841	0.0830
		5D	0.0830	0.0978	0.0814	0.1153	0.0967	0.1668	0.1511	0.1109	0.1129
		7D	0.1064	0.1236	0.1114	0.1452	0.1335	0.2015	0.1823	0.1354	0.1424
		Avg.	0.0666	0.0796	0.0682	0.0974	0.0864	0.1438	0.1241	0.0935	0.0949
	StemGNN	1D	0.0636	0.0445	0.0335	0.0635	0.0586	0.1001	0.0599	0.0489	0.0591
		3D	0.1114	0.1001	0.0788	0.1273	0.1028	0.1524	0.1421	0.1408	0.1195
		5D	0.1690	0.1688	0.1022	0.1698	0.1352	0.1980	0.2366	0.2161	0.1745
		7D	0.2094	0.2090	0.1719	0.2016	0.1625	0.2325	0.2514	0.2730	0.2139
		Avg.	0.1384	0.1306	0.0966	0.1406	0.1148	0.1707	0.1725	0.1697	0.1417
LLM	GPT4TS	1D	0.0209	0.0287	0.0261	0.0482	0.0407	0.0740	0.0596	0.7614	0.1324
		3D	0.0467	0.0638	0.0553	0.0845	0.0730	0.1431	0.1105	0.0869	0.0830
		5D	0.0702	0.0946	0.0832	0.1141	0.0980	0.1823	0.1455	0.1120	0.1125
		7D	0.0909	0.1231	0.1105	0.1392	0.1160	0.2087	0.1715	0.1397	0.1375
		Avg.	0.0572	0.0776	0.0688	0.0965	0.0819	0.1520	0.1218	0.2750	0.1163
	AutoTimes	1D	0.0228	0.0282	0.0199	0.0429	0.0321	0.0680	0.0542	0.0407	0.0386
		3D	0.0475	0.0615	0.0486	0.0760	0.0638	0.1240	0.0993	0.0751	0.0745
		5D	0.0692	0.0965	0.0737	0.1075	0.0892	0.1632	0.1315	0.1056	0.1045
		7D	0.0921	0.1218	0.1038	0.1304	0.1083	0.1900	0.1573	0.1285	0.1290
		Avg.	0.0579	0.0770	**0.0615**	0.0892	0.0734	0.1363	0.1106	0.0875	0.0867

Table 30: Benchmark(MSE) on part 3(Fort Myers area) stations(MLP,CNN,Transformer)

	Method	T	S0	S1	S2	S3	S4	S5	S6	S7	Avg.
MLP	MLP	1D	0.0036	0.0046	0.0052	0.0165	0.0137	0.0368	0.0139	0.0095	0.0130
		3D	0.0156	0.0159	0.0199	0.0359	0.0318	0.0888	0.0374	0.0252	0.0338
		5D	0.0295	0.0300	0.0345	0.0538	0.0486	0.1253	0.0552	0.0426	0.0524
		7D	0.0461	0.0442	0.0494	0.0729	0.0635	0.1537	0.0701	0.0562	0.0695
		Avg.	**0.0237**	**0.0237**	0.0272	**0.0448**	**0.0394**	**0.1011**	**0.0441**	**0.0334**	**0.0422**
	TSMixer	1D	0.0047	0.0056	0.0070	0.0182	0.0163	0.0420	0.0159	0.0116	0.0152
		3D	0.0176	0.0174	0.0217	0.0381	0.0353	0.0983	0.0403	0.0280	0.0371
		5D	0.0348	0.0315	0.0372	0.0561	0.0522	0.1410	0.0605	0.0452	0.0573
		7D	0.0548	0.0465	0.0531	0.0740	0.0679	0.1735	0.0778	0.0624	0.0763
		Avg.	0.0280	0.0253	0.0297	0.0466	0.0429	0.1137	0.0486	0.0368	0.0465
	NLinear	1D	0.0031	0.0044	0.0050	0.0174	0.0158	0.0392	0.0138	0.0098	0.0136
		3D	0.0153	0.0159	0.0202	0.0378	0.0349	0.0970	0.0383	0.0263	0.0357
		5D	0.0321	0.0298	0.0362	0.0561	0.0518	0.1392	0.0581	0.0433	0.0558
		7D	0.0520	0.0449	0.0526	0.0742	0.0677	0.1724	0.0754	0.0607	0.0750
		Avg.	0.0256	0.0238	0.0285	0.0464	0.0426	0.1120	0.0464	0.0350	0.0450
CNN	TCN	1D	0.0925	0.0196	0.0078	0.0383	0.0743	0.0452	0.0900	0.1310	0.0623
		3D	0.1029	0.1063	0.0244	0.0440	0.0804	0.1231	0.0514	0.1998	0.0916
		5D	0.1186	0.0304	0.0379	0.0681	0.1249	0.1691	0.0767	0.2183	0.1055
		7D	0.1905	0.1158	0.0575	0.0808	0.1354	0.1655	0.1613	0.1934	0.1375
		Avg.	0.1261	0.0680	0.0319	0.0578	0.1038	0.1257	0.0949	0.1856	0.0992
	ModernTCN	1D	0.0048	0.0050	0.0045	0.0208	0.0142	0.0451	0.0148	0.0100	0.0149
		3D	0.0219	0.0210	0.0187	0.0451	0.0345	0.1297	0.0455	0.0276	0.0430
		5D	0.0466	0.0406	0.0363	0.0757	0.0548	0.1949	0.0722	0.0451	0.0708
		7D	0.0710	0.0626	0.0527	0.1014	0.0705	0.2231	0.0981	0.0619	0.0927
		Avg.	0.0361	0.0323	0.0280	0.0607	0.0435	0.1482	0.0576	0.0362	0.0553
	TimesNet	1D	0.0035	0.0052	0.0066	0.0215	0.0262	0.0586	0.0206	0.0163	0.0198
		3D	0.0159	0.0181	0.0214	0.0461	0.0445	0.1318	0.0553	0.0331	0.0458
		5D	0.0315	0.0351	0.0369	0.0654	0.0684	0.2087	0.0811	0.0509	0.0723
		7D	0.0514	0.0543	0.0537	0.0919	0.0871	0.2343	0.1012	0.0706	0.0931
		Avg.	0.0256	0.0282	0.0297	0.0562	0.0565	0.1584	0.0645	0.0427	0.0577
Transformer	iTransformer	1D	0.0035	0.0047	0.0050	0.0177	0.0157	0.0436	0.0140	0.0094	0.0142
		3D	0.0171	0.0171	0.0209	0.0403	0.0352	0.1103	0.0410	0.0255	0.0384
		5D	0.0343	0.0335	0.0356	0.0623	0.0527	0.1582	0.0674	0.0423	0.0608
		7D	0.0518	0.0522	0.0539	0.0807	0.0714	0.1897	0.0847	0.0590	0.0804
		Avg.	0.0267	0.0269	0.0288	0.0503	0.0437	0.1254	0.0518	0.0341	0.0485
	PatchTST	1D	0.0032	0.0048	0.0044	0.0179	0.0154	0.0444	0.0144	0.0096	0.0143
		3D	0.0161	0.0205	0.0212	0.0420	0.0353	0.1100	0.0432	0.0266	0.0393
		5D	0.0385	0.0364	0.0374	0.0608	0.0531	0.1632	0.0668	0.0438	0.0625
		7D	0.0564	0.0578	0.0514	0.0832	0.0700	0.2020	0.0825	0.0598	0.0829
		Avg.	0.0285	0.0299	0.0286	0.0510	0.0435	0.1299	0.0517	0.0350	0.0498

Table 31: Benchmark(MSE) on part 3(Fort Myers area) stations(RNN,GNN,LLM)

	Method	T	S0	S1	S2	S3	S4	S5	S6	S7	Avg.
RNN	LSTM	1D	0.0183	0.0087	0.0109	0.0287	0.0217	0.0748	0.0274	0.0181	0.0261
		3D	0.0420	0.0271	0.0312	0.0588	0.0444	0.1455	0.0540	0.0381	0.0551
		5D	0.0624	0.0427	0.0506	0.0774	0.0630	0.1761	0.0717	0.0552	0.0749
		7D	0.0949	0.0621	0.0773	0.0985	0.0797	0.2013	0.0880	0.0714	0.0967
		Avg.	0.0544	0.0352	0.0425	0.0659	0.0522	0.1494	0.0603	0.0457	0.0632
	DeepAR	1D	0.0408	0.0090	0.0108	0.0298	0.0224	0.0750	0.0266	0.0173	0.0290
		3D	0.0634	0.0251	0.0316	0.0568	0.0463	0.1353	0.0580	0.0370	0.0567
		5D	0.0682	0.0414	0.0506	0.0743	0.0642	0.1775	0.0754	0.0564	0.0760
		7D	0.0910	0.0569	0.0728	0.0969	0.0799	0.1947	0.0899	0.0703	0.0941
		Avg.	0.0659	0.0331	0.0414	0.0644	0.0532	0.1457	0.0625	0.0453	0.0639
	DilatedRNN	1D	0.0172	0.0048	0.0056	0.0194	0.0162	0.0408	0.0175	0.0104	0.0165
		3D	0.0395	0.0193	0.0225	0.0442	0.0356	0.1128	0.0489	0.0300	0.0441
		5D	0.0583	0.0347	0.0401	0.0675	0.0560	0.1787	0.0786	0.0509	0.0706
		7D	0.0808	0.0583	0.0578	0.0958	0.0747	0.2167	0.0990	0.0714	0.0943
		Avg.	0.0489	0.0293	0.0315	0.0567	0.0457	0.1372	0.0610	0.0407	0.0564
GNN	GCN	1D	0.0108	0.0094	0.0060	0.3682	0.0982	0.0392	0.0227	0.0923	0.0809
		3D	0.0267	0.0246	0.0196	0.3854	0.1184	0.0918	0.0472	0.1217	0.1044
		5D	0.0434	0.0359	0.0339	0.4006	0.1337	0.1285	0.0674	0.1440	0.1234
		7D	0.0569	0.0499	0.0486	0.4154	0.1489	0.1565	0.0868	0.1794	0.1428
		Avg.	0.0344	0.0300	**0.0270**	0.3924	0.1248	<u>0.1040</u>	0.0560	0.1343	0.1129
	FourierGNN	1D	0.0037	0.0049	0.0063	0.0178	0.0153	0.0430	0.0145	0.0108	0.0145
		3D	0.0154	0.0166	0.0207	0.0379	0.0364	0.0938	0.0399	0.0268	0.0359
		5D	0.0298	0.0302	0.0359	0.0555	0.0496	0.1312	0.0609	0.0432	0.0545
		7D	0.0477	0.0434	0.0542	0.0769	0.0691	0.1594	0.0787	0.0591	0.0736
		Avg.	<u>0.0241</u>	**0.0237**	0.0293	0.0471	0.0426	0.1069	0.0485	0.0350	<u>0.0446</u>
	StemGNN	1D	0.0390	0.0081	0.0070	0.0221	0.0281	0.0535	0.0164	0.0145	0.0236
		3D	0.0816	0.0405	0.0270	0.0609	0.0599	0.1179	0.0722	0.0861	0.0683
		5D	0.1100	0.0850	0.0433	0.1015	0.0809	0.1587	0.1540	0.1312	0.1081
		7D	0.1554	0.1173	0.1096	0.1232	0.1079	0.1982	0.1746	0.2072	0.1492
		Avg.	0.0965	0.0628	0.0467	0.0769	0.0692	0.1321	0.1043	0.1098	0.0873
LLM	GPT4TS	1D	0.0038	0.0050	0.0060	0.0202	0.0223	0.0542	0.0183	0.6054	0.0919
		3D	0.0151	0.0174	0.0205	0.0442	0.0474	0.1530	0.0496	0.0339	0.0476
		5D	0.0321	0.0319	0.0371	0.0648	0.0716	0.2071	0.0829	0.0526	0.0725
		7D	0.0494	0.0489	0.0528	0.0872	0.0841	0.2397	0.0996	0.0734	0.0919
		Avg.	0.0251	0.0258	0.0291	0.0541	0.0564	0.1635	0.0626	0.1913	0.0760
	AutoTimes	1D	0.0037	0.0052	0.0048	0.0183	0.0159	0.0447	0.0161	0.0106	0.0149
		3D	0.0159	0.0167	0.0189	0.0396	0.0342	0.1026	0.0409	0.0263	0.0369
		5D	0.0321	0.0314	0.0337	0.0564	0.0519	0.1485	0.0614	0.0429	0.0573
		7D	0.0522	0.0466	0.0508	0.0745	0.0661	0.1807	0.0781	0.0586	0.0760
		Avg.	0.0260	0.0250	<u>0.0271</u>	0.0472	<u>0.0420</u>	0.1191	0.0491	0.0346	0.0463

Table 32: Benchmark(SEDI10) on part 3(Fort Myers area) stations(MLP,CNN,Transformer)

	Method	T	S0	S1	S2	S3	S4	S5	S6	S7	Avg.
MLP	MLP	1D	0.6714	0.9580	0.6989	0.7088	0.4910	0.6202	0.5661	0.8442	0.6948
		3D	0.6107	0.8594	0.6242	0.7260	0.4937	0.4783	0.5238	0.8326	0.6436
		5D	0.5833	0.7752	0.6230	0.6262	0.4892	0.5590	0.5791	0.7968	0.6290
		7D	0.5649	0.7550	0.5619	0.5997	0.5046	0.4772	0.4864	0.6886	0.5798
		Avg.	<u>0.6076</u>	<u>0.8369</u>	0.6270	<u>0.6652</u>	**0.4946**	**0.5337**	<u>0.5389</u>	**0.7906**	**0.6368**
	TSMixer	1D	0.6675	0.9189	0.6900	0.7345	0.5080	0.6620	0.6030	0.8160	0.7000
		3D	0.5919	0.8285	0.6258	0.6505	0.4595	0.5203	0.4941	0.7342	0.6131
		5D	0.5567	0.7866	0.5754	0.6006	0.4316	0.4412	0.4199	0.6803	0.5615
		7D	0.5350	0.7498	0.5379	0.5651	0.4129	0.3812	0.3557	0.6375	0.5219
		Avg.	0.5878	0.8209	0.6073	0.6377	0.4530	<u>0.5012</u>	0.4682	0.7170	0.5991
	NLinear	1D	0.6653	0.9466	0.7012	0.7387	0.5234	0.6204	0.6081	0.8296	0.7041
		3D	0.5963	0.8470	0.6314	0.6528	0.4532	0.5048	0.4892	0.7448	0.6149
		5D	0.5604	0.7925	0.5800	0.6023	0.4297	0.4342	0.4069	0.6914	0.5622
		7D	0.5393	0.7539	0.5417	0.5660	0.4113	0.3787	0.3420	0.6494	0.5228
		Avg.	0.5903	0.8350	0.6136	0.6399	0.4544	0.4845	0.4615	0.7288	0.6010
CNN	TCN	1D	0.6607	0.9349	0.7126	0.6214	0.3251	0.6057	0.3817	0.4229	0.5831
		3D	0.5849	0.7254	0.6607	0.6150	0.3200	0.3803	0.4778	0.3677	0.5165
		5D	0.4883	0.8096	0.5672	0.5006	0.2824	0.3337	0.3708	0.4034	0.4695
		7D	0.2490	0.6355	0.5764	0.6034	0.2939	0.3018	0.2916	0.3836	0.4169
		Avg.	0.4957	0.7763	0.6292	0.5851	0.3054	0.4054	0.3805	0.3944	0.4965
	ModernTCN	1D	0.6643	0.9457	0.6975	0.7506	0.5325	0.6309	0.5645	0.8346	0.7026
		3D	0.5833	0.8013	0.6528	0.6401	0.4782	0.4488	0.4296	0.7353	0.5962
		5D	0.5274	0.7259	0.5842	0.6140	0.4395	0.3732	0.3519	0.6687	0.5356
		7D	0.4967	0.6819	0.5463	0.5468	0.4399	0.3177	0.2592	0.6290	0.4897
		Avg.	0.5679	0.7887	0.6202	0.6379	0.4725	0.4426	0.4013	0.7169	0.5810
	TimesNet	1D	0.6628	0.8907	0.6824	0.7392	0.4722	0.5926	0.5199	0.7606	0.6651
		3D	0.5922	0.8103	0.6122	0.6461	0.4452	0.4391	0.3654	0.6902	0.5751
		5D	0.5666	0.7517	0.5491	0.6090	0.4134	0.3682	0.3255	0.6374	0.5276
		7D	0.5199	0.7043	0.5105	0.5579	0.3969	0.2931	0.2576	0.5950	0.4794
		Avg.	0.5854	0.7892	0.5885	0.6380	0.4319	0.4233	0.3671	0.6708	0.5618
Transformer	iTransformer	1D	0.6753	0.9308	0.6948	0.7630	0.5149	0.6342	0.5745	0.8270	0.7018
		3D	0.5920	0.8284	0.6263	0.6781	0.4784	0.4697	0.4621	0.7383	0.6092
		5D	0.5688	0.7619	0.5898	0.6217	0.4517	0.4084	0.3802	0.6824	0.5581
		7D	0.5440	0.7203	0.5514	0.5852	0.4287	0.3532	0.3130	0.6412	0.5171
		Avg.	0.5950	0.8103	0.6156	0.6620	0.4684	0.4664	0.4325	0.7222	0.5965
	PatchTST	1D	0.6779	0.9328	0.7007	0.7626	0.5236	0.6109	0.5828	0.8365	0.7035
		3D	0.6072	0.8306	0.6327	0.6674	0.4839	0.4845	0.4406	0.7434	0.6113
		5D	0.5537	0.7707	0.5892	0.6232	0.4570	0.4017	0.3710	0.6887	0.5569
		7D	0.5374	0.7078	0.5492	0.5853	0.4358	0.3455	0.3136	0.6471	0.5152
		Avg.	0.5941	0.8105	0.6180	0.6596	0.4751	0.4606	0.4270	<u>0.7289</u>	0.5967

Table 33: Benchmark(SEDI10) on part 3(Fort Myers area) stations(RNN,GNN,LLM)

	Method	T	S0	S1	S2	S3	S4	S5	S6	S7	Avg.
RNN	LSTM	1D	0.6375	0.8919	0.6771	0.7127	0.5130	0.6141	0.4802	0.6979	0.6530
		3D	0.5603	0.7366	0.5969	0.7031	0.4666	0.4219	0.4553	0.6716	0.5765
		5D	0.5230	0.7399	0.5582	0.6459	0.4201	0.3505	0.4925	0.6755	0.5507
		7D	0.5015	0.7195	0.5452	0.5964	0.4224	0.3320	0.4663	0.6533	0.5296
		Avg.	0.5556	0.7720	0.5943	0.6645	0.4555	0.4296	0.4736	0.6746	0.5775
	DeepAR	1D	0.6113	0.9191	0.5886	0.7494	0.5485	0.4949	0.4766	0.7039	0.6365
		3D	0.5456	0.7545	0.6393	0.6426	0.4689	0.3235	0.3871	0.7007	0.5578
		5D	0.5199	0.7361	0.5829	0.6406	0.3841	0.2802	0.2172	0.5790	0.4925
		7D	0.5267	0.7149	0.4846	0.5765	0.4471	0.2646	0.3546	0.5960	0.4956
		Avg.	0.5509	0.7811	0.5738	0.6523	0.4621	0.3408	0.3589	0.6449	0.5456
	DilatedRNN	1D	0.6157	0.9270	0.7114	0.8285	0.4265	0.5347	0.4866	0.7628	0.6616
		3D	0.5809	0.7952	0.6612	0.5798	0.4546	0.3865	0.3726	0.7252	0.5695
		5D	0.5291	0.8040	0.5665	0.6098	0.4765	0.2496	0.2638	0.6925	0.5239
		7D	0.5392	0.6853	0.5523	0.5684	0.4365	0.2247	0.3043	0.5970	0.4885
		Avg.	0.5662	0.8029	0.6228	0.6466	0.4485	0.3489	0.3568	0.6944	0.5609
GNN	GCN	1D	0.6792	0.8309	0.7292	0.4914	0.4288	0.5120	0.4721	0.7129	0.6071
		3D	0.6144	0.8262	0.6910	0.4325	0.3749	0.4319	0.5107	0.6594	0.5676
		5D	0.5949	0.7921	0.6016	0.4126	0.3364	0.3577	0.3270	0.6403	0.5078
		7D	0.5728	0.7445	0.6076	0.3891	0.3311	0.2809	0.3782	0.6840	0.4985
		Avg.	**0.6153**	0.7984	**0.6574**	0.4314	0.3678	0.3956	0.4220	0.6741	0.5453
	FourierGNN	1D	0.6606	0.9310	0.7011	0.7420	0.5204	0.5268	0.6103	0.7723	0.6831
		3D	0.6044	0.8487	0.6062	0.6820	0.4898	0.5028	0.5337	0.7566	0.6281
		5D	0.5545	0.8082	0.6223	0.6375	0.4579	0.3712	0.5406	0.7085	0.5876
		7D	0.5737	0.7776	0.6044	0.6699	0.4793	0.4239	0.5228	0.6609	0.5891
		Avg.	0.5983	**0.8414**	0.6335	**0.6828**	0.4869	0.4562	**0.5519**	**0.7246**	0.6219
	StemGNN	1D	0.6429	0.9027	0.6334	0.6619	0.4429	0.4493	0.5562	0.7738	0.6329
		3D	0.5120	0.8540	0.6633	0.6193	0.4460	0.3921	0.3833	0.6762	0.5683
		5D	0.4908	0.7262	0.6228	0.5595	0.3974	0.3235	0.3157	0.6449	0.5101
		7D	0.4009	0.6838	0.4941	0.5233	0.3831	0.2672	0.2345	0.5653	0.4440
		Avg.	0.5116	0.7917	0.6034	0.5910	0.4173	0.3580	0.3724	0.6650	0.5388
LLM	GPT4TS	1D	0.6635	0.9232	0.6942	0.7230	0.4875	0.6188	0.5335	0.7614	0.6757
		3D	0.6057	0.8277	0.6177	0.6298	0.4394	0.4481	0.4085	0.6951	0.5840
		5D	0.5684	0.7776	0.5751	0.5932	0.4164	0.3858	0.3212	0.6346	0.5340
		7D	0.5243	0.7301	0.5333	0.5432	0.3953	0.3318	0.2623	0.5767	0.4871
		Avg.	0.5905	0.8147	0.6051	0.6223	0.4347	0.4462	0.3814	0.6670	0.5702
	AutoTimes	1D	0.6599	0.9250	0.6921	0.7510	0.5256	0.6094	0.5451	0.8114	0.6899
		3D	0.6089	0.8376	0.6380	0.6568	0.4840	0.4850	0.4504	0.7400	0.6126
		5D	0.5746	0.7828	0.5837	0.6040	0.4538	0.4243	0.3857	0.6793	0.5610
		7D	0.5422	0.7350	0.5560	0.5717	0.4415	0.3649	0.3277	0.6459	0.5231
		Avg.	0.5964	0.8201	0.6175	0.6459	0.4762	0.4709	0.4272	0.7191	0.5967

Table 34: Benchmark(SEDI5) on part 3(Fort Myers area) stations(MLP,CNN,Transformer)

	Method	T	S0	S1	S2	S3	S4	S5	S6	S7	Avg.
MLP	MLP	1D	0.4894	0.8078	0.7149	0.4916	0.3294	0.5618	0.3728	0.6667	0.5543
		3D	0.4773	0.7190	0.6372	0.5178	0.3379	0.4137	0.3164	0.6467	0.5083
		5D	0.4737	0.6523	0.5924	0.4466	0.3030	0.4697	0.3772	0.6306	0.4932
		7D	0.4645	0.6408	0.5297	0.4251	0.3127	0.3881	0.2769	0.5457	0.4479
		Avg.	0.4762	0.7050	0.6186	0.4703	0.3208	**0.4583**	0.3358	**0.6224**	**0.5009**
	TSMixer	1D	0.4885	0.7318	0.7059	0.5263	0.3722	0.5500	0.3410	0.6631	0.5474
		3D	0.4713	0.6731	0.6384	0.4570	0.3260	0.3770	0.2068	0.5727	0.4653
		5D	0.4577	0.6479	0.5783	0.4103	0.3053	0.2971	0.1542	0.5068	0.4197
		7D	0.4474	0.6274	0.5311	0.3795	0.2879	0.2336	0.1456	0.4626	0.3894
		Avg.	0.4662	0.6700	0.6134	0.4433	0.3229	0.3644	0.2119	0.5513	0.4554
	NLinear	1D	0.4908	0.8016	0.7131	0.5444	0.3801	0.5330	0.3531	0.6808	0.5621
		3D	0.4729	0.6957	0.6459	0.4658	0.3114	0.3720	0.2127	0.5928	0.4711
		5D	0.4581	0.6564	0.5865	0.4188	0.2919	0.2901	0.1535	0.5293	0.4231
		7D	0.4475	0.6307	0.5373	0.3836	0.2755	0.2271	0.1539	0.4864	0.3927
		Avg.	0.4673	0.6961	0.6207	0.4532	0.3147	0.3555	0.2183	0.5724	0.4623
CNN	TCN	1D	0.4885	0.5418	0.6754	0.4250	0.0903	0.5215	0.1972	0.1387	0.3848
		3D	0.2287	0.4575	0.4992	0.3864	0.0903	0.2572	0.2046	0.1727	0.2871
		5D	0.2222	0.6698	0.3806	0.3737	0.1045	0.2205	0.1504	0.1179	0.2799
		7D	0.2372	0.4134	0.4001	0.3923	0.1494	0.2020	0.1318	0.1100	0.2545
		Avg.	0.2941	0.5206	0.4888	0.3943	0.1086	0.3003	0.1710	0.1348	0.3016
	ModernTCN	1D	0.4916	0.8000	0.7168	0.5206	0.3806	0.5178	0.3296	0.6500	0.5509
		3D	0.4736	0.6654	0.6446	0.4359	0.3385	0.2951	0.1874	0.5540	0.4493
		5D	0.4546	0.6087	0.5675	0.3828	0.3163	0.2291	0.1094	0.4870	0.3944
		7D	0.4437	0.5747	0.5238	0.3442	0.2964	0.1796	0.0746	0.4491	0.3607
		Avg.	0.4659	0.6622	0.6132	0.4209	0.3329	0.3054	0.1752	0.5350	0.4388
	TimesNet	1D	0.4887	0.7914	0.6931	0.5047	0.3416	0.4730	0.2862	0.5783	0.5196
		3D	0.4738	0.6845	0.6056	0.4265	0.3145	0.3008	0.1060	0.4963	0.4260
		5D	0.4572	0.6307	0.5365	0.3854	0.2857	0.2354	0.0782	0.4423	0.3814
		7D	0.4477	0.6095	0.4801	0.3425	0.2637	0.1745	0.0602	0.3952	0.3467
		Avg.	0.4669	0.6790	0.5788	0.4148	0.3013	0.2959	0.1327	0.4780	0.4184
Transformer	iTransformer	1D	0.4861	0.7835	0.7049	0.5526	0.3745	0.5381	0.3514	0.6485	0.5549
		3D	0.4722	0.6740	0.6211	0.4677	0.3346	0.3229	0.2136	0.5557	0.4577
		5D	0.4566	0.6520	0.5766	0.4145	0.3157	0.2654	0.1486	0.5018	0.4164
		7D	0.4463	0.6171	0.5237	0.3832	0.2963	0.2088	0.1013	0.4623	0.3799
		Avg.	0.4653	0.6817	0.6066	0.4545	0.3303	0.3338	0.2037	0.5421	0.4522
	PatchTST	1D	0.4924	0.8199	0.7104	0.5501	0.3796	0.4983	0.3188	0.6643	0.5542
		3D	0.4747	0.6933	0.6454	0.4688	0.3416	0.3528	0.1760	0.5698	0.4653
		5D	0.4567	0.6503	0.5773	0.4337	0.3168	0.2647	0.1300	0.5138	0.4179
		7D	0.4544	0.6030	0.5288	0.3971	0.2896	0.2039	0.1030	0.4685	0.3810
		Avg.	0.4695	0.6916	0.6154	0.4624	0.3319	0.3299	0.1820	0.5541	0.4546

Table 35: Benchmark(SEDI5) on part 3(Fort Myers area) stations(RNN,GNN,LLM)

	Method	T	S0	S1	S2	S3	S4	S5	S6	S7	Avg.
RNN	LSTM	1D	0.4820	0.6970	0.6832	0.5265	0.3526	0.4093	0.2297	0.5224	0.4878
		3D	0.4696	0.6260	0.5874	0.4875	0.2963	0.1749	0.2572	0.4429	0.4177
		5D	0.4635	0.6474	0.3289	0.4312	0.2716	0.1569	0.0442	0.4783	0.3528
		7D	0.4340	0.6733	0.3075	0.3608	0.2654	0.1364	0.0542	0.4455	0.3347
		Avg.	0.4623	0.6609	0.4768	0.4515	0.2965	0.2194	0.1463	0.4723	0.3982
	DeepAR	1D	0.4587	0.7348	0.5771	0.5112	0.3805	0.3081	0.1743	0.4682	0.4516
		3D	0.4104	0.6217	0.3898	0.4468	0.3524	0.1630	0.1703	0.4901	0.3806
		5D	0.3463	0.6626	0.3252	0.4434	0.2483	0.1350	0.0699	0.3937	0.3280
		7D	0.4636	0.6772	0.2954	0.4170	0.2511	0.1049	0.1605	0.4080	0.3472
		Avg.	0.4197	0.6741	0.3969	0.4546	0.3081	0.1778	0.1437	0.4400	0.3769
	DilatedRNN	1D	0.4427	0.7950	0.7256	0.6408	0.2791	0.4482	0.2522	0.5895	0.5216
		3D	0.4861	0.6492	0.6471	0.3783	0.3198	0.2445	0.1764	0.5450	0.4308
		5D	0.3852	0.6652	0.5548	0.4024	0.3185	0.1632	0.1136	0.5060	0.3886
		7D	0.4685	0.5954	0.5216	0.3734	0.2855	0.1483	0.1444	0.4271	0.3705
		Avg.	0.4456	0.6762	0.6123	0.4487	0.3007	0.2510	0.1716	0.5169	0.4279
GNN	GCN	1D	0.4893	0.7551	0.7258	0.3366	0.3070	0.3908	0.2399	0.5583	0.4754
		3D	0.4817	0.7295	0.6715	0.2813	0.2968	0.2954	0.2091	0.5118	0.4346
		5D	0.4785	0.7154	0.5946	0.2677	0.2595	0.2635	0.0498	0.4793	0.3885
		7D	0.4697	0.6812	0.5678	0.2610	0.2722	0.2174	0.1484	0.5102	0.3910
		Avg.	**0.4798**	**0.7203**	**0.6399**	0.2867	0.2839	0.2918	0.1618	0.5149	0.4224
	FourierGNN	1D	0.4873	0.7843	0.7085	0.5126	0.3541	0.4430	0.4340	0.6063	0.5412
		3D	0.4800	0.7305	0.6125	0.4674	0.3419	0.3558	0.3325	0.5709	0.4864
		5D	0.4773	0.6881	0.5911	0.4507	0.3064	0.2782	0.3179	0.5243	0.4543
		7D	0.4705	0.6634	0.5482	0.4566	0.3343	0.3072	0.3234	0.4842	0.4485
		Avg.	0.4788	<u>0.7166</u>	0.6151	**0.4718**	**0.3342**	0.3460	**0.3519**	0.5464	<u>0.4826</u>
	StemGNN	1D	0.4950	0.7993	0.6503	0.4581	0.3070	0.3161	0.3138	0.5819	0.4902
		3D	0.4878	0.6894	0.6336	0.4333	0.2762	0.2694	0.1468	0.4612	0.4247
		5D	0.4762	0.6203	0.6074	0.4065	0.2529	0.2048	0.1256	0.4329	0.3908
		7D	0.2821	0.5487	0.4545	0.3398	0.2205	0.1658	0.0749	0.3691	0.3069
		Avg.	0.4353	0.6644	0.5865	0.4094	0.2642	0.2390	0.1653	0.4613	0.4032
LLM	GPT4TS	1D	0.4909	0.7803	0.6876	0.4807	0.3624	0.4659	0.2754	0.6054	0.5186
		3D	0.4731	0.6916	0.6056	0.4087	0.3166	0.3103	0.1481	0.4977	0.4315
		5D	0.4595	0.6523	0.5701	0.3712	0.2935	0.2494	0.0887	0.4326	0.3896
		7D	0.4498	0.6217	0.5153	0.3324	0.2688	0.2017	0.0738	0.3889	0.3566
		Avg.	0.4683	0.6865	0.5947	0.3983	0.3103	0.3068	0.1465	0.4811	0.4241
	AutoTimes	1D	0.4910	0.7669	0.6932	0.5324	0.3777	0.5069	0.3207	0.6462	0.5419
		3D	0.4693	0.6760	0.6316	0.4674	0.3322	0.3641	0.2025	0.5692	0.4640
		5D	0.4547	0.6498	0.5702	0.4229	0.3073	0.2926	0.1335	0.5071	0.4173
		7D	0.4421	0.6195	0.5349	0.3920	0.2933	0.2368	0.1115	0.4639	0.3868
		Avg.	0.4643	0.6781	0.6075	0.4537	0.3277	0.3501	0.1920	0.5466	0.4525

Table 36: Benchmark(SEDI1) on part 3(Fort Myers area) stations(MLP,CNN,Transformer)

	Method	T	S0	S1	S2	S3	S4	S5	S6	S7	Avg.
MLP	MLP	1D	0.4747	0.4387	0.5051	0.2137	0.1295	0.3272	0.0017	0.2836	0.2968
		3D	0.4444	0.4520	0.2868	0.2392	0.1628	0.2860	0.0006	0.3115	0.2729
		5D	0.4302	0.2950	0.1017	0.1766	0.1696	0.3612	0.0005	0.3690	0.2380
		7D	0.4116	0.2920	0.2236	0.1575	0.1613	0.2435	0.0004	0.2357	0.2157
		Avg.	**0.4402**	0.3694	0.2793	**0.1968**	0.1558	**0.3045**	**0.0008**	**0.3000**	**0.2558**
	TSMixer	1D	0.4450	0.5180	0.4305	0.2132	0.1929	0.2698	0.0000	0.3516	0.3026
		3D	0.3848	0.3874	0.2667	0.1432	0.1651	0.1587	0.0000	0.2378	0.2180
		5D	0.3283	0.3044	0.2146	0.1247	0.1417	0.1347	0.0000	0.1959	0.1805
		7D	0.2849	0.2479	0.1902	0.1069	0.1197	0.1177	0.0000	0.1482	0.1519
		Avg.	0.3607	0.3644	0.2755	0.1470	0.1548	0.1702	0.0000	0.2334	0.2133
	NLinear	1D	0.4657	0.5401	0.4711	0.2360	0.2096	0.3693	0.0017	0.3968	0.3363
		3D	0.4022	0.3957	0.2858	0.1465	0.1677	0.2077	0.0006	0.2691	0.2344
		5D	0.3454	0.3299	0.2238	0.1311	0.1556	0.1897	0.0003	0.2083	0.1980
		7D	0.3003	0.2835	0.1990	0.1112	0.1377	0.1638	0.0002	0.1777	0.1717
		Avg.	0.3784	**0.3873**	0.2949	0.1562	0.1676	0.2326	0.0007	0.2630	0.2351
CNN	TCN	1D	0.3817	0.3979	0.5681	0.1620	0.1078	0.2254	0.0001	0.2565	0.2624
		3D	0.3269	0.2261	0.2620	0.1106	0.1482	0.1507	0.0000	0.1577	0.1728
		5D	0.3281	0.3077	0.2576	0.1217	0.1144	0.1199	0.0000	0.1687	0.1773
		7D	0.2895	0.2433	0.2785	0.0881	0.0582	0.1289	0.0000	0.1664	0.1566
		Avg.	0.3315	0.2938	**0.3415**	0.1206	0.1072	0.1562	0.0000	0.1873	0.1923
	ModernTCN	1D	0.4700	0.3796	0.4606	0.1984	0.1834	0.2864	0.0003	0.3521	0.2913
		3D	0.4134	0.2972	0.3154	0.1244	0.1610	0.1089	0.0000	0.2540	0.2093
		5D	0.3802	0.2393	0.2666	0.0989	0.1319	0.0585	0.0000	0.1811	0.1696
		7D	0.3497	0.2258	0.2511	0.0857	0.1173	0.0431	0.0000	0.1418	0.1518
		Avg.	0.4033	0.2855	0.3234	0.1269	0.1484	0.1242	0.0001	0.2322	0.2055
	TimesNet	1D	0.4591	0.3666	0.4525	0.1548	0.1686	0.1891	0.0000	0.2756	0.2583
		3D	0.4283	0.2930	0.2820	0.1182	0.1470	0.0856	0.0000	0.1680	0.1902
		5D	0.3777	0.2554	0.2337	0.1004	0.1092	0.0487	0.0000	0.1362	0.1577
		7D	0.3632	0.2254	0.1776	0.0801	0.0995	0.0378	0.0000	0.0923	0.1345
		Avg.	0.4071	0.2851	0.2865	0.1134	0.1311	0.0903	0.0000	0.1680	0.1852
Transformer	iTransformer	1D	0.4584	0.4340	0.4950	0.2389	0.1775	0.3983	0.0005	0.3726	0.3219
		3D	0.4305	0.2699	0.2939	0.1542	0.1563	0.1485	0.0001	0.2423	0.2120
		5D	0.3914	0.2541	0.2244	0.1336	0.1363	0.1145	0.0001	0.1856	0.1800
		7D	0.3506	0.2224	0.1918	0.1115	0.1161	0.0841	0.0000	0.1842	0.1576
		Avg.	0.4077	0.2951	0.3013	0.1595	0.1465	0.1863	0.0002	0.2462	0.2179
	PatchTST	1D	0.4734	0.4614	0.4548	0.2418	0.1918	0.3446	0.0003	0.3847	0.3191
		3D	0.4278	0.3069	0.2981	0.1757	0.1645	0.1653	0.0001	0.2403	0.2223
		5D	0.3990	0.2060	0.2292	0.1506	0.1415	0.0919	0.0000	0.1697	0.1735
		7D	0.3603	0.1898	0.1968	0.1058	0.1200	0.0701	0.0000	0.1344	0.1472
		Avg.	0.4151	0.2910	0.2947	0.1685	0.1544	0.1680	0.0001	0.2323	0.2155

Table 37: Benchmark(SEDI1) on part 3(Fort Myers area) stations(RNN,GNN,LLM)

	Method	T	S0	S1	S2	S3	S4	S5	S6	S7	Avg.
RNN	LSTM	1D	0.2500	0.3899	0.0246	0.1762	0.1810	0.1240	0.0000	0.2035	0.1686
		3D	0.2375	0.0599	0.0035	0.1100	0.1246	0.0055	0.0000	0.1008	0.0802
		5D	0.0000	0.0617	0.0000	0.0920	0.0927	0.0081	0.0000	0.0967	0.0439
		7D	0.2466	0.0486	0.0230	0.0938	0.0791	0.0256	0.0000	0.0555	0.0715
		Avg.	0.1835	0.1400	0.0128	0.1180	0.1194	0.0408	0.0000	0.1141	0.0911
	DeepAR	1D	0.1603	0.0000	0.0998	0.1648	0.1890	0.1125	0.0000	0.1389	0.1082
		3D	0.2332	0.1744	0.0000	0.0798	0.0822	0.0015	0.0000	0.0887	0.0825
		5D	0.2488	0.0519	0.0000	0.1098	0.0928	0.0190	0.0000	0.0000	0.0653
		7D	0.0000	0.0091	0.0056	0.0657	0.0243	0.0088	0.0000	0.0961	0.0262
		Avg.	0.1606	0.0589	0.0263	0.1050	0.0971	0.0355	0.0000	0.0809	0.0705
	DilatedRNN	1D	0.1049	0.3690	0.3560	0.3224	0.0969	0.3043	0.0003	0.2794	0.2291
		3D	0.2490	0.2811	0.0161	0.1159	0.1277	0.0744	0.0001	0.1527	0.1271
		5D	0.0949	0.2827	0.2367	0.1348	0.1246	0.0415	0.0000	0.2265	0.1427
		7D	0.2413	0.1618	0.2236	0.1230	0.1192	0.0497	0.0000	0.0805	0.1249
		Avg.	0.1725	0.2736	0.2081	0.1740	0.1171	0.1175	0.0001	0.1848	0.1560
GNN	GCN	1D	0.3817	0.3979	0.5681	0.1620	0.1078	0.2254	0.0001	0.2565	0.2624
		3D	0.3269	0.2261	0.2620	0.1106	0.1482	0.1507	0.0000	0.1577	0.1728
		5D	0.3281	0.3077	0.2576	0.1217	0.1144	0.1199	0.0000	0.1687	0.1773
		7D	0.2895	0.2433	0.2785	0.0881	0.0582	0.1289	0.0000	0.1664	0.1566
		Avg.	0.3315	0.2938	**0.3415**	0.1206	0.1072	0.1562	0.0000	0.1873	0.1923
	FourierGNN	1D	0.4363	0.3351	0.3967	0.2117	0.1928	0.2551	0.0018	0.2885	0.2647
		3D	0.4293	0.2745	0.2772	0.1733	0.2145	0.1698	0.0000	0.2810	0.2274
		5D	0.4124	0.3231	0.2661	0.1731	0.1441	0.2090	0.0000	0.2253	0.2191
		7D	0.3564	0.2544	0.2314	0.1561	0.2023	0.1808	0.0000	0.1790	0.1951
		Avg.	0.4086	0.2968	0.2928	<u>0.1785</u>	**0.1884**	0.2037	0.0005	0.2434	0.2266
	StemGNN	1D	0.1616	0.4190	0.1862	0.1781	0.1094	0.1578	0.0002	0.2462	0.1823
		3D	0.2372	0.2514	0.1446	0.1443	0.0443	0.1068	0.0000	0.1309	0.1324
		5D	0.0956	0.1130	0.0178	0.1026	0.0790	0.0844	0.0000	0.1162	0.0761
		7D	0.0360	0.0911	0.0384	0.1245	0.0247	0.1175	0.0000	0.0726	0.0631
		Avg.	0.1326	0.2186	0.0968	0.1374	0.0644	0.1167	0.0001	0.1415	0.1135
LLM	GPT4TS	1D	0.4586	0.4502	0.4421	0.1424	0.1876	0.2122	0.0000	0.2792	0.2715
		3D	0.4088	0.3268	0.2713	0.1127	0.1530	0.0738	0.0000	0.1810	0.1909
		5D	0.3916	0.2650	0.2210	0.1011	0.1201	0.0412	0.0000	0.1263	0.1583
		7D	0.3606	0.2190	0.1939	0.0847	0.1091	0.0466	0.0000	0.1000	0.1392
		Avg.	0.4049	0.3153	0.2821	0.1102	0.1424	0.0935	0.0000	0.1716	0.1900
	AutoTimes	1D	0.4710	0.3713	0.4458	0.2398	0.1955	0.3082	0.0000	0.3205	0.2940
		3D	0.4297	0.2009	0.2890	0.1551	0.1653	0.1697	0.0000	0.2165	0.2033
		5D	0.3880	0.1895	0.2212	0.1363	0.1375	0.1271	0.0000	0.1561	0.1695
		7D	0.3494	0.1505	0.1984	0.1012	0.1175	0.0965	0.0000	0.1250	0.1423
		Avg.	0.4095	0.2280	0.2886	0.1581	0.1539	0.1753	0.0000	0.2045	0.2023

Table 38: Benchmark(MAE) on all stations

Method	T	S0	S1	S2	S3	S4	S5	S6	S7	Avg.
MLP	1D	0.1324	0.1424	0.1441	0.1043	0.1098	0.1192	0.1423	0.1310	0.1282
	3D	0.2158	0.2352	0.2471	0.1838	0.1875	0.1903	0.2516	0.2082	0.2150
	5D	0.2810	0.2902	0.3178	0.2277	0.2437	0.2354	0.3228	0.2565	0.2719
	7D	0.3329	0.3374	0.3666	0.2661	0.2837	0.2719	0.3793	0.2915	0.3162
	Avg.	**0.2405**	**0.2513**	**0.2689**	**0.1955**	**0.2062**	**0.2042**	**0.2740**	**0.2218**	**0.2328**
TCN	1D	0.3079	0.2613	0.2634	0.2414	0.2079	0.1885	0.2957	0.2740	0.2550
	3D	0.4332	0.3215	0.3490	0.3061	0.2900	0.2554	0.3944	0.3465	0.3370
	5D	0.4324	0.3788	0.4040	0.3563	0.3457	0.3070	0.4547	0.3992	0.3848
	7D	0.4842	0.3951	0.4429	0.3915	0.3803	0.3397	0.4979	0.4242	0.4195
	Avg.	0.4144	0.3392	0.3648	0.3238	0.3060	0.2727	0.4107	0.3610	0.3491
LSTM	1D	0.1867	0.2613	0.2736	0.1595	0.2496	0.1697	0.3087	0.1836	0.2241
	3D	0.2862	0.3516	0.3751	0.2391	0.3291	0.2446	0.4267	0.2704	0.3153
	5D	0.3475	0.4012	0.4475	0.2892	0.3753	0.2944	0.4867	0.3172	0.3699
	7D	0.4174	0.4312	0.5125	0.3261	0.4193	0.3261	0.5173	0.3429	0.4116
	Avg.	0.3094	0.3613	0.4022	0.2535	0.3433	0.2587	0.4348	0.2785	0.3302
GCN	1D	0.1850	0.2317	0.2365	0.2061	0.1953	0.1681	0.1944	0.2152	0.2040
	3D	0.2668	0.3177	0.3426	0.2735	0.2782	0.2385	0.3119	0.2914	0.2901
	5D	0.3329	0.3673	0.4137	0.3184	0.3256	0.2796	0.3977	0.3336	0.3461
	7D	0.3863	0.3860	0.4624	0.3484	0.3646	0.3102	0.4265	0.3620	0.3808
	Avg.	0.2928	0.3257	0.3638	0.2866	0.2909	0.2491	0.3326	0.3005	0.3053

Table 39: Benchmark(MSE) on all stations

Method	T	S0	S1	S2	S3	S4	S5	S6	S7	Avg.
MLP	1D	0.1144	0.1360	0.1284	0.0684	0.1124	0.0747	0.1674	0.1256	0.1159
	3D	0.2226	0.3080	0.2875	0.1478	0.3256	0.1424	0.5486	0.2405	0.2779
	5D	0.3117	0.4687	0.4318	0.2081	0.6883	0.1928	1.2099	0.3317	0.4804
	7D	0.3808	0.6967	0.6094	0.2648	1.0917	0.2369	1.8233	0.3899	0.6867
	Avg.	**0.2574**	**0.4024**	**0.3643**	**0.1723**	**0.5545**	**0.1617**	**0.9373**	**0.2719**	**0.3902**
TCN	1D	0.3964	0.5800	0.4714	0.2575	0.3783	0.2180	1.3093	0.5552	0.5208
	3D	0.6306	0.6849	0.6180	0.3337	0.5102	0.2900	1.5333	0.6517	0.6566
	5D	0.5709	0.7997	0.7216	0.3930	0.6323	0.3534	1.6885	0.7298	0.7362
	7D	0.6880	0.8404	0.7966	0.4639	0.7027	0.3941	1.8442	0.7434	0.8092
	Avg.	0.5715	0.7263	0.6519	0.3620	0.5559	0.3139	1.5938	0.6700	0.6807
LSTM	1D	0.2550	1.4732	1.0367	0.1620	5.2575	0.1497	6.8509	0.4084	1.9492
	3D	0.3871	1.3765	1.0735	0.2642	5.7927	0.2476	8.5420	0.5052	2.2736
	5D	0.4911	1.5590	1.4324	0.3373	5.8335	0.3032	8.3886	0.5652	2.3638
	7D	0.6198	1.6812	1.8663	0.3982	6.0814	0.3494	8.5648	0.6176	2.5224
	Avg.	0.4383	1.5225	1.3522	0.2904	5.7413	0.2625	8.0866	0.5241	2.2772
GCN	1D	0.1994	0.2886	0.7728	0.3590	0.2534	0.1165	0.2171	6.2444	1.0564
	3D	0.3102	0.4645	1.0667	0.4061	0.5848	0.1883	0.9433	3.7576	0.9652
	5D	0.4273	0.5908	1.3546	0.4490	0.8592	0.2408	2.4139	2.7351	1.1338
	7D	0.5166	0.5968	1.5264	0.4728	1.3609	0.2752	1.8411	2.3212	1.1139
	Avg.	0.3634	0.4852	1.1801	0.4217	0.7646	0.2052	1.3539	3.7646	1.0673

Table 40: Benchmark(SEDI10) on all stations

Method	T	S0	S1	S2	S3	S4	S5	S6	S7	Avg.
MLP	1D	0.7865	0.8159	0.8152	0.7883	0.7313	0.7192	0.7116	0.7581	0.7658
	3D	0.7108	0.7527	0.7714	0.7639	0.6709	0.5924	0.6336	0.6414	0.6921
	5D	0.6823	0.6972	0.7482	0.7092	0.6185	0.5809	0.5830	0.6343	0.6567
	7D	0.6455	0.6726	0.7134	0.6753	0.6142	0.5620	0.5496	0.5815	0.6268
	Avg.	**0.7063**	**0.7346**	**0.7621**	**0.7342**	**0.6587**	**0.6136**	**0.6195**	**0.6538**	**0.6853**
TCN	1D	0.6211	0.7314	0.7264	0.6545	0.5807	0.6232	0.5594	0.4628	0.6199
	3D	0.4990	0.6284	0.6505	0.5697	0.4678	0.5020	0.4852	0.3738	0.5221
	5D	0.4997	0.6025	0.6164	0.5319	0.4059	0.4549	0.4289	0.3187	0.4824
	7D	0.4366	0.5680	0.5829	0.4747	0.3637	0.4181	0.3906	0.3059	0.4426
	Avg.	0.5141	0.6326	0.6440	0.5577	0.4545	0.4996	0.4660	0.3653	0.5167
LSTM	1D	0.7478	0.7266	0.7410	0.7615	0.6781	0.6422	0.6255	0.6716	0.6993
	3D	0.6290	0.6424	0.6606	0.6671	0.5615	0.5070	0.5091	0.5369	0.5892
	5D	0.5632	0.5683	0.6139	0.6053	0.5035	0.4434	0.4307	0.4694	0.5247
	7D	0.5249	0.5386	0.5845	0.5758	0.4605	0.3974	0.3886	0.4256	0.4870
	Avg.	0.6162	0.6190	0.6500	0.6524	0.5509	0.4975	0.4885	0.5259	0.5751
GCN	1D	0.7461	0.7112	0.7543	0.7031	0.6442	0.6466	0.6565	0.6686	0.6913
	3D	0.6725	0.6669	0.6912	0.6308	0.5846	0.5725	0.5800	0.6044	0.6254
	5D	0.6331	0.6218	0.6668	0.5908	0.5515	0.5247	0.5314	0.5519	0.5840
	7D	0.5989	0.5811	0.6531	0.5765	0.5183	0.4903	0.5025	0.5109	0.5539
	Avg.	0.6626	0.6452	0.6913	0.6253	0.5746	0.5585	0.5676	0.5840	0.6137

Table 41: Benchmark(SEDI5) on all stations

Method	T	S0	S1	S2	S3	S4	S5	S6	S7	Avg.
MLP	1D	0.7136	0.7660	0.7338	0.7105	0.6322	0.6125	0.6060	0.6216	0.6745
	3D	0.6163	0.7050	0.6930	0.6926	0.5791	0.4788	0.5176	0.5137	0.5995
	5D	0.5987	0.6437	0.6679	0.6416	0.5329	0.4810	0.4710	0.5052	0.5678
	7D	0.5702	0.6306	0.6431	0.6119	0.5267	0.4753	0.4457	0.4662	0.5462
	Avg.	**0.6247**	**0.6863**	**0.6845**	**0.6642**	**0.5678**	**0.5119**	**0.5101**	**0.5267**	**0.5970**
TCN	1D	0.4196	0.6603	0.6184	0.5291	0.4095	0.4960	0.4138	0.3313	0.4848
	3D	0.3450	0.5523	0.5307	0.4549	0.2944	0.3870	0.3365	0.2404	0.3926
	5D	0.3236	0.5302	0.5064	0.4307	0.2343	0.3585	0.2869	0.2074	0.3597
	7D	0.2981	0.4912	0.4486	0.3805	0.1940	0.3273	0.2666	0.1886	0.3243
	Avg.	0.3466	0.5585	0.5260	0.4488	0.2831	0.3922	0.3259	0.2419	0.3904
LSTM	1D	0.6546	0.6720	0.6402	0.6737	0.5568	0.5009	0.4883	0.5126	0.5874
	3D	0.5112	0.5662	0.5342	0.5557	0.4398	0.3529	0.3555	0.3751	0.4613
	5D	0.4395	0.4974	0.4877	0.4993	0.3820	0.3008	0.2920	0.2929	0.3990
	7D	0.3879	0.4701	0.4458	0.4642	0.3109	0.2694	0.2556	0.2664	0.3588
	Avg.	0.4983	0.5514	0.5270	0.5482	0.4224	0.3560	0.3479	0.3618	0.4516
GCN	1D	0.6660	0.6406	0.6734	0.6192	0.5498	0.5445	0.5430	0.5278	0.5955
	3D	0.5885	0.6013	0.6062	0.5427	0.4961	0.4673	0.4629	0.4690	0.5292
	5D	0.5593	0.5528	0.5793	0.5059	0.4684	0.4301	0.4192	0.4291	0.4930
	7D	0.5471	0.5177	0.5610	0.4934	0.4320	0.4081	0.3855	0.3945	0.4674
	Avg.	0.5902	0.5781	0.6050	0.5403	0.4866	0.4625	0.4526	0.4551	0.5213

Table 42: Benchmark(SEDI1) on all stations

Method	T	S0	S1	S2	S3	S4	S5	S6	S7	Avg.
MLP	1D	0.5452	0.6313	0.5586	0.5222	0.3956	0.3222	0.3557	0.3511	0.4602
	3D	0.4265	0.5790	0.5332	0.5326	0.3359	0.2318	0.2916	0.2890	0.4025
	5D	0.4535	0.5114	0.5228	0.4968	0.3349	0.2440	0.2813	0.3036	0.3935
	7D	0.4738	0.5377	0.5065	0.4550	0.3195	0.2545	0.2705	0.2740	0.3864
	Avg.	**0.4748**	**0.5649**	**0.5303**	**0.5017**	**0.3465**	**0.2631**	**0.2998**	**0.3044**	**0.4107**
TCN	1D	0.1333	0.4546	0.4028	0.3001	0.0736	0.2119	0.1582	0.1412	0.2345
	3D	0.1118	0.3684	0.3182	0.2284	0.0440	0.1646	0.1282	0.0833	0.1809
	5D	0.1033	0.3531	0.3050	0.2328	0.0305	0.1499	0.1147	0.0757	0.1706
	7D	0.0802	0.3176	0.2611	0.2063	0.0249	0.1433	0.0978	0.0746	0.1507
	Avg.	0.1071	0.3734	0.3218	0.2419	0.0432	0.1674	0.1247	0.0937	0.1842
LSTM	1D	0.4140	0.4712	0.4004	0.4026	0.2813	0.1812	0.2226	0.2254	0.3249
	3D	0.2247	0.2719	0.2113	0.2167	0.1419	0.0936	0.1123	0.1012	0.1717
	5D	0.1839	0.1920	0.1746	0.1489	0.1184	0.0703	0.0868	0.0744	0.1312
	7D	0.1173	0.1752	0.1429	0.1642	0.0394	0.0573	0.0715	0.0608	0.1036
	Avg.	0.2350	0.2776	0.2323	0.2331	0.1453	0.1006	0.1233	0.1155	0.1828
GCN	1D	0.4770	0.4553	0.4873	0.4167	0.3108	0.2708	0.3098	0.2742	0.3752
	3D	0.4046	0.4419	0.3886	0.3418	0.2585	0.2237	0.2572	0.2331	0.3187
	5D	0.3840	0.3823	0.3712	0.3168	0.2323	0.1991	0.2144	0.2147	0.2894
	7D	0.3641	0.3583	0.3773	0.2930	0.2013	0.1843	0.1942	0.1889	0.2702
	Avg.	0.4074	0.4095	0.4061	0.3421	0.2507	0.2195	0.2439	0.2277	0.3134

Table 43: MAE results of input factors ablation study on S6. All, G, R, and C represent all factors, groundwater, rainfall, and human control(pump and gate).

Method	T	w/ All	w/o G	w/o R	w/o C	w/o GR	w/o RC	w/o WC	w/o WRC
iTransformer	1D	0.0738	0.0735	0.0729	0.0733	0.0739	0.0737	0.0739	0.0742
	3D	0.1275	0.1279	0.1278	0.1275	0.1290	0.1280	0.1265	0.1276
	5D	0.1660	0.1662	0.1664	0.1662	0.1660	0.1660	0.1658	0.1671
	7D	0.1953	0.1953	0.1953	0.1948	0.1954	0.1961	0.1947	0.1955
	Avg.	0.1406	0.1407	0.1406	0.1405	0.1411	0.1410	**0.1402**	0.1411
PatchTST	1D	0.0726	0.0731	0.0713	0.0719	0.0732	0.0722	0.0727	0.0772
	3D	0.1252	0.1262	0.1252	0.1255	0.1273	0.1273	0.1254	0.1295
	5D	0.1615	0.1639	0.1624	0.1618	0.1649	0.1649	0.1634	0.1667
	7D	0.1910	0.1933	0.1923	0.1916	0.1938	0.1941	0.1927	0.1951
	Avg.	**0.1376**	0.1391	0.1378	0.1377	0.1398	0.1396	0.1385	0.1421
TSMixer	1D	0.1004	0.0781	0.1599	0.1443	0.0778	0.1789	0.0782	0.0782
	3D	0.1471	0.1296	0.2611	0.2216	0.1297	0.2506	0.1299	0.1299
	5D	0.1802	0.1658	0.3104	0.2350	0.1657	0.3018	0.1664	0.1663
	7D	0.2107	0.1941	0.2776	0.2435	0.1939	0.3914	0.1947	0.1944
	Avg.	0.1596	0.1419	0.2523	0.2111	**0.1418**	0.2807	0.1423	0.1422
NLinear	1D	0.0937	0.0977	0.0854	0.0933	0.0850	0.0804	0.0983	0.0780
	3D	0.1429	0.1461	0.1363	0.1422	0.1366	0.1328	0.1462	0.1314
	5D	0.1769	0.1796	0.1713	0.1764	0.1717	0.1689	0.1797	0.1678
	7D	0.2050	0.2074	0.2003	0.2043	0.2008	0.1978	0.2072	0.1970
	Avg.	0.1546	0.1577	0.1483	0.1540	0.1485	0.1450	0.1579	**0.1435**
TimesNet	1D	0.0986	0.0936	0.0986	0.0986	0.0928	0.0970	0.0924	0.0930
	3D	0.1513	0.1446	0.1511	0.1525	0.1465	0.1529	0.1448	0.1468
	5D	0.1883	0.1838	0.1889	0.1890	0.1843	0.1908	0.1830	0.1814
	7D	0.2187	0.2177	0.2262	0.2200	0.2131	0.2219	0.2111	0.2109
	Avg.	0.1642	0.1599	0.1662	0.1650	0.1592	0.1656	**0.1578**	0.1580

Table 44: MSE results of input factors ablation study on S6. All, G, R, and C represent all factors, groundwater, rainfall, and human control(pump and gate).

Method	T	w/ All	w/o G	w/o R	w/o C	w/o GR	w/o RC	w/o WC	w/o WRC
iTransformer	1D	0.0400	0.0407	0.0398	0.0402	0.0405	0.0400	0.0405	0.0409
	3D	0.0817	0.0828	0.0821	0.0818	0.0827	0.0825	0.0818	0.0832
	5D	0.1175	0.1172	0.1170	0.1167	0.1166	0.1169	0.1164	0.1184
	7D	0.1419	0.1430	0.1407	0.1430	0.1429	0.1431	0.1407	0.1424
	Avg.	0.0953	0.0960	**0.0949**	0.0954	0.0957	0.0956	**0.0949**	0.0962
PatchTST	1D	0.0395	0.0393	0.0392	0.0393	0.0405	0.0399	0.0389	0.0432
	3D	0.0798	0.0807	0.0806	0.0797	0.0831	0.0819	0.0797	0.0850
	5D	0.1107	0.1128	0.1122	0.1105	0.1154	0.1140	0.1123	0.1173
	7D	0.1368	0.1400	0.1388	0.1367	0.1412	0.1393	0.1385	0.1428
	Avg.	0.0917	0.0932	0.0927	**0.0916**	0.0950	0.0938	**0.0923**	0.0971
TSMixer	1D	0.0562	0.0415	0.1891	0.2590	0.0414	0.4396	0.0419	0.0416
	3D	0.0957	0.0827	0.4979	0.2580	0.0830	0.4833	0.0825	0.0826
	5D	0.1243	0.1145	0.5722	0.3232	0.1145	0.4855	0.1139	0.1141
	7D	0.1557	0.1396	0.3653	0.2389	0.1394	1.2701	0.1389	0.1382
	Avg.	0.1080	0.0946	0.4061	0.2698	0.0946	0.6697	0.0943	**0.0941**
NLinear	1D	0.0477	0.0497	0.0450	0.0471	0.0459	0.0434	0.0494	0.0426
	3D	0.0878	0.0898	0.0848	0.0871	0.0856	0.0837	0.0895	0.0829
	5D	0.1178	0.1196	0.1154	0.1171	0.1160	0.1145	0.1191	0.1139
	7D	0.1434	0.1451	0.1411	0.1425	0.1417	0.1400	0.1444	0.1395
	Avg.	0.0992	0.1011	0.0966	0.0984	0.0973	0.0954	0.1006	0.0947
TimesNet	1D	0.0564	0.0518	0.0580	0.0573	0.0521	0.0550	0.0515	0.0517
	3D	0.1049	0.0970	0.1043	0.1049	0.0985	0.1086	0.0966	0.1015
	5D	0.1409	0.1357	0.1419	0.1416	0.1397	0.1485	0.1338	0.1338
	7D	0.1729	0.1770	0.1863	0.1770	0.1677	0.1826	0.1624	0.1624
	Avg.	0.1188	0.1154	0.1226	0.1202	0.1145	0.1237	**0.1111**	0.1123

Table 45: SEDI(10%) results of input factors ablation study on S6. All, G, R, and C represent all factors, groundwater, rainfall, and human control(pump and gate).

Method	T	w/ All	w/o G	w/o R	w/o C	w/o GR	w/o RC	w/o WC	w/o WRC
iTransformer	1D	0.6508	0.6479	0.6510	0.6551	0.6525	0.6548	0.6512	0.6520
	3D	0.5526	0.5429	0.5485	0.5510	0.5393	0.5485	0.5513	0.5533
	5D	0.4856	0.4793	0.4831	0.4877	0.4786	0.4864	0.4824	0.4779
	7D	0.4384	0.4323	0.4408	0.4399	0.4301	0.4380	0.4320	0.4326
	Avg.	0.5318	0.5256	0.5308	**0.5334**	0.5251	0.5319	0.5292	0.5289
PatchTST	1D	0.6632	0.6629	0.6665	0.6644	0.6686	0.6618	0.6621	0.6561
	3D	0.5696	0.5614	0.5704	0.5717	0.5616	0.5586	0.5658	0.5455
	5D	0.5028	0.5013	0.4997	0.5043	0.4926	0.4945	0.4993	0.4857
	7D	0.4562	0.4518	0.4498	0.4544	0.4442	0.4465	0.4476	0.4364
	Avg.	0.5480	0.5443	0.5466	**0.5487**	0.5418	0.5404	0.5437	0.5309
TSMixer	1D	0.6052	0.6538	0.5202	0.5722	0.6475	0.5493	0.6499	0.6525
	3D	0.5267	0.5571	0.4251	0.4290	0.5580	0.4402	0.5581	0.5596
	5D	0.4732	0.4959	0.3523	0.4067	0.4963	0.3709	0.4932	0.4973
	7D	0.4245	0.4487	0.3516	0.3703	0.4497	0.3206	0.4454	0.4474
	Avg.	0.5074	0.5389	0.4123	0.4446	0.5379	0.4202	0.5367	**0.5392**
NLinear	1D	0.6477	0.6485	0.6485	0.6481	0.6506	0.6529	0.6602	0.6561
	3D	0.5476	0.5556	0.5521	0.5472	0.5521	0.5566	0.5517	0.5582
	5D	0.4868	0.4928	0.4905	0.4865	0.4904	0.4936	0.4960	0.4950
	7D	0.4356	0.4355	0.4383	0.4345	0.4381	0.4440	0.4345	0.4450
	Avg.	0.5294	0.5331	0.5324	0.5291	0.5328	0.5368	0.5356	**0.5386**
TimesNet	1D	0.5936	0.6093	0.5855	0.5884	0.6067	0.5939	0.6086	0.6089
	3D	0.4772	0.5059	0.4986	0.4925	0.5117	0.4854	0.5093	0.5046
	5D	0.4304	0.4489	0.4264	0.4305	0.4460	0.4202	0.4456	0.4396
	7D	0.3878	0.3959	0.3696	0.3837	0.4095	0.3839	0.4091	0.4082
	Avg.	0.4723	0.4900	0.4700	0.4738	**0.4935**	0.4709	0.4931	0.4903

Table 46: MAE results of temporal information ablation study on S6.

Method	T	6H	12H	1D	2D	3D	4D	5D	6D
	1D	0.1136	0.1123	0.1097	0.1123	0.1133	0.1198	0.1214	0.1209
	3D	0.1999	0.1978	0.1980	0.2025	0.2071	0.2121	0.2168	0.2137
iTransformer	5D	0.2571	0.2537	0.2547	0.2586	0.2725	0.2776	0.2815	0.2779
	7D	0.3036	0.3007	0.3015	0.3059	0.3179	0.3242	0.3221	0.3261
	Avg.	0.2185	0.2161	**0.2160**	0.2198	0.2277	0.2334	0.2354	0.2346
	1D	0.1266	0.1164	0.1135	0.1127	0.1094	0.1099	0.1106	0.1159
	3D	0.2123	0.2067	0.1988	0.1979	0.1963	0.1940	0.1979	0.2011
PatchTST	5D	0.2693	0.2650	0.2566	0.2530	0.2554	0.2518	0.2522	0.2559
	7D	0.3143	0.3116	0.3039	0.2988	0.2984	0.2983	0.3011	0.3069
	Avg.	0.2306	0.2249	0.2182	0.2156	0.2149	**0.2135**	0.2155	0.2199
	1D	0.1197	0.1216	0.1237	0.1269	0.1258	0.1269	0.1289	0.1266
	3D	0.2021	0.2033	0.2058	0.2087	0.2051	0.2073	0.2074	0.2052
TSMixer	5D	0.2586	0.2592	0.2618	0.2639	0.2576	0.2604	0.2585	0.2582
	7D	0.3046	0.3049	0.3070	0.3092	0.3007	0.3029	0.2997	0.3009
	Avg.	**0.2213**	0.2222	0.2246	0.2272	0.2223	0.2244	0.2236	0.2227
	1D	0.1159	0.1180	0.1211	0.1462	0.1505	0.1508	0.1587	0.1586
	3D	0.1998	0.2011	0.2047	0.2220	0.2289	0.2305	0.2388	0.2382
NLinear	5D	0.2568	0.2577	0.2605	0.2743	0.2796	0.2870	0.2871	0.2925
	7D	0.3031	0.3036	0.3064	0.3186	0.3234	0.3293	0.3323	0.3355
	Avg.	**0.2189**	0.2201	0.2232	0.2403	0.2456	0.2494	0.2542	0.2562
	1D	0.1175	0.1234	0.1357	0.1565	0.1750	0.1903	0.2066	0.2184
	3D	0.2017	0.2084	0.2235	0.2423	0.2618	0.2775	0.2880	0.3012
TimesNet	5D	0.2602	0.2635	0.2757	0.2887	0.2989	0.3235	0.3386	0.3657
	7D	0.3086	0.3097	0.3254	0.3272	0.3570	0.3636	0.3804	0.4016
	Avg.	**0.2220**	0.2262	0.2401	0.2537	0.2732	0.2887	0.3034	0.3217

Table 47: MSE results of temporal information ablation study on S6.

Method	T	6H	12H	1D	2D	3D	4D	5D	6D
	1D	0.0829	0.0815	0.0793	0.0825	0.0844	0.0878	0.0899	0.0899
	3D	0.2093	0.2068	0.2082	0.2152	0.2218	0.2281	0.2379	0.2306
iTransformer	5D	0.3186	0.3162	0.3174	0.3219	0.3472	0.3551	0.3556	0.3594
	7D	0.4170	0.4149	0.4139	0.4220	0.4499	0.4614	0.4614	0.4757
	Avg.	0.2569	0.2549	**0.2547**	0.2604	0.2758	0.2831	0.2862	0.2889
	1D	0.0888	0.0860	0.0851	0.0827	0.0795	0.0787	0.0788	0.0835
	3D	0.2151	0.2104	0.2107	0.2078	0.2064	0.2050	0.2072	0.2089
PatchTST	5D	0.3243	0.3214	0.3210	0.3156	0.3130	0.3256	0.3408	0.3187
	7D	0.4236	0.4187	0.4270	0.4193	0.4275	0.4548	0.4255	0.4348
	Avg.	0.2630	0.2592	0.2609	0.2563	0.2566	0.2660	0.2631	**0.2615**
	1D	0.0899	0.0899	0.0888	0.0887	0.0860	0.0853	0.0855	0.0837
	3D	0.2152	0.2145	0.2141	0.2121	0.2047	0.2042	0.2034	0.1992
TSMixer	5D	0.3241	0.3228	0.3226	0.3170	0.3060	0.3050	0.3035	0.3024
	7D	0.4235	0.4222	0.4214	0.4142	0.3999	0.3982	0.3968	0.3985
	Avg.	0.2632	0.2623	0.2617	0.2580	0.2491	0.2482	0.2473	**0.2460**
	1D	0.0852	0.0858	0.0873	0.1111	0.1135	0.1122	0.1196	0.1176
	3D	0.2111	0.2115	0.2148	0.2370	0.2444	0.2436	0.2535	0.2509
NLinear	5D	0.3201	0.3206	0.3236	0.3439	0.3490	0.3587	0.3563	0.3629
	7D	0.4199	0.4200	0.4235	0.4427	0.4480	0.4555	0.4586	0.4623
	Avg.	**0.2591**	0.2595	0.2623	0.2836	0.2887	0.2925	0.2970	0.2984
	1D	0.0866	0.0937	0.1104	0.1357	0.1603	0.1750	0.2039	0.2297
	3D	0.2177	0.2333	0.2594	0.2953	0.3156	0.3607	0.3811	0.4114
TimesNet	5D	0.3316	0.3372	0.3781	0.3997	0.4169	0.4597	0.5154	0.5691
	7D	0.4363	0.4407	0.4918	0.4891	0.5910	0.5837	0.5953	0.6566
	Avg.	**0.2681**	0.2762	0.3100	0.3299	0.3710	0.3948	0.4239	0.4667

Table 48: SEDI(10%) results of temporal information ablation study on S6.

Method	T	6H	12H	1D	2D	3D	4D	5D	6D
iTransformer	1D	0.7825	0.7945	0.7941	0.7898	0.7703	0.7857	0.7728	0.7632
	3D	0.6792	0.6945	0.6987	0.6957	0.6847	0.6801	0.6691	0.6627
	5D	0.6220	0.6392	0.6420	0.6318	0.6201	0.6189	0.6178	0.6022
	7D	0.5797	0.5984	0.6006	0.5992	0.5867	0.5841	0.5738	0.5665
	Avg.	0.6659	0.6816	**0.6838**	0.6791	0.6654	0.6672	0.6584	0.6487
PatchTST	1D	0.7522	0.7946	0.8004	0.8033	0.8100	0.8118	0.8058	0.8099
	3D	0.6324	0.6425	0.6977	0.7010	0.7046	0.7030	0.7033	0.7032
	5D	0.5820	0.5796	0.6389	0.6427	0.6404	0.6467	0.6362	0.6326
	7D	0.5415	0.5314	0.5959	0.6024	0.5986	0.5957	0.5929	0.5982
	Avg.	0.6270	0.6370	0.6832	0.6874	0.6884	**0.6893**	0.6846	0.6860
TSMixer	1D	0.7812	0.7886	0.7954	0.7912	0.7931	0.7965	0.7905	0.7952
	3D	0.6861	0.6906	0.6971	0.7005	0.7016	0.7067	0.6946	0.6983
	5D	0.6307	0.6351	0.6397	0.6463	0.6445	0.6503	0.6400	0.6385
	7D	0.5917	0.5942	0.5984	0.6054	0.6003	0.6038	0.5959	0.5900
	Avg.	0.6724	0.6771	0.6827	0.6859	0.6849	**0.6893**	0.6803	0.6805
NLinear	1D	0.7915	0.8002	0.8029	0.7843	0.7891	0.7933	0.7929	0.7904
	3D	0.6956	0.6989	0.7019	0.6857	0.6958	0.6974	0.6925	0.6940
	5D	0.6359	0.6383	0.6447	0.6320	0.6329	0.6373	0.6422	0.6373
	7D	0.5944	0.5995	0.6016	0.5875	0.5889	0.5951	0.5973	0.5994
	Avg.	0.6794	0.6842	**0.6878**	0.6724	0.6767	0.6808	0.6812	0.6803
TimesNet	1D	0.7590	0.7610	0.7482	0.7130	0.6908	0.6854	0.6548	0.6392
	3D	0.6582	0.6606	0.6499	0.6148	0.5993	0.5889	0.5790	0.5731
	5D	0.5976	0.6096	0.5988	0.5779	0.5631	0.5461	0.5458	0.5246
	7D	0.5647	0.5692	0.5451	0.5447	0.5269	0.5263	0.5062	0.5060
	Avg.	0.6449	**0.6501**	0.6355	0.6126	0.5950	0.5867	0.5714	0.5607

Table 49: MAE results of spatial information ablation study on S6.

		MAE					MSE					SEDI(10%)				
Method	T	$1.0R$	$1.2R$	$1.4R$	$1.6R$	$1.8R$	$1.0R$	$1.2R$	$1.4R$	$1.6R$	$1.8R$	$1.0R$	$1.2R$	$1.4R$	$1.6R$	$1.8R$
iTransformer	1D	0.1123	0.1135	0.1125	0.1099	0.1119	0.0825	0.0825	0.0818	0.0822	0.0807	0.7898	0.7810	0.7894	0.7863	0.7939
	3D	0.2025	0.2038	0.2020	0.2024	0.2021	0.2152	0.2144	0.2117	0.2136	0.2119	0.6957	0.7011	0.6952	0.7022	0.7036
	5D	0.2586	0.2650	0.2584	0.2538	0.2513	0.3219	0.3314	0.3241	0.3257	0.3186	0.6318	0.6294	0.6329	0.6353	0.6361
	7D	0.3059	0.3040	0.3017	0.3006	0.2995	0.4220	0.4239	0.4181	0.4176	0.4197	0.5992	0.5973	0.5989	0.5972	0.5965
	Avg.	0.2198	0.2216	0.2187	0.2167	**0.2162**	0.2604	0.2631	0.2589	0.2598	**0.2577**	0.6791	0.6772	0.6791	0.6803	**0.6825**
PatchTST	1D	0.1127	0.1131	0.1139	0.1113	0.1118	0.0827	0.0833	0.0829	0.0825	0.0821	0.8033	0.8030	0.8066	0.8068	0.8095
	3D	0.1979	0.1967	0.1990	0.1976	0.1976	0.2078	0.2060	0.2087	0.2082	0.2083	0.7010	0.7036	0.7048	0.7040	0.7073
	5D	0.2530	0.2531	0.2548	0.2556	0.2550	0.3156	0.3133	0.3151	0.3182	0.3160	0.6427	0.6440	0.6433	0.6437	0.6483
	7D	0.2988	0.2971	0.2994	0.3000	0.2991	0.4193	0.4102	0.4102	0.4115	0.4097	0.6024	0.6035	0.6049	0.6056	0.6065
	Avg.	0.2156	**0.2150**	0.2168	0.2161	0.2159	0.2563	**0.2532**	0.2542	0.2551	0.2540	0.6874	0.6885	0.6899	0.6900	**0.6929**
TSMixer	1D	0.1269	0.1259	0.1255	0.1271	0.1256	0.0887	0.0882	0.0876	0.0888	0.0879	0.7912	0.7896	0.7918	0.7895	0.7891
	3D	0.2087	0.2082	0.2072	0.2075	0.2064	0.2121	0.2125	0.2096	0.2093	0.2096	0.7005	0.6996	0.7026	0.7011	0.7001
	5D	0.2639	0.2638	0.2621	0.2632	0.2625	0.3170	0.3182	0.3136	0.3147	0.3146	0.6463	0.6451	0.6503	0.6484	0.6492
	7D	0.3092	0.3086	0.3074	0.3082	0.3062	0.4142	0.4151	0.4117	0.4114	0.4097	0.6054	0.6042	0.6078	0.6066	0.6055
	Avg.	0.2272	0.2266	0.2255	0.2265	**0.2252**	0.2580	0.2585	0.2556	0.2560	**0.2554**	0.6859	0.6846	**0.6881**	0.6864	0.6860
NLinear	1D	0.1462	0.1482	0.1473	0.1464	0.1449	0.1111	0.1133	0.1123	0.1113	0.1097	0.7843	0.7816	0.7807	0.7811	0.7821
	3D	0.2220	0.2238	0.2227	0.2213	0.2205	0.2370	0.2397	0.2381	0.2358	0.2347	0.6857	0.6836	0.6850	0.6865	0.6876
	5D	0.2743	0.2756	0.2746	0.2744	0.2735	0.3439	0.3461	0.3443	0.3437	0.3423	0.6320	0.6300	0.6315	0.6317	0.6310
	7D	0.3186	0.3199	0.3191	0.3181	0.3173	0.4427	0.4450	0.4435	0.4415	0.4402	0.5875	0.5888	0.5904	0.5930	0.5932
	Avg.	0.2403	0.2419	0.2409	0.2400	**0.2390**	0.2836	0.2860	0.2845	0.2831	**0.2817**	0.6724	0.6710	0.6719	0.6731	**0.6735**
TimesNet	1D	0.1565	0.1582	0.1597	0.1655	0.1661	0.1357	0.1423	0.1392	0.1458	0.1492	0.7130	0.7099	0.7155	0.7093	0.7007
	3D	0.2423	0.2451	0.2408	0.2424	0.2454	0.2953	0.3075	0.2847	0.2893	0.3104	0.6148	0.6168	0.6174	0.6202	0.6131
	5D	0.2887	0.2935	0.3038	0.2924	0.2985	0.3997	0.4087	0.4531	0.4028	0.4239	0.5779	0.5812	0.5651	0.5824	0.5674
	7D	0.3272	0.3399	0.3380	0.3422	0.3413	0.4891	0.5223	0.5136	0.5219	0.5451	0.5447	0.5377	0.5359	0.5426	0.5410
	Avg.	**0.2537**	0.2592	0.2606	0.2606	0.2628	**0.3299**	0.3452	0.3476	0.3400	0.3571	0.6126	0.6114	0.6085	**0.6136**	0.6056